The Dissertation Committee for Chris Eugene Brough Certifies that this is the approved version of the following dissertation:

Novel Uses of Pharmaceutical Polymers as enabled by KinetiSol® Dispersing

Committee:

Robert O. Williams III, Supervisor

James W. McGinity

Christopher R. Frei

Sean M. Kerwin

Dave A. Miller

Novel Uses of Pharmaceutical Polymers as enabled by KinetiSol® Dispersing

by

Chris Eugene Brough, B.S., M.S., M.B.A.

Dissertation

Presented to the Faculty of the Graduate School of

The University of Texas at Austin

in Partial Fulfillment

of the Requirements

for the Degree of

Doctor of Philosophy

The University of Texas at Austin

August, 2015

Dedication

To my wife, Jessica, who has been a huge support in all of my business and scholastic adventures.

To my three kids, Ezra, Scarlett & Levi, who have been patient with their dad as he has had some late nights and early mornings.

To my father, who always wanted one of his boys to become a ‘doctor’.

Acknowledgements

I would like to thank my boss, Gershon Yaniv, for pushing me to pursue this Ph.D. and for also allowing me to be employed full-time to allow it to happen. I would like to thank Robert O. Williams III for being such a wonderful supervisor and allowing me the flexibility to juggle school and work. I could not have completed the program without his patience, understanding, support and guidance. James W. McGinity's support of the technology has not only helped DisperSol get its start, but also sparked interest within me for this particular field of study, of which I am very grateful.

I would like to thank the faculty and the members on my committee. I cannot take the time here to write all of the things I learned nor the ways I was influenced, but I am very grateful for them. This may sound cheesy, but I really felt that every one of them genuinely cared about my success. In the vigor of this program, it was nice to feel that everyone was on my side.

I need to specifically thank Dave Miller, Justin Keen and Justin Hughey. As I think about the hours that these men spent with me, I am humbled by their generosity, knowledge and kindness. I could not have done this without them. Also, as funny as this sounds, I want to thank Texas. I know I would not have ever gotten involved in this industry, if my company wasn't bought and moved to Texas.

There is no way that I can adequately thank my wife, Jessica. She has had to handle most parental duties without me. I know that being a 'single mother' to our three kids has been a real challenge at times, but she has been amazing. She is SuperMom and SuperWife, but the world will never know it. I just want her to know that I do.

Finally, I would like to thank my Father in Heaven. As I was contemplating getting this Ph.D. (rather as Gershon was pushing me to do it), I really didn't want to because I felt that my two master's degrees were more than sufficient for what I wanted to do in life. As I made it a matter of prayer, it was clear to me that this was something that God wanted me to do. I could not count the times that I wanted to quit or the times that I felt bad as I saw how this program was negatively effecting my wife and kids. But, each time I turned to Him, I received comfort and strength. I honestly still don't know why I did this. If I knew how hard it was going to be, I probably wouldn't have done it. But, I have faith that there is a reason. At the end of the day, I just want to be His servant and to make the world a little better place. I just hope that the sacrifice this bundle of paper represents actually results in the outcome that He wanted.

Novel Uses of Pharmaceutical Polymers as enabled by KinetiSol® Dispersing

Chris Eugene Brough, Ph.D.

The University of Texas at Austin, 2015

Supervisor: Robert O. Williams III

Poor water-solubility is a common characteristic of drug candidates in pharmaceutical development pipelines today. Various processes have been developed to increase the solubility, dissolution rate and bioavailability of these active ingredients belonging to BCSII and IV classifications. Over the last decade, nano-crystal delivery forms and amorphous solid dispersions have become well established in commercially available products and industry literature. Chapter 1 is a comparative analysis of these two methodologies primarily for orally delivered medicaments. The thermodynamic and kinetic theories relative to these technologies are presented along with a survey of commercial relevant scientific literature. Marketed products from both technologies are presented, but there appears to be more amorphous dispersion products on the U.S. market today and current development trends are showing an industry preference for amorphous solid dispersions.

Many pharmaceutical polymers have been investigated as the primary component in amorphous solid dispersions for their ability to increase the apparent water solubility of poorly water-soluble drugs. Polyvinyl alcohol (PVAL) has not been investigated as a concentration enhancing polymer owing to its high melting point/high viscosity and poor organic solubility. Due to the unique attributes of the KinetiSol® Dispersing (KSD)

technology, PVAL has been enabled for this application and Chapter 2 contains an initial investigation into various grades for improvement of the solubility and bioavailability of the poorly water-soluble model drug, itraconazole (ITZ). Polymer grades were chosen with variation in molecular weight and degree of hydroxylation to determine the effects on performance. Differential scanning calorimetry, powder x-ray diffraction, polarized light microscopy, size exclusion chromatography and dissolution testing were used to characterize the amorphous dispersions. An *in vivo* pharmacokinetic study in rats was also conducted to compare the selected formulation to current market formulations of ITZ.

Chapter 3 continues the investigation into the use of PVAL as a concentration enhancing polymer for amorphous solid dispersion. The previous chapter revealed that the 88% hydrolyzed grade was optimal for ITZ compositions with regard to solid-state properties, non-sink dissolution performance and bioavailability enhancement. This chapter explores the influence of molecular weight for the 88% hydrolyzed grade in the range of 4 to 8 mPa·s with the top performing grade from both chapters emerging as PVAL 4-88. Amorphous dispersions at 10, 20, 30, 40 and 50% ITZ drug loads in PVAL 4-88 were compared by dissolution performance. Analytical tools of diffusion-ordered spectroscopy and Fourier transform infrared spectroscopy were employed to understand the interaction between drug and polymer. Finally, results from a 30 month stability test of a 30% drug loaded ITZ:PVAL 4-88 composition shows that stable amorphous dispersions can be achieved.

The KinetiSol® Dispersing (KSD) technology has been shown to create solid dispersion systems from challenging drugs and highly viscous polymers. The focus has been primarily using this technology for solubility enhancement, but it can be advantageous for other obstacles facing the pharmaceutical development industry. Chapter 4 contains an investigation into the use of the technology for producing abuse deterrent formulations for

the drug, theophylline, which is used as a model for oxycodone. Various high molecular weight polymers are combined with plasticizers to produce mechanical and chemical properties sufficient to resist alcohol dose dumping, size reduction for immediate release and syringeability for injection. Thus, the KinetiSol® Dispersing (KSD) technology can be used as a formulation platform for creating abuse deterrent delivery forms in addition to solid amorphous dispersions for solubility enhancement.

Table of Contents

List of Tables

List of Figures

List of Equations

Chapter 1

Amorphous Solid Dispersions and Nano-crystal Technologies for Poorly Water-Soluble Drug Delivery [1]

[1] Previously published: Brough, C. and R.O. Williams III, *Amorphous solid dispersions and nano-crystal technologies for poorly water-soluble drug delivery.* International Journal of Pharmaceutics, 2013. **453**(1): p. 157-166.

Research and writing was supervised by Robert O. Williams III.

1.1 INTRODUCTION

Poorly-water soluble drug substances are a significant percentage of the molecular entities in the industry's drug development pipeline and are a growing percentage of those commercially available [2-4]. In the past, the industry consensus was to view these as highly risky development candidates [5]. However, given their prevalence, industry consensus has shifted from an attitude of avoidance to one of acceptance as increasing research dedication is given to solving solubility challenges [6]. Whether the increase in number of poorly water-soluble entities is due to modern high-through put screening methodologies [7] or credited to development on increasingly biocomplex diseases requiring higher lipophilicity and larger molecular weight, the challenge of poor solubility is not disappearing in the foreseeable future [8, 9].

Addressing this issue, the pharmaceutical industry has developed multiple methods for increasing the apparent solubility of crystalline drugs. Traditionally, salt formation was preferred by medicinal and synthetic chemists for weak bases or weak acids [10]. Unfortunately, only 20-30% of new molecules form salts easily, so 70-80% of those entities must find another route to improved solubility [11]. Cyclodextrins [12], self-emulsifying drug delivery systems (SEDDS)[13], solid lipid nanoparticles [14], liposomes [15], micelles [16], soft gelatin capsules [17], co-crystals [18], pH micro-environmental

modifiers [19], and high energy polymorphs [20] are some of the routes available to pharmaceutical scientists. However, the last decade has shown the prevalence of two solubility/dissolution rate improvement methods both in scientific literature and marketed products: nano-crystal delivery forms and solid amorphous dispersions.

1.2 SCIENTIFIC FOUNDATION

Solubility of the drug substances plays a significant role in its bioavailability. The Biopharmaceutical classification system (BCS) was established in order to classify intestinal absorption [21]. Poorly water-soluble compounds are grouped into BCS Class II (high permeability, low solubility) or BCS Class IV (low permeability, low solubility) depending upon their permeability categorization [22].

There are multiple complex factors in drug absorption, but a straightforward conceptual approach to understanding solubility's role can be expressed by the maximum absorbable dose (*MAD*) formula:

$$\mathrm{MAD} = K_a \cdot S_{pH} \cdot V_{SI} \cdot t$$

Equation 1.1: Maximum absorbable dose (MAD) formula.

Where K_a is the intestinal absorption rate constant (related to permeability), S_{pH} is the solubility at intestinal pH, V_{SI} is the volume of fluid in the small intestine available for drug dissolution and t is the transit time through the small intestine [23, 24]. While this is a more simplistic model, it does illustrate important points in the challenge of poorly soluble drug absorption. First, the solubility at the site of absorption is critical after the pH transition from the acidic gastric environment [25]. Delivery forms must either include dissolution in the gastric environment and maintenance of solubility through the pH transition into the intestines or acceptably rapid dissolution rates at intestinal pH to achieve

solubility during the intestinal transit time. Second, K_a, the intestinal absorption rate, must also be considered with increased solubility. At low solubility, the S_{pH} is likely the limiting factor in the maximum absorbable dose. If the drug solubility is increased substantially, the limiting factor can shift from solubility to the intestinal absorption rate [26]. Thus, it may be more important to stabilize drug solubility for the entire intestinal transit time rather than to maximize solubility for a portion of it.

1.2.1 Nano-crystal Delivery Forms

Both nano-crystal delivery forms and solid amorphous dispersions increase the amount of drug dissolved at the site of absorption, but they achieve this by different mechanisms. Nano-crystal delivery relies on reduced particle size for increased solubility and dissolution rate [27]. The Nernst-Brunner equation (Noyes-Whitney equation modified with Fick's second law) illustrates the effect of smaller particle size on dissolution as seen in Equation 1.2:

$$\frac{dC}{dt} = \frac{DS}{Vh}(C_s - C)$$

Equation 1.2: The Nernst-Brunner equation.

Where dC/dt is the change of concentration over time (dissolution), D is the diffusion coefficient, S is the surface area, V is the volume of the dissolution medium, h is the thickness of the diffusion layer, C_S is the saturation solubility and C is the instantaneous concentration at time t [28]. As particles are reduced in size the surface area increases; as particles are reduced to the nano scale the surface area increases dramatically. In addition to affecting surface area, with particle sizes less than about 50μm the thickness of the diffusion layer appears to decreases as well [29]. Thus, nano sizing increases dissolution

by simultaneously increasing surface area in the numerator and decreasing the diffusion layer thickness in the denominator of Equation 1.2.

The relationship of solubility of a small particle in a bulk solution is given by the Ostwald-Freundlich equation (Equation 1.3), which is analogous to the Gibbs-Kelvin equation [30].

$$\ln\left(\frac{x_R}{x_\infty}\right) = \frac{2\sigma^{\alpha\gamma}\upsilon_2^{\gamma}}{k_B RT}$$

Equation 1.3: Ostwald-Freundlich equation.

Where the solubility, x_R, of a small solid particle (phase γ) in the ideal bulk solution (phase α) is related to radius, R. The other variables are as follows: x_∞ is the relative concentration of solute in phase α, $\sigma^{\alpha\gamma}$ is the surface tension of the solid particle at its boundary with phase α, υ_2^{γ} is the volume per molecule in the solid particle, k_B is the Boltzmann constant and T is the temperature. According to the equation, particles with a very small radius will have increased solubility. This indicates that nanoparticles not only affect surface area, S, and the diffusion layer thickness, h, in the Nernst-Brunner equation, but also the saturation solubility, C_S. Entering values to simulate a drug in intestinal fluid (assuming a drug molecular weight of 500 and an $\sigma^{\alpha\gamma}$ value of 15-20 mN m^{-1} for the crystal-intestinal fluid surface tension) Equation 1.3 predicts an approximate 10-15% increase in solubility for a particle size of 100 nm [31].

Further illustrations of increased solubility of small particles have been reported [32, 33]. Junghanns et al. used an equation related to the Ostwald-Freundlich equation, the Kelvin equation, which describes the relationship between the radius of a liquid droplet and the vapor pressure leading to evaporation. Equation 1.4 is the Kelvin equation.

$$\ln\left(\frac{p}{p_o}\right) = \frac{2\gamma V_m}{\hat{R}RT}$$

Equation 1.4: Kelvin equation.

Where p is the vapor pressure, p_o is the saturated vapor pressure, γ is the surface tension, V_m is the molar volume, $\hat{R}$ is the universal gas constant, R is the radius of the droplet and T is the temperature. Under the assumption that a transfer of molecules from a liquid phase to a gas phase is in principal identical to the transfer of molecules from a solid phase to a liquid phase, the properties of $BaSO_4$ were entered into the Equation 1.4. Using the curvature of the nanoparticle surfaces to estimate pressures, the Kelvin equation shows an increase in saturation solubility for particles smaller than 1 μm.

Nanoparticles are much more unstable than microparticles because of the extra Gibbs free energy contribution related to reducing particle size and primarily due to surface energy [34]. Addressing this extra contribution is key to formulating pharmaceutical nanoparticles because they will tend to agglomerate to minimize their total energy [35]. Approaches to stabilizing drug nanoparticles can be categorized into two groups: thermodynamic stabilization which uses surfactants or block copolymers for particle stability or kinetic stabilization which uses energy input to compensate for Gibbs free energy [34]. For maximum effectiveness, the two approaches are often combined [36]. Careful selection of the amount of stabilizer is as important as the selection of the type of stabilizer. For example, one obstacle to stabilization is Ostwald ripening, which is the phenomenon in which smaller particles in solution dissolve and deposit on larger particles in order to reach a more thermodynamically stable state by minimizing the surface to area

ratio [37]. Too little stabilizer allows agglomeration of nanoparticles and too much stabilizer promotes Ostwald ripening [38].

1.2.2 Amorphous Dispersions

Understanding the benefit of solid amorphous dispersions must be explained in terms of enthalpic energy. There are three basic quantities governing the solubility (*S*) of a given solid solute [8]:

$$S = f(Crystal\ Packing\ Energy + Cavitation\ Energy + Solvation\ Energy)$$

Equation 1.5: Three basic quantities governing solubility.

The crystal packing energy term accounts for the energy necessary to disrupt the crystal lattice and remove isolated molecules. The cavitation energy term accounts for the energy required to disrupt water in order to create a cavity in which to host the solute molecule. The solvation energy term accounts for the release of energy as favorable interactions are formed between the solvent and solute. A graphical representation is shown in Figure 1.1.

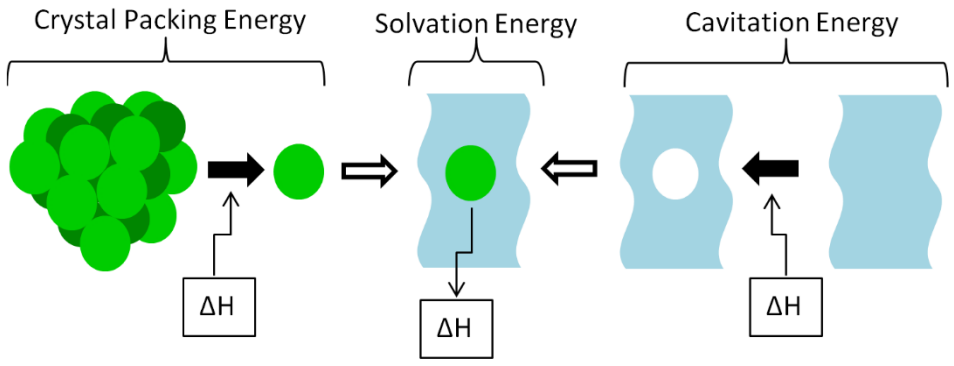

Figure 1.1: Three basic quantities that determine solubility of solid solute.

In relative terms, the crystal packing energy is larger than both cavitation and solvation energies and thus, the driving force behind solubility. The intent in formulating an amorphous solid dispersion is to minimize this energy component by disrupting the drug crystal lattice in the delivery form. In conjunction with solubility enhancing polymeric carriers, the apparent solubility can be increased by up to 10,000 fold or more [39-42]. In terms of the Nernst-Brunner equation, drastic increases of the saturation solubility, C_S, result in a much faster dissolution rate.

Solid amorphous dispersions essentially contain stored potential energy that can 'spring' the molecular entity into a supersaturated state [43, 44]. Since supersaturation is thermodynamically unstable, the formulation must also provide a 'parachute' to keep the solubility from rapidly returning to the crystalline drug equilibrium solubility (Figure 1.2) to maintain elevated drug concentrations for the duration of intestinal transit to achieve the maximum absorbable dose. In general, solubility enhancing polymers are reported to function well as a parachute or stabilizer due to drug-polymer interactions in solution and by adsorption of the polymer on the growing crystal [45]. Other solubility enhancing formulations may require additional excipients to function as the parachute to retard the descent from high to low energy forms of the drug. Examples of polymers that have been investigated for their stabilizing effect are PVP [46], PEG [47], methylcellulose (MC) [48] and HPMC [49].

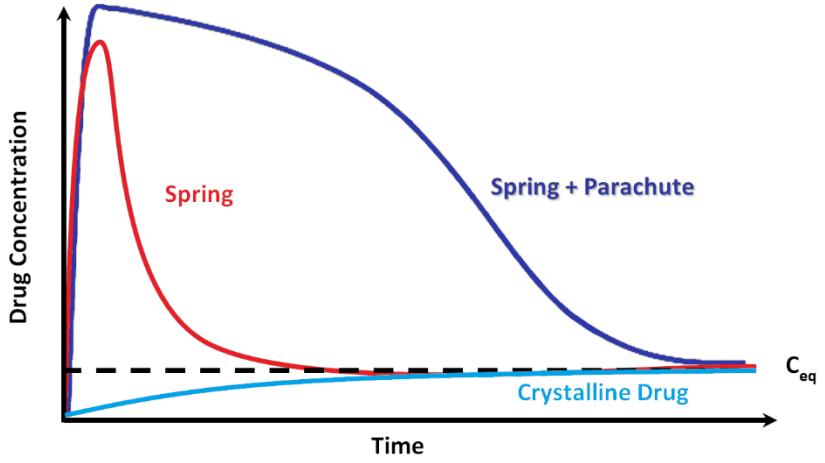

Figure 1.2: 'Spring & Parachute' concept for supersaturation stability [44] (adapted).

A concern with solid dispersions is the possibility of the amorphous drug substance undergoing crystallization on storage. The effect of moisture on storage stability is an another concern because the presence of water may increase drug mobility and promote drug crystallization [50]. Additionally, some polymers used in solid dispersions are hygroscopic, which may result in phase separation, crystal growth or conversion from a metastable crystalline form to a more stable crystalline structure during storage [51]. This would result in continually decreasing the solubility and dissolution rate as well as lower the *in vivo* performance during the product's shelf-life.

The above challenges can be mitigated by proper polymer selection, drug loading optimization and appropriate product packaging selection. Amorphous solid dispersions can be rendered physically stable via kinetic stabilization: i.e., freezing the amorphous drug substance in the polymer matrix to restrict molecular mobility to prevent nucleation and crystal growth. It has been reported that for adequate kinetic stability, the T_g of the composite matrix should be 50 °C above the maximum storage temperature [52]. From this perspective, polymer selection is important to ensure a high composite T_g for the

preservation of the amorphous drug. A polymer may also stabilize an amorphous drug substance via drug-polymer intermolecular interactions such as hydrogen bonding, Van der Waals forces, etc. Such interactions can be estimated a priori utilizing calculated solubility parameters or empirically via the use of analytical techniques such as Fourier transform infrared spectroscopy (FTIR) [53-55]. These interactions provide thermodynamic stability to the amorphous drug substance and can result in product stability irrespective of T_g [56]. Drug loading can impact both kinetic and thermodynamic stability of an amorphous solid dispersion. For a low T_g drug in a kinetically stabilized dispersion, the higher the drug loading means the lower the composite T_g, and hence the more unstable the composition. For a thermodynamically stabilized amorphous solid dispersion, increasing drug loading can saturate bonding sites, and thus result in a less stable amorphous dispersion. Practically speaking, most amorphous solid dispersions are formulated in a metastable region where the mode of stabilization is a combination of both kinetic and thermodynamic mechanisms [57]. As drug loading impacts both of these stabilizing mechanisms it is critical to conduct accelerated stability studies on a range of drug loadings to arrive at a physically stable amorphous dispersion with an acceptable drug load. Finally, packaging is critical when the amorphous solid dispersion is susceptible to destabilization by moisture absorption [58]. Adsorbed moisture can lead to crystallization by plasticizing the polymer matrix and increasing the molecular mobility, displacing drug substances from bonding sites on the polymer, or both. Utilizing the appropriate dosage form, the packaging configuration can eliminate moisture contact and stabilize the amorphous product for an acceptable shelf-life.

1.3 PROCESSES

1.3.1 Nano-crystal Technologies

Wet ball milling (also called bead milling or pearl milling) is the most frequently used production method for drug nano-crystals in the pharmaceutical industry [59]. This can be attributed in part to the simplicity of the process allowing it to be performed in almost every lab. The simplest way of doing ball milling is feeding coarse drug substance into a jar filled with milling media with at least one stabilizing agent. Then, agitate the milling media by magnetic stirrer or by rotating or tumbling the jar. This will generally yield very fine particles with a narrow size distribution when allowed to operate long enough.

Alternatively, wet ball milling operations based on higher energy media movement can accomplish particle size reduction in times more suitable for industrial pharmaceutical applications [60]. The NanoCrystal™ process is a high energy wet ball milling process regarded as the standard procedure to produce nanosuspensions [61]. To operate, the milling chamber is filled with milling media, water, drug and stabilizer. A shaft with projectiles spins within the milling chamber which allows drug particles to collide with the chamber wall, milling media and other drug particles. The high shear forces provide the energy input to fracture drug crystals into nanometer-size particles. Normal processing times ranging from 30 minutes to 2 hours yield nanosuspensions of good quality. The process has demonstrated scalability; batch mode R&D equipment can process 10 mg of drug substance and larger continuous mode equipment is being used to produce commercial products [62]. Because it is part of the process, one inherent benefit of wet ball milling is creating a very stable aqueous suspension. This suspension can be directly formed into liquid oral, injectable and nebulized inhalation delivery forms [63].

High pressure homogenization can be considered the second most frequently used technique to produce nano-crystals [59]. Like wet ball milling, it is a particle size reduction technology, but uses jet-stream homogenization by pumping drug, dispersion medium, surfactants and/or stabilizers under high pressure through a micro fluidizing nozzle. The particle size reduction is caused by cavitation forces, shear forces and collision through multiple homogenization cycles. The number of passes depends upon many factors comprising the type of homogenizer and process conditions, which has led to various technologies: IDD-P™, Dissocubes® and Nanopure® [32].

Combination technologies have also been developed that integrate a pre-treatment step with a subsequent high energy step, like high pressure homogenization. The NANOEDGE™ technology is one example that combines a first classical precipitation step with a subsequent annealing step by applying high energy (high pressure homogenization)[32]. The term annealing was used meaning nanoparticles achieve a lower surface energy by application of energy followed by thermal relaxation. Other combination technologies, bottom-up methodologies and other processes are available to produce nano-crystal drug delivery forms [64-66].

1.3.2 Amorphous Dispersion Technologies

Processes for the preparation of solid amorphous dispersions can be categorized into two general types: solvent methods and fusion or melting methods. With solvent methods, solid dispersions are obtained by evaporating a common solvent from a drug and carrier solution. In general, fusion methods heat a drug and carrier composition above their melting or glass transition temperatures, mix at the elevated temperature, and then cool the composition in such a way to keep the active ingredient in its amorphous state. Operating temperatures for solvent techniques are generally lower than fusion techniques and are

advantageous for thermolabile drug substances. However, finding a common solvent is not always straightforward. For example, in the case for solid dispersions for immediate drug release, hydrophobic drugs are typically combined with hydrophilic carriers, which can limit solvent selection. A secondary drying step is often required to reduce residual solvent below accepted levels for safety issues. In addition, small amounts of residual solvent could negatively affect drug chemical stability and can plasticize the solid dispersion matrix to subsequently impact physical stability [45].

Practical applications of the solvent method are spray drying and freeze drying. In spray drying, the drug and carrier solution is atomized into hot gas that causes the solvent to evaporate resulting in spherical particles containing amorphous drug [67]. Freeze drying or lyophilization is a technique in which the drug and polymer solution is frozen and the solvent is sublimed under vacuum. Another solvent method is using a fluidized bed system to coat multiparticulates (i.e., beads or pellets) with drug-carrier solutions resulting in pellets with a solid amorphous dispersion coating [68].

Hot-melt extrusion (HME), a well-known fusion technique, has been a topic of interest in recent pharmaceutical research literature [69]. HME is the process of pumping compositions through a heated barrel by one or more screws under pressure followed by discharging the extrudate through a die. Solvents are not necessary thereby eliminating the aforementioned solvent related issues. The intense mixing and agitation imposed by the rotating screw(s) causes uniform distribution of drug and the processes is continuous and efficient. The extrudate discharge is dense and can be post-processed without the bulk density issues of some solvent methods. Viscous compositions may require the aid of a plasticizing agent to allow the composition to flow through the heated barrel and out the die without over torqueing the electric motor. Plasticizers increase molecular mobility

upon storage and can allow for crystallization if the composition's glass transition temperature is not at least 50°C above the storage condition [52].

Other fusion processes have been explored in creating amorphous dispersions. Spray congealing is a process where molten compositions are atomized into particles of spherical shape and then cooled to solidification [70]. KinetiSol® Dispersing is a fusion based process that has been shown to create amorphous dispersions of high temperature, thermolabile drug substances without degradation [71]. It does not have the same viscosity limitations as HME and thus compositions are processed without the need of a plasticizer. Scalability is a non-issue as the equipment is used in non-pharmaceutical industrial applications, but no current marketed products are produced by this technology.

1.4 RESEARCH COMPARISONS

Numerous papers have been published on amorphous solid dispersions and nano-crystal formulations. For the purposes of this comparison review, only original research papers that directly compare the two in a formulation development effort are discussed. Additionally, literature was limited to those studies that included participation and/or support from a pharmaceutical company as this was considered to be an indicator of the study's commercial relevance.

Fakes et al reported on the enhancement of an HIV-attachment inhibitor, BMS-488043 [72]. The molecule was classified as a BSC class II compound with low aqueous solubility of 0.04 mg/ml and a permeability of 178 nm/s in a caco2 cell-line model. To increase bioavailability of the molecule, a nanosuspension formulation was developed and compared to an amorphous solid dispersion made by a solvent evaporation method. The nanosuspension formula was produced by a Nanomill™ at a 10% (w/w) concentration using hydroxypropyl cellulose (HPC-SL) at 2% (w/w) and sodium lauryl sulfate (SLS) at 0.1% (w/w). The mean cumulative particle size was 0.120 μm and the suspension was physically stable when stored at room temperature up to 4 weeks.

The amorphous dispersion was produced by flash evaporation from an acetonitrile solution in a Buchi Rotovap. Polyvinylpyrrolidone (PVP, K-30) was the selected polymer with drug loadings of 20 and 40%. The dispersions were determined to be XRD amorphous following storage at 50 °C up to 3 weeks. Further, an extremely high drug load amorphous dispersion of 80/20 BMS-488043/PVP was found to remain amorphous after storage at 50 °C for 17 weeks. The two amorphous formulations and a single nanosuspension formula were compared to wet-milled crystalline drug capsule in a crossover beagle dog study. The two solid dispersions were dosed as 200 mg tablets with the nanosuspension administered via a standard gavage tube at the equivalent dose. The nanosuspension showed a 4.7 fold

increase in C_{max} and 4.6 fold increase in AUC over the capsule. The 20% amorphous dispersion showed an 18.2 and 7.0 fold increase in C_{max} and AUC respectively. The 40% dispersion showed a 15.7 fold increase in C_{max} and 8.7 fold increase in AUC. The authors concluded that the amorphous dispersions were the superior option for increased bioavailability of BMS-488043.

Zheng et al reported on the commercial development of LCQ789, a BCS Class II compound, investigated particle size reduction, amorphous dispersions, lipid based formulations and co-crystals [73]. LCQ789 is a crystalline, neutral compound with a molecular weight of 476.93 and a ClogP of 5.4 with extremely low solubility (<1 μg/ml). Each formulation method was carefully screened: co-crystal screening was performed with four solvents and 27 co-crystal formers, solid dispersion screening was conducted with seven polymers and a total of 64 variants, and lipid-based formulations were screened with 25 GRAS listed excipients. Particle size reduction on a research compound from the same scaffold at LCQ789 showed minimal impact on its oral bioavailability, as confirmed by GastroPlus™ and *in vivo* rat study. Consequently, the nanoparticle approach was not pursued for LCQ789.

Optimized formulations were compared in rat and dog single dose pharmacokinetic studies. Minimal exposure was observed with suspensions of crystalline LCQ789 and co-crystal formula in rats, but the co-crystal did show some improved exposure in dogs. In both species, significant improvement in bioavailability was achieved with the solid dispersion and lipid-based formulations. The *in vivo* pharmacokinetic studies indicated that the solid dispersion improved the oral bioavailability by 18-fold in rats and 50-fold in dogs, while the lipid-based formula increased the oral bioavailability by 25-fold in rats and 80-fold in dogs. The lipid-based formula achieved the highest exposure, and the solid dispersion demonstrated less inter-subject variability. These two formulas continued on to

dose escalation studies. Higher exposure was achieved with the lipid-based formula, but it also exhibited higher variability as compared to the solid dispersion. In addition, overall high organic content was a concern for the long-term safety studies. As a result, the solid dispersion formulation was selected for use in safety studies.

Vogt et al investigated micronization, co-grinding and spray-drying formulations of fenofibrate and compared their release profiles to German and French commercial products [74]. Micronization was conducted by jet milling while nanosizing was performed by bead milling. Co-grinding was achieved by particle size reduction with lactose, polyvinylpyrrolidone (PVP), sodium lauryl sulphate (SLS) and combinations of the three excipients. Spray dried particles were produced by bead milling with lactose and SLS in water, then fed directly into a Buchi Mini Spray Dryer. All formulations were compared by dissolution in biorelevant media. The fenofibrate drug products commercially available on the German and French markets dissolved similarly to crude or micronized fenofibrate and were slower than the co-ground and spray-dried formulas. The co-ground formulations had faster dissolution rates, but reached the same equilibrium concentration as the commercially available products. The spray-dried formula produced substantial initial supersaturation, but returned to concentrations only slightly better than equilibrium in 180 minutes because formulation did not contain a parachute component. This was termed as unstable by the authors, but they concluded that both co-grinding and spray-drying could potentially lead to better bioavailability of fenofibrate drug products.

Kwong et al reported that toxicity is one of the leading causes of attrition in the clinic, and that good safety margins are imperative to reach proof of concept in clinical studies [75]. Research was conducted to identify a conventional formulation that would provide the maximum exposure possible to define the dose limiting toxicity for a molecule referred to as compound 3. Compound 3 existed as a crystalline free base with poor

solubility in water (0.0002 mg/ml in water, 0.0003 mg/ml in SGF and 0.004 mg/ml in FaSSIF), but was highly permeable. Thus, drug dissolution was the rate limiting step for absorption.

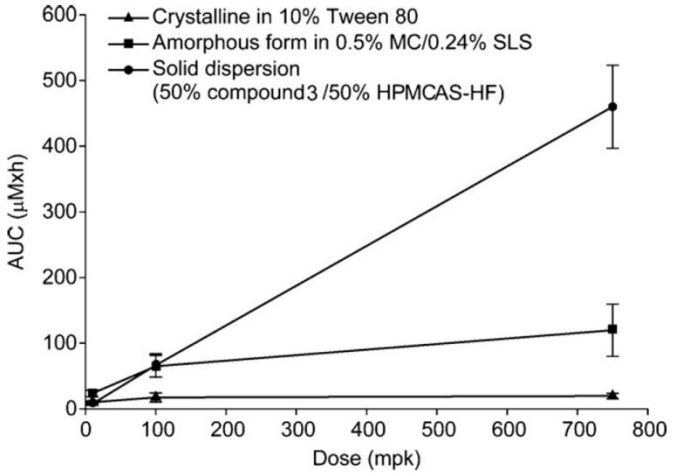

Figure 1.3: Dose proportionality of compound 3 in 10% Tween (-▲-) as the crystalline form; in 0.5% Methocel/0.24% SLS as the amorphous form (-■-) and in solid dispersion at 50% drug loading in HPMC-AS given as suspension in Methocel (-●-) from 10 mpk to 750 mpk dosed at 5 ml/kg in Sprague Dawley rats (n=4) [75] (corrected).

Various preparation methods and excipients were screened and the leading formulations were compared in a preclinical dose range finding study in rats. The three leading formulas were (1) crystalline form in 10% Tween 80, (2) amorphous form in 0.5% methylcellulose and 0.24% sodium lauryl sulfate and (3) a solid dispersion with 50% drug loading in HPMCAS-HF as seen in Figure 1.3. The particle size for compound 3 was not specifically mentioned; however, looking at another reported project within the article, the particle size is conservatively below 10 µm. At the lowest dose, 10 mpk, the exposure was similar for all three compounds. As the dose was increased to 100 mpk, the solubility of the crystalline phase limited the absorption of the compound and resulted in a lower exposure. It is interesting to note that the exposure obtained from the amorphous form is

comparable to the solid dispersion at this level. Finally, at 750 mpk the amorphous dispersion provided a significant increase in exposure over the other two formulations (4x AUC as compared to the crystalline phase).

Thombre et al compared amorphous, nanocrystalline and crystalline formulations of ziprasidone to commercially available Geodon® capsules in order to minimize food effect [76]. The three formulations in the study were (A) an amorphous inclusion complex of ziprasidone mesylate and a cyclodextrin, (B) a nanosuspension of crystalline ziprasidone free base made by wet-milling, and (C) jet-milled ziprasidone HCl coated crystals made by spray drying the drug with hypromellose acetate succinate. The pharmacokinetic studies in dogs showed that the three formulations performed differently. Formulation B yielded the best fasted state absorption enhancement, indicating that improved dissolution rate with a low potential for precipitation might be the best combination to improve ziprasidone absorption in the fasted state. The *in vivo* data for formulation B was highly variable, but the mean summary parameters were comparable to the control capsule dosed in the fed state.

Formulation A also showed increase absorption of ziprasidone in the fasted state compared to the commercial capsule. Because of the solubilization technology used, ziprasidone likely went quickly into solution and was absorbed (formulation A had the shortest observed T_{max}). But, the extent of absorption was less than the control capsule dosed in the fed state, indicating possible precipitation in intestinal pH media. *In vitro* testing demonstrated that some amorphous complex formulations can achieve high enough supersaturation to cause precipitation of a lower solubility drug form such as the free base. Formulation C did not show enhanced absorption in the fasted state compared to the commercial capsule control.

In humans, both formulations A and B showed improved absorption in the fasted state while formulation C did not [77]. Thus, the *in vivo* performance in dogs was qualitatively similar to the *in vivo* performance of these formulations in humans.

Sigfridsson et al compared crystalline and amorphous nanosuspensions to a solution of AZ68 [78]. AZ68 is a neurokinin NK receptor antagonist intended for schizophrenia treatment. The compound has high permeability and low solubility in the gastrointestinal track and thus fulfills the criteria for a BCS II compound. Crystalline nanosuspensions were prepared by bead milling; amorphous nanosuspensions were prepared by a solvent evaporation process and confirmed amorphous by XRPD (Powder X-ray Diffraction). Particle sizes for both suspensions were approximately 200 nm and both formulations were dosed in rats by gavage at similar concentrations. The results indicate that AZ68 is absorbed at a lower rate for crystalline nanosuspensions compared to amorphous nanosuspensions and solutions. However, the absorbed extent of the compound is similar.

1.5 MARKETED PRODUCTS

1.5.1 Nano-crystal Products

Perhaps the best way to understand the utility of a technology is to review its application in marketed products. Table 1.1 contains examples of current marketed products produced using nano-crystal technologies.

Trade Name	Generic Name	Processing Technology	Company	FDA Approval
Rapamune	Sirolimus	NanoCrystal	Pfizer (Wyeth)	2000
Emend	Aprepitant	NanoCrystal	Merck	2003
Tricor	Fenofibrate	NanoCrystal	Fournier Pharma (AbbVie)	2004
Triglide	Fenofibrate	IDD-P	Sciele Pharma, SkyePharma	2005
Megace ES	Megestrole acetate	NanoCrystal	PAR Pharmaceuticals	2005
Invega Sustenna	Paliperidone palmitate	NanoCrystal	Janssen	2009

Table 1.1: Examples of commercial nano crystal products [59]

The first commercial product using a pure nanoparticle technology was Rapamune®, a tablet formulation containing the immunosuppressant drug, sirolimus. It was originally marketed as an unpleasant tasting lipid based liquid solution that required cold storage and a dispensing protocol. Sirolimus is poorly water soluble (~2 μg/ml) and processed by NanoCrystal® technology into a fine nanoparticle dispersion with a mean particle size of <200 nm. The NanoCrystal Colloidal Dispersion® intermediate is then post processed into tablets of 1 mg, 2 mg and 5 mg. The tablets have increased bioavailability (~ 27%), do not require special storage conditions and have better patient compliance due to a more convenient dosage form [62, 79].

The second product, Emend®, is an antiemetic for the prevention of nausea and vomiting following chemotherapy and surgery. It is a spray coated capsule formulation of aprepitant that has been formulated as a nanosuspension. Aprepitant (water solubility 3-7

μg/ml) is a free base crystalline compound that was processed into a fine particle dispersion using a wet milling technology, and then processed into a solid dosage capsule formulation. The original dosage form showed significant food effect with exposures of 3-fold increase under fed conditions for a 100 mg dose. The food effect was significantly higher at a 300 mg dose [80]. The NanoCrystal® formulation was able to eliminate the food effect by increasing surface area 40 fold which resulted in a 4 fold increase in AUC values in the fasted state of beagle dogs. The elimination of the food effect for antiemetic drug is significant as the commercial success may have been limited if required to consume with food [62].

Tricor® is the successor product for fenofibrate (for hypercholesterolemia) after patent expiration. Triglide is also a fenofibrate nano-crystal product, but produced by the IDD-P® technology. Tricor® has a dose of 48 mg or 145 mg in a tablet form. The nano-crystal technology provided a life-cycle extension in the creation of a superior performing product. Fenofibrate showed 35% higher absorption in the fed state and significantly reduced the food effect [32].

Megace ES® (ES stands for enhanced solubility) is for the delivery of megestrol acetate, a synthetic progestin used to treat anorexia, cachexia and AIDS-related wasting. The commercial formulation is an aqueous nanosuspension. The dose is 625 mg/ 5 ml and the nanosuspension reduces bioavailability differences between fed and fasted conditions. It also has less administration volume than the previously given oral formulation (only ¼) while being less viscous [32].

The last approved nano-crystal product to be discussed is Janssen's INVEGA® SUSTENNA®. This product, an atypical antipsychotic, is a once monthly intramuscular extended release injectable dosage form of paliperidone palmitate. It is a liquid dispersion product in prefilled syringes that has physical stability without the need for special storage

conditions for a two year shelf life. This is a sterile product by way of conventional sterilization methods. Terminal heat is the preferred route, but filtration, gamma irradiation and aseptic approaches are employed as alternatives [81]. The particulate nature of the formulation allowed for sustained release and in a patient population where compliance is a concern, the once a month dosage is a valuable option [62].

1.5.2 Amorphous Dispersion Products

Table 1.2 contains examples of current marketed products produced using solid amorphous dispersion technologies.

Trade Name	Generic Name	Processing Technology	Company	FDA Approval
Cesamet	Nabilone	Solvent evaporation	Meda Pharmaceuticals	1985
Sporanox	Itraconazole	Fluid bed bead layering	Janssen	1992
Prograf	Tacrolimus	Spray drying	Astellas Pharma	1994
Kaletra	Lopinavir, ritonavir	Melt extrusion	AbbVie	2007
Intelence	Etravirin	Spray drying	Janssen	2008
Zortress	Everolimus	Spray drying	Novartis	2010
Norvir tablet	Ritonavir	Melt extrusion	AbbVie	2010
Onmel	Itraconazole	Melt extrusion	Merz Pharma	2010
Incivek	Telaprevir	Spray drying	Vertex	2011
Zelboraf	Vemurafenib	Solvent/anti-solvent precipitation	Roche	2011
Kalydeco	Ivacaftor	Spray drying	Vertex	2012

Table 1.2: Examples of current amorphous dispersion products [82] (modified).

The original solid oral formulation of Kaletra® was a soft-gelatin capsule (SGC) containing 133.3 mg of lopinavir (an HIV protease inhibitor) with 33.3 mg of ritonavir, with ritonavir acting as a bioavailability enhancer for lopinavir [83]. The SGC dosage form required refrigeration and the recommended adult dosage was 6 capsules daily with food to maximize the bioavailability of lopinavir. Toward the end of end of enhancing therapy

with Kaletra, the product was reformulated as a solid amorphous dispersion utilizing HME technology. The result was a 200/50 mg lopinavir/ritonavir tablet formulation that reduced the number of dosage units and eliminated the requirement for refrigeration. Compared with the SGC formulation, the HME formed tablet resulted in more consistent lopinavir and ritonavir exposures across meal conditions, which minimized the likelihood of extreme high or low blood plasma concentrations. In addition, the removal of the refrigeration requirement allowed for worldwide distribution into underdeveloped areas that could not support a cold distribution chain.

The path toward the development of ritonavir into a solid oral dosage form based on amorphous solid dispersion technology was very similar to that of Kaletra. Ritonavir was originally developed because it possesses anti-HIV activity, but it is no longer prescribed as a sole protease inhibitor in antiretroviral regimens today. However, as a pharmacokinetic enhancer, ritonavir has become a mainstay in the management of both treatment-naïve and treatment-experienced patients. The basis for this enhancement is the inhibition of cytochrome P-450 (CYP) metabolic pathways [84]. Inhibition of CYP 3A4 leads to a reduction in the metabolism of most protease inhibitors and increases pharmacokinetic properties including area-under-the-plasma concentration curve (AUC), maximum plasma concentration (C_{max}), and half-life ($t_{½}$). These enhancements allow for a reduction of pill burden, dosing frequency and food restrictions while maintaining efficacy.

Because ritonavir is not bioavailable in the crystalline solid state, it was formulated in ethanol/water based solutions. It was available as an oral solution in 1996 and as SGC since 1998. Only one crystal form of ritonavir was identified during development and the initial 240 lots of Norvir® capsules had no stability problems [85]. However, in mid-1998 several lots of capsules failed the dissolution requirement and investigation revealed a polymorph with greatly reduced solubility compared to the original crystal form. Within

weeks, this new polymorph (Form II) appeared throughout both the bulk drug and formulation areas. Since the manufacturing of Norvir® capsules required a certain concentration in the ethanol/water solutions, Form II made the formulation unproducible.

With the emergence and dominance of polymorph Form II, Abbott Laboratories reevaluated their manufacturing process [86]. They reported a new method to control the conversion of Form I to Form II by choosing an appropriate ratio of solvent to antisolvent in a reactor process. Following the HME formulation development for Kaletra® in 2005, Abbott began developing a 100 mg HME-based amorphous dispersion formula for ritonavir. In the bioequivalence studies, the HME tablet demonstrated equivalence with SGC for AUC parameters. However, the ritonavir tablet C_{max} was 26% higher than the SGC formulation [84]. This increase in C_{max} was not expected to alter the safety or pharmacokinetic enhancing profile of ritonavir. The tablet also exhibits less food effect than the SGC formulation.

Itraconazole is another interesting example of a drug product that was commercialized using an amorphous solid dispersion technology. The compound is a potent broad-spectrum triazole antifungal drug, is insoluble in water (solubility ~4 ng/ml) and was among the first marketed solid amorphous dispersion products. Itraconazole is so insoluble in intestinal fluids that drug therapy with the compound could not be achieved without substantial solubility enhancement by formulation intervention. The original solid oral formulation, Sporanox® Capsule, was produced by a fluid bed bead layering process that used a co-solvent system of dichloromethane and methanol to dissolve itraconazole and hydroxypropyl methylcellulose (HPMC) which was then sprayed on inert sugar spheres [87]. The resultant product provided a significant enhancement of itraconazole bioavailability with approximately 55% of the administered dose absorbed [88]. Itraconazole has recently been reformulated into a tablet composition that contains an

amorphous dispersion in HPMC 2910 by HME utilizing the MeltRx Technology®. The trade name is Onmel®; it is available in a 200 mg strength for once-daily administration and was approved by the FDA in April 2010 for the treatment of onychomycosis. The HME formulation not only eliminated the use of organic solvents in manufacturing, but also reduced dosing frequency from twice-daily to once daily [89].

Like itraconazole, Zelboraf™ is another compound for which the drug therapy was enabled by the application of amorphous solid dispersion technology. The product is a tablet dosage form containing an amorphous dispersion of vemurafenib in HPMCAS-LF produced by a solvent/anti-solvent precipitation called microprecipitated bulk powder (MBP) technology [90]. The process utilizes N,N-dimethylacetamide to dissolve the drug and the ionic polymer. The solution is precipitated into acidified aqueous media, the precipitates are then filtered, repeatedly washed to remove residual acid and solvent content, dried, and then milled to form the amorphous powder intermediate, MBP. The MBP product provides substantial enhancement of the solubility/ dissolution properties and oral bioavailability of vemurafenib with excellent physical stability. The stability of the amorphous dispersion is attributed to the high composite T_g, intermolecular interactions between the drug and polymer as well as the moisture protective effect provided by the polymer.

In initial Phase I clinical studies with a conventional formulation of vemurafenib, patients did not respond, i.e. no tumor regression, to doses as high as 1,600 mg [91]. The issue was identified as low oral bioavailability stemming from poor solubility, which caused a halt to the clinical study until it could be reformulated into a more bioavailable form. Due to melting point and organic solubility limitations, traditional amorphous solid dispersion processes could not be applied, therefore necessitating the application of the MBP technology. When clinical trials resumed with the new MBP-based formulation,

substantial tumor regression was achieved in a majority of patients as a result of the enhanced formulation [92]. The application of the MBP technology to vemurafenib is a compelling case study for the application of amorphous solid dispersion technology because formulation intervention was directly responsible for enabling the drug therapy and prolonging the lives of terminal patients suffering from metastatic melanoma.

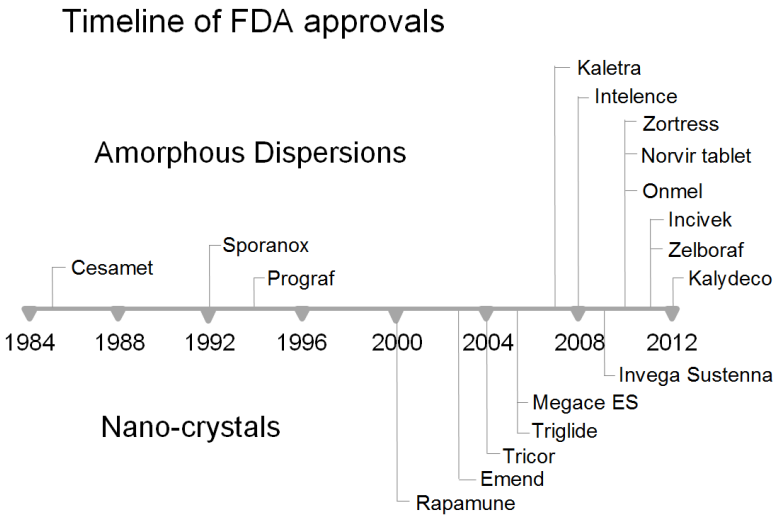

Figure 1.4: Timeline of FDA approved amorphous dispersion and nano-crystal products.

In concluding this section, viewing the nano-crystal and amorphous dispersion FDA approved products on a timeline might indicate a possible trend in the drug development industry (see Figure 1.4). From this analysis, it appears poorly water-soluble drug candidates were formulated for commercialization in the 1980s and 1990s using solid amorphous dispersion technologies. In the late 1990s it seems as if the industry turned to nano-crystalline technologies as the method of choice for development of BCS class II and IV active ingredients. However, from 2006 to 2012 only one nano-crystal product was approved by the FDA while 8 amorphous solid dispersion products were accepted.

Additionally, the last two FDA approved nano-crystal products were suspensions; the last one being an intramuscular injection product. This is a small sampling, but it looks like the current industry preference for solving water-solubility challenges for oral delivery is through the use of amorphous solid dispersion technologies.

1.6 CONCLUSION

Nano-crystal delivery forms and amorphous solid dispersions are well established techniques for addressing poor water solubility in pharmaceutical compounds, however, the methodologies are quite different. While several marketed products are made by both nano-crystal technologies and amorphous solid dispersion technologies, it appears there are more amorphous dispersion products on the U.S. market today. A timeline of FDA approved drugs suggests current industry preference for solving solubility challenges for oral delivery is leaning toward amorphous solid dispersion technologies.

Chapter 2

New Use of Polyvinyl Alcohol as a Solubility Enhancing Polymer for Poorly Water-soluble Drug Delivery (Part 1)

2.1 INTRODUCTION

Poor water solubility has been documented as a common characteristic for new chemical entities in development pipelines and commercially available products in the pharmaceutical industry today [2-4]. Among the options for dealing with poor solubility, the incorporation of the drug substance in a solid amorphous dispersion dosage form is gaining popularity. There are many reasons for this increase in popularity with only a few being mentioned here. First, conventional chemistry methods for solubility enhancement like salt formation reportedly only work for 20-30% of new molecules, leaving the 70-80% remaining to find other routes to improved solubility [11]. Second, solid dispersions containing solubility enhancing polymers can dramatically increase apparent solubility for durations sufficient to enable absorption form the intestinal lumen. Specifically, in the case of ITZ, solubility increases of 10,000 fold or more have been demonstrated [40-42]. Third, nano-crystal technologies have not proven as capable and industry trends show preference to solid dispersions [1]. Fourth, compared with other noncrystalline drug delivery approaches such as cosolvent systems or self-emulsifying drug delivery systems (SEDDS), amorphous solid dispersions are more amenable to be developed into tablets, which is the preferred solid dosage form for distribution, and amorphous dispersions demonstrate highly desirable advantages over liquid or semisolid formulations including lower manufacturing cost, smaller pill burden, and improved physical and chemical stability [57]. Finally, the various grades of polymers used for solid dispersions can not only increase solubility, but also allow for targeted release and the tailoring of release profiles of a drug substance. Thus, solving multiple problems simultaneously.

While numerous studies have been published on amorphous solid dispersions, there are a limited number of polymers suitable for creating those systems. Polymers that have been reported as a major component in solid dispersion formulations for improved solubility are as follows: povidone (PVP) [93], copovidone (PVPVA) [94], crospovidone (CrosPVP) [95], polyethyleneglycols (PEG) [96, 97], polymethacrylates [98, 99], hydroxypropylmethylcellulose or hypromellose (HPMC) [87, 89], hypromellose acetate succinate (HPMCAS) [100, 101], hypromellose phthalate (HPMCP) [102], hydroxyethylcellulose (HEC) [103], hydroxypropylcellulose (HPC) [104], polyvinyl acetate phthalate (PVAP) [42], cellulose acetate phthalate (CAP) [42], poloxamers [105], carbomers [106], and Soluplus® [107]. As additional polymers are identified as options, a broader range of challenging drug substances may be enabled for oral delivery systems. Furthermore, existing prohibitive intellectual property could be circumvented and unique release profiles could be created. Due to the high cost of development and regulatory compliance verification, repurposing an existing excipient would seem a financial and time efficient path.

Polyvinyl Alcohol (PVAL) is a water-soluble synthetic polymer represented by the formula $(C_2H_4O)_n$. The value of n for commercially available materials is between 500 and 5,000, which is roughly equivalent to a molecular weight range of 20,000 to 200,000 [108]. PVAL is unique among the vinyl polymers in the fact that the monomer, vinyl alcohol, cannot exist in the free form. So, it is manufactured by the polymerization of vinyl acetate and then converted by a hydrolysis (alcoholysis) process. Various grades based on extent of hydrolysis exists with unconverted fractions being polyvinyl acetate. Since EMD Millipore PVAL was used in this research, a brief explanation of their nomenclature is prudent. Each grade of PVAL has two groups of numbers separated by a dash. The first group of numbers represents the viscosity of the 4% aqueous solution at 20 °C as a relative

indication of the molar mass. The second group of numbers is the degree of hydrolysis of the polyvinyl acetate. For example, an 88 in the second group would represent 88% hydrolysis with 98% being considered a fully hydrolyzed grade. Thus, a 5-88 grade would have the viscosity of 5 mPa·s in a 4% aqueous solution at 20 °C with the polymer chain being approximately 88% PVAL and 12% polyvinyl acetate [109]. Table 2.1 contains additional properties.

Available molecular weights	14,000 – 205,000 g/mol for partially hydrolyzed grades; 16,000 – 195,000 for fully hydrolyzed grades.
Crystallite melting point (T_k)	180 – 240 °C
Glass transition temperature (T_g)	40 – 80 °C
Percent crystallinity	Varies; increases with percentage hydrolysis.
Solubility in water	Solutions can be prepared at any concentration. However, because viscosity rises rapidly with solids content, certain practical limits exist for processable solutions.
Solubility in organics	Insoluble in most organic solvents. Slightly soluble in ethanol, practically insoluble in acetone.
Temperature onset of degradation	Approximately 180 °C
Aqueous solution pH	(4% solution at room temperature) 5.0 – 6.5
Hygroscopicity	DVS measurements reveal below a relative humidity of 50%, the change in mass is less than 1%. At 90% relative humidity, mass changes of 8 – 17% depending upon polymer type.

Table 2.1: Properties of PVAL (EMD Millipore) [109]

PVAL is currently being used in a variety of pharmaceutical applications. It is used as a stabilizing agent for emulsions [110], in topical pharmaceutical [111] and ophthalmic formulations [112, 113]. It is used in artificial tears [114] and integrated into contact lenses for lubrication purposes [115]. Polyvinyl alcohol can be made into microspheres [116] and is used as an emulsifier in creating PLGA nanoparticles [117, 118]. It has also been used in sustained-release formulations for oral administration [119] and transdermal patches [120]. Oral toxicity has been evaluated and found safe even at high levels of consumption;

the no-observed-adverse-effect level (NOAEL) for rats in a 3 month study was 5,000 mg/kg body weight / day [121].

To the authors' knowledge, PVAL has not been reported as the polymeric carrier in binary amorphous solid dispersions [122]. A brief discussion of the limitations of conventional methods for creating amorphous dispersions provides insight to probable reasons for this. Solvent processes (e.g., like spray drying and precipitation approaches) require a drug/polymer solution prepared with a common solvent or co-solvents. PVAL is insoluble in most organic solvents and only slightly soluble in ethanol while typical pipeline drug molecules are only slightly soluble in more aggressive organic solvents. Even if suitable solvents were ascertained, the required concentration of polymer would render the solution too viscous for practical processing (like preventing flow through a small orifice needed for spray drying). Alternatively, the application of conventional fusion processes like hot melt extrusion (HME) and injection molding is limited due to the high melting point of PVAL and high viscosity of the resulting melt. These technologies are not suitable for processing thermally sensitive and viscous formulations, however KinetiSol® has been demonstrated in these applications [123]. KinetiSol® Dispersing is a novel fusion process that does not have torque limitations like HME and has been shown to create unique solid dispersions [71]. Through this enabling technology, solid amorphous dispersions containing PVAL as the primary polymer can now be evaluated.

The pH independence of PVAL presents some advantages in bioavailability enhancement. The dissolution of pharmaceutical excipients with pH dependent ionizing properties can be variable across the gastrointestinal pH range [124]. For example, dissolution rate and apparent solubility of weakly basic drugs in gastric pH and weakly acidic drugs in intestinal pH would be higher due to the ionization at those pH conditions [40, 41, 125]. Anionic and cationic polymers are prone to those same ionization effects,

which allows for differing dissolution rates across the gastrointestinal tract. This may become clinically significant for formulations utilizing ionic polymers in both inter-patient and intra-patient variation. The dissolution behavior of non-ionic polymers is expected to be the same across the gastrointestinal track, which should lower variability and provide a more predictable bioavailability improvement [126]. Anionic polymers, even with variation challenges, are still often chosen in formulation development due to their ability to improve solubility compared to non-ionic polymers [127]. Anionic polymers have been shown to increase dissolution rate and apparent solubility of both weakly basic and neutral drugs in amorphous dispersions due to polymer/drug interactions likely occurring between polymer functional groups and the drug substance [128]. The few non-ionic polymers used for solid dispersions, primarily HPMC, PVP and PVPVA, do not exhibit tunable ratios of hydrogen bond donors and receptors like HMPCAS and polymethacrylates. However, PVAL has a tunable density of hydrogen bond donating hydroxyl groups and hydrogen bond receptors along its polymer backbone while still having pH independent solubility. In theory, this would allow it to function strongly as a solubility enhancer like the anionic polymers, but also have the low variability of the non-ionic polymers.

It is hypothesized that the pH independent solubility along with tunable density of functional groups of PVAL would be ideal in the creation of solid dispersions especially for weakly basic drugs. While other groups have shown stability with semicrystalline polymers, PVAL will need be investigated to establish the polymer crystalline structure does not create nucleation sites for drug recrystallization during processing and storage [129]. As a first step in investigating that PVAL will function as a solubility enhancing polymer, ITZ was selected as the model drug to be formulated in various grades. Varying molecular weight grades with identical degree of hydrolysis were used to create solid dispersions to determine its effect on performance. Conversely, the best performing

molecular weight range of PVAL from the first group of formulations were selected in grades of changing degrees of hydrolysis. The best performing polymer grade would then be compared to commercially available ITZ products.

2.2 MATERIALS

Itraconazole was purchased from Hawkins, Inc. (Minneapolis, MN). All grades of EMD Millipore PVAL were donated by Merck Millipore. All other chemicals used in this study were ACS grade.

2.3 METHODS

2.3.1 KinetiSol® Dispersing (KSD)

All compositions for this study were produced by a lab scale, GMP pharmaceutical compounder designed and manufactured my DisperSol Technologies, L.L.C. (Georgetown, TX, USA). Prior to KSD processing, materials were weighed, placed into a polyethylene bag, manually shaken for approximately 1 minute, and charged into the compounder chamber. During processing, real time computer controls monitor various parameters and eject the material at a pre-set ejection temperature. Discharged material was immediately quenched in a cooling die under pressure in a pneumatic press. Cooled material was then milled in a FitzMill L1A and screened through a 60 mesh screen (250 μm). All further analyses was conducted on this powder.

2.3.2 Differential Scanning Calorimetry (DSC)

Modulated DSC analysis was conducted using a TA Instruments Model mQ20 DSC (New Castle, DE) equipped with a refrigerated cooling system and auto sampler. Samples were weighed to 5 - 10 mg in aluminum-crimped pans. Samples were heated at a ramp rate of 10 °C/min from 0 to 210 °C with a modulation temperature amplitude of 1.0 ºC and a modulation period of 60 seconds for all studies. Ultrahigh purity nitrogen was used as the purge gas at a flow rate of 50 mL/min. All data analyses were performed using TA Universal Analysis software. The thermogram for amorphous ITZ used in the DSC analysis

of the solid dispersions formulations was obtained on a second heating of crystalline ITZ following an initial heating to 200 ºC followed by rapid cooling (40 ºC/min) to 0 ºC.

2.3.3 Powder X-Ray Diffraction (XRD)

An Inel Equinox 100 X-ray diffractometer (INEL, Artenay, France) was used to detect the presence of ITZ crystallinity. Milled compositions, physical mixtures or unprocessed ITZ were loaded on a rotating aluminum sample holder and placed in the radiation chamber. The Equinox 100 utilizes Cu K Alpha radiation (λ = 1.5418 Å) with a curved radius detector to simultaneously measure a 2Θ range of 5 - 110°. Operating voltage and amperage were adjusted to 41 kV and 0.8 mA respectively and the scan time for each sample was 10 minutes.

2.3.4 Polarized Light Microscopy (PLM)

While XRD has been shown to have limits of detection of less than 1% [130], PLM can serve as a qualitative confirmation of XRD results. PLM analysis was conducted on a Meiji Techno MT 9300 Polarizing microscope with a first order red compensator. Pulverized samples were dusted on a glass slide and viewed under 400x magnification. The slide holder was rotated at least 90 degrees while being observed to detect any light refractions. Images were taken by an Infinity CMOS camera.

2.3.5 Size Exclusion Chromatography (SEC)

Molecular weights of PVAL in both processed and unprocessed samples were analyzed with a Dionex Ultimate 3000 H/UPLC system equipped with a Shodex (Showa Denko K.K., Japan) Refractive Index detector. Two Shodex Asahipak 7.6mm x 300mm (GF-7M HQ) columns were placed series and maintained at 40 °C. A 50nM LiCl aqueous solution was utilized at the mobile phase at a constant flow rate of 0.7 mL/min. Sample injection volumes were 100 µL [131].

2.3.6 Non-sink Dissolution Analysis

Non-sink dissolution analysis was conducted with a VK 7000 dissolution tester (Varian, Inc., Palo Alto, CA, USA) in accordance with USP XXXIV Method A for delayed release dosage form. Solid dispersions (n=3) were weighed to achieve an equivalent of 37.5 mg ITZ and placed in dissolution vessels containing 750 ml of 0.1 N HCl (~10x ITZ equilibrium solubility in acid) equilibrated to a temperature of 37.0 ± 1 °C with a paddle rotation of 50 rpm. After 2 hours, a buffer medium of 250 mL of 0.2M Na3PO4, preheated to 37.0 ± 1 °C, was added to the dissolution vessels to adjust the pH to 6.80 and reach 1000 mL in volume. Samples were taken at 1, 2, 2.25, 2.5, 3, 4 and 5 hours. Samples were immediately filtered using 0.2 μm PTFE membrane, 13 mm filters, diluted to a 1:1 ratio with mobile phase, mixed and then transferred into 1 mL vials for HPLC analysis.

2.3.7 High Performance Liquid Chromatography

The ITZ content in processed samples and dissolution aliquots were analyzed with a Dionex Ultimate 3000 H/UPLC system equipped with diode array detector extracting at 263 nm. The system was operated under isocratic conditions with a 70:30:0.05 acetonitrile:water:diethanolamine mobile phase equipped with a Phenomenex Luna 5 μm C18(2) 100 Å, 150 mm x 4.6 mm (Phenomenex, Torrance, CA) HPLC column. Dionex Chromeleon 7.2 software was used to analyze all chromatography data.

2.3.8 *In Vivo* Studies

In vivo studies were conducted at Charles River Laboratories (Wilmington, Massachusetts Facility) under NIH guidelines with IACUC approval. Male Sprague-Dawley rats equipped with a surgically-implanted jugular vein catheters to facilitate blood collection were prepared for the study. Animals were assigned to the study based on catheter patency and acceptable health as determined by a staff veterinarian and placed into

groups of four animals (See Table 2.2 for details). All animals were fasted overnight prior to dose administration and food was returned following the 4-hour post-dose blood collection. All dosage forms were milled to a fine powder and suspended in an aqueous dosing vehicle to insure accurate ITZ to rat body weight medicating.

Group No.	No. of Males	Treatment					
		Test Article	Dose Level (mg API/kg)	Dose Conc. (mg API/mL)	Dose Volume (mL/kg)	Dose Vehicle	Dose Route
1	4	KSD [ITZ:PVAL 4-88 (1:4)]	30	6	5	2% HPC/ 0.1% Tween 80/ pH 2.0	Oral gavage
2	4	Onmel™ tablets (pulverized)	30	6	5		

Table 2.2: Rat PK study design

Blood samples (0.25 mL; sodium heparin anticoagulant) were collected from the jugular vein catheter or by venipuncture of a tail vein if the catheter became blocked. Blood samples were collected from each animal at 2, 3, 3.5, 4, 5, 6, 8, 12, and 24 hours following oral dosing. All whole blood samples were placed on wet ice immediately after collection and were centrifuged at 2-8ºC to isolate plasma. The resulting plasma was transferred to individual polypropylene tubes and immediately placed on dry ice until storage at nominally -20°C before transfer to the Charles River's Bioanalytical Chemistry Department for concentration analysis.

Plasma samples were analyzed for itraconazole concentration using a proprietary in-house research grade LC-MS/MS Assay. Pharmacokinetic parameters were estimated from the plasma concentration-time data using standard noncompartmental methods and utilizing suitable analysis software (Watson 7.2 Bioanalytical LIMS, Thermo Electron Corp).

2.4 RESULTS AND DISCUSSION

2.4.1 Preliminary Evaluation of PVAL Molecular Weight

Due to the uniqueness of the KinetiSol® technology, screening methods do not exist to determine the processability of a new polymer. So, three viscosity grades representing a low (PVAL 4-88), medium (PVAL 26-88) and high (PVAL 40-88) with the same level of hydrolysis were selected with an arbitrary ITZ loading of 20%. Because of the feasibility nature of this study, KSD processing parameters were not optimized but considered acceptable if ITZ was rendered amorphous as determined by XRD and PLM analysis and drug assays were at least 96%. This was easily achieved for the 4-88 grade as the discharged material was a single agglomerated, semi-molten mass similar in character to other previously processed formulations. The 26-88 and 40-88 grades behaved differently in that the discharged material was a slightly densified powder. Variance in processing RPM or increases in discharge temperature would not render an agglomerated discharge which is typical of the KSD processes (preliminary results not reported). Other polymers with larger molecular weights have been used in previous research without incident [132]. Thus, this phenomena must be attributed to the specific sintering properties or crystalline nature of high viscosity grades of PVAL. The addition of 4-88 to 26-88 as a minor component allowed for an agglomerated discharge, however a 1:1 ratio of 4-88 to 40-88 was required to achieve the same result. For consistency, a 1:1 ratio of 4-88 to both 26-88 and 40-88 was chosen as the compositions to continue this portion of the study.

Size exclusion chromatography was performed on unprocessed polymer grades as controls and on the KSD processed compositions of ITZ with 4-88, 4-88:26-88 and 4-88:40-88. Comparison of unprocessed and KSD processed 4-88 is shown in Figure 2.1A while comparison of unprocessed, one-to-one physical mixture of 4-88 and 40-88 to the KSD process composition is shown in Figure 2.1B.

A

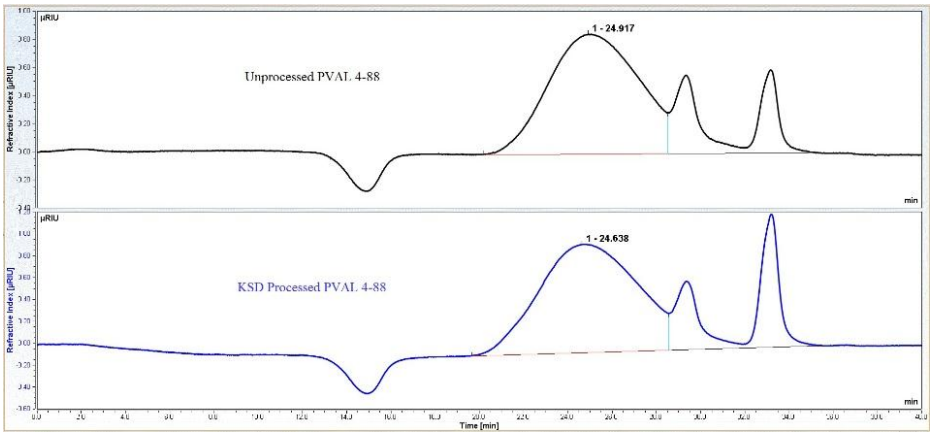

B

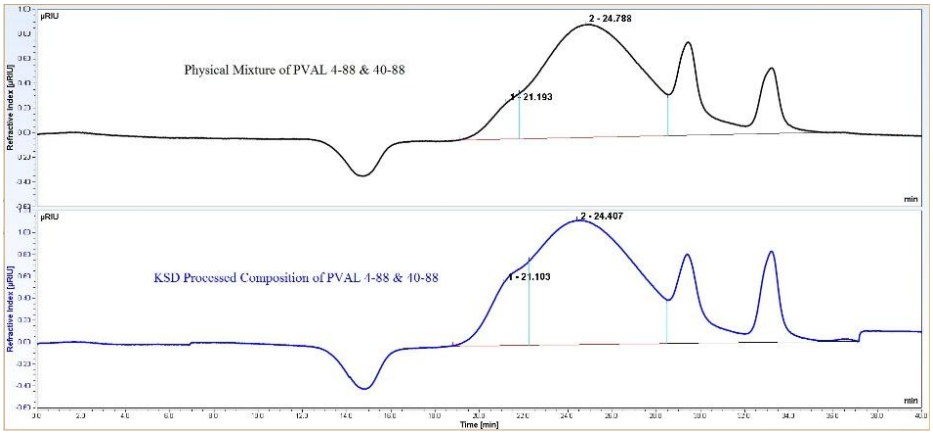

Figure 2.1: SEC profiles of unprocessed powders and processed compositions.

Peaks associated with polymer have been numbered, followed by the elution time (longer elution times signifies a smaller molecular weight). Each sample was analyzed in triplicate, and representative chromatograms are presented herein. Unprocessed 4-88 had a peak elution time of 24.917 minutes compared to the KSD processed 4-88 with a peak time of 24.638. The physical mixture of 4-88 and 40-88 exhibited a first polymer peak at 21.193 minutes, which corresponds with the 40-88 grade, and the second peak at 24.788, which is associated with the 4-88. The KSD composition showed elution times of the respective peaks at 21.103 and 24.407. The small difference in the times can be explained by sampling variance and it can be concluded that KSD processing did not change the

molecular weight of PVAL. However, it was noted that the KSD compositions always eluded at an earlier time compared to the corresponding unprocessed powder, which would indicate a slight increase in molecular weight. It is plausible that a portion of the solubilized ITZ remains bound on the polymer following dissolution of the sample in the diluent and while traversing the column, which would increase the apparent size of the polymer coil and manifest as an increase in molecular weight. The key result of this analysis is that there is no indication of a reduction in the molecular weight of the starting PVAL material after KSD processing.

Dissolution profiles of the three compositions were compared (data not shown). The ITZ:4-88 and ITZ:4-88:26-88 compositions performed similarly, but the ITZ:4-88:40-88 composition did not maintain ITZ supersaturation to the same extent following the pH change. With its ease of processing and good dissolution profile, the 4 mPa·s grade of PVAL was selected as the molecular weight to continue evaluation of the effect of degree of hydrolysis on polymer performance.

2.4.2 Solid-state Analysis

Various hydrolysis grades of the same viscosity were selected for comparison with 4-88, namely 4-38, 4-75 and 4-98. Polyvinyl alcohol is known to be a crystalline polymer and XRD profiles were generated for each polymer used in this study to determine the effect of molecular weight and degree of hydrolysis has on the crystallinity (see Figure 2.2). The XRD data matches the reported information in that crystallinity does appear to increase with degree of hydrolysis. The 4-38 grade, contains a greater component of polyvinyl acetate than PVAL, is the only grade that is XRD amorphous. All the other grades had a primary peak between 19 and 20 2-theta with two other easily distinguishable peaks between 22 and 23 and between 40 and 42 2-theta. The 26-88 and 40-88 grades

showed larger peak intensities than the 4-88 grade that might indicate increased crystallinity with molecular weight and would explain why these grades were more difficult to process at the selected conditions. The 4-98 grade, which is the only fully hydrolyzed grade, demonstrated the highest peak intensities of all the grades tested.

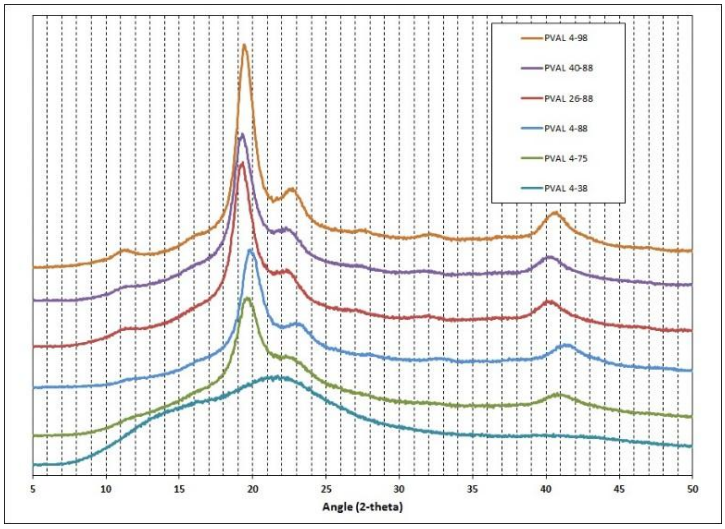

Figure 2.2: XRD profiles of PVAL grades used in study

XRD profiles were also generated for ITZ and the processed compositions as illustrated in Figure 2.3.

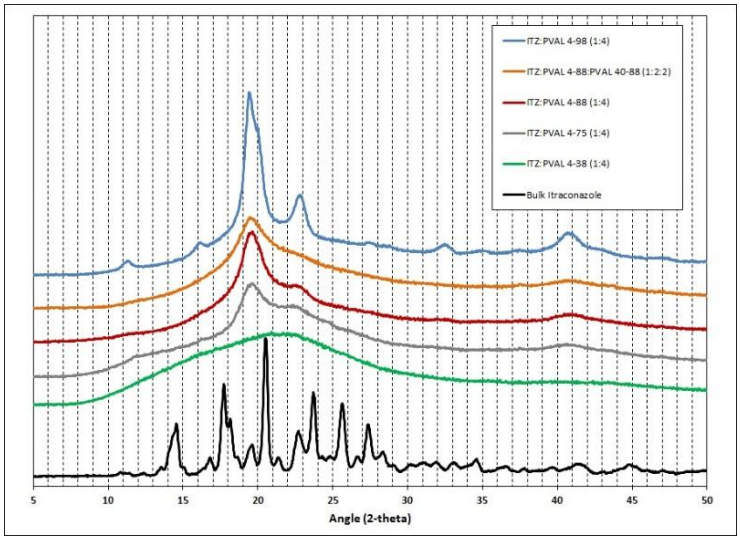

Figure 2.3: XRD profiles of ITZ and KSD compositions

For the 4-38, 4-75, 4-88 and 4-98 compositions, the profile demonstrates that the drug substance is amorphous while the polymers retain their crystalline structure. In the compositions with a one to one polymer ratio of low molecular weight with higher molecular weight (only the 4-88:40-88 profile is shown, but the 4-88:26-88 profile was identical), the major crystalline peak is visible, but with lower intensity. Other peaks are barely distinguishable. It appears that the combination of different molecular weights interact in such a way as to reduce the crystalline structure of the polymer portion of the composite.

mDSC analysis was conducted on the pure PVAL polymers to understand the thermal characteristic of each grade prior to analyzing the ITZ:PVAL KSD compositions. Considering that PVAL is a copolymer of polyvinyl acetate (PVAC) and PVAL one would expect to see by DSC analysis a T_g of the PVAC component and a melting endotherm of the crystalline PVAL component, the prominence of both being a function of the degree of hydrolysis. That is to say that with increasing degree of hydrolysis, the T_g of the PVAC component will be less pronounced and the melting endotherm of PVAL will be more distinct. Thus, a fully hydrolyzed grade would exhibit essentially no T_g associated with PVAC and a strong melting endotherm associated with PVAL. The DSC thermograms for the four 4 mPa·s grades of PVAL and their corresponding KSD compositions provided in Figure 2.4 (nonreversing heat flow) and Figure 2.5 (reversing heat flow) demonstrate this expected trend.

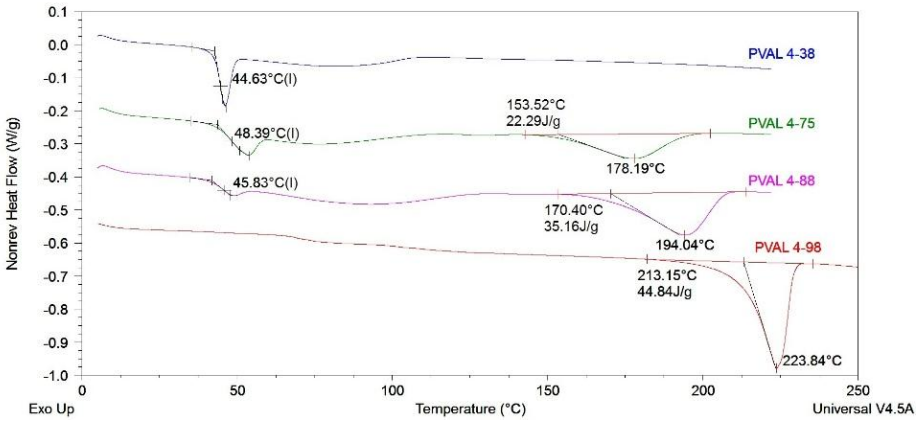

Figure 2.4: Nonreversing Heat Flow DSC thermograms for 4 mPa·s grades of PVAL

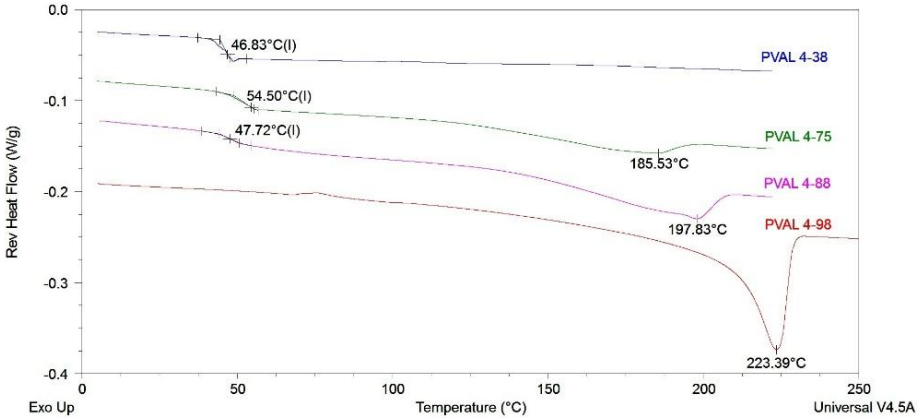

Figure 2.5: Reversing Heat Flow DSC thermograms for 4 mPa·s grades of PVAL

It is seen that the 4-38 grade, which is predominantly PVAC, exhibits a strong T_g associated with the PVAC component and no detectable melting endotherm for PVAL [133]. The amorphous nature of this grade as demonstrated by DSC is in agreement with the previously discussed XRD result. Hence, it is understood that below a critical degree of hydrolysis the PVAL component is unable to interact with itself to form crystallite structures due to the density of PVAC on the polymer chain. Examining the thermograms for the 4-75 and the 4-88 grades, the expected trend is seen in that the T_g becomes less noticeable and the melting endotherm becomes more pronounced with an increased T_m as

the degree of hydrolysis is increased: consistent with increasing crystalline content of the polymer. The thermal profile obtained for the 4-98 grade matches industry literature for fully hydrolyzed polyvinyl alcohol with a melting point around 223 °C. The reversing heat flow profile for PVAL 4-98 shows a slight thermal event around 70 °C which others have suggested was the T_g [134]. This event was much less prominent than the T_g events for 4-88, 4-75 and 4-38 as would be expected considering the low PVAC content and was not able to be accurately quantified by the analysis software. The DSC profile for the 4-98 grade corroborates the XRD result indicating high crystallinity of the fully hydrolyzed grade.

mDSC analysis was performed on the ITZ:PVAL KSD compositions to investigate the dispersed state of ITZ in each polymer grade and to evaluate the influence of the dispersed drug on the thermal properties of the polymers. Figure 2.6 contains the nonreversing heat flow thermograms for the KSD composition and ITZ while Figure 2.7 contains the reversing heat flow thermograms.

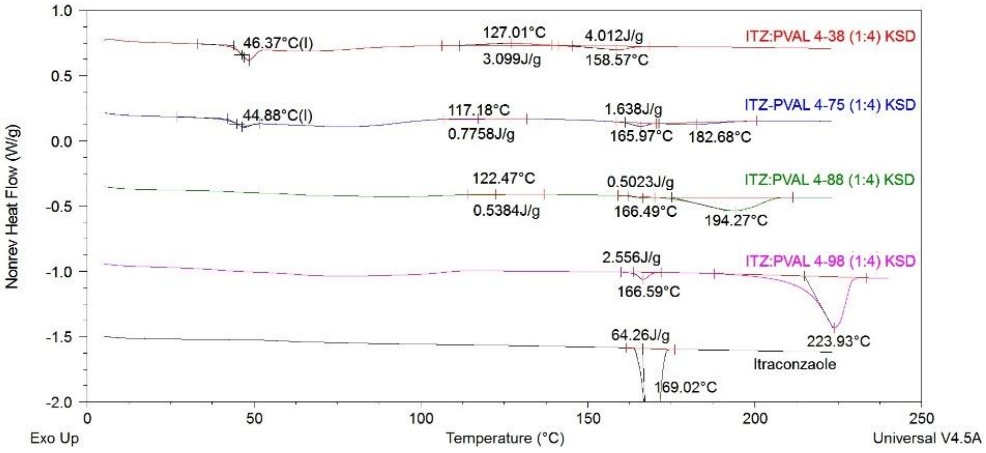

Figure 2.6: Nonreversing Heat Flow DSC thermograms for KSD compositions and ITZ

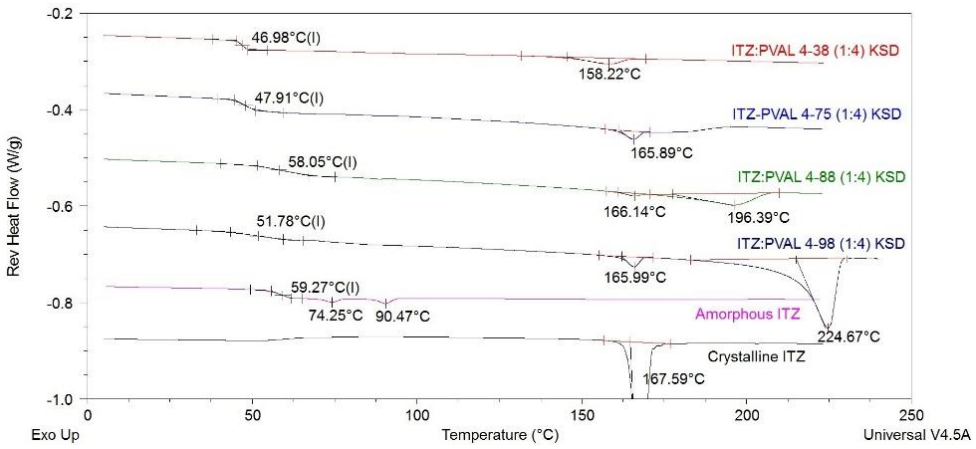

Figure 2.7: Reversing Heat Flow DSC thermograms for KSD compositions and ITZ

The nonreversing heat flow thermogram in Figure 2.6 shows a general trend of broadening and/or reduction in the magnitude of the glass transition event for the 4-38, 4-75 and 4-88 grades relative to the pure polymers. This could be attributed to dilution and/or anti-plasticizing effect of the dispersed ITZ phase. Consistent with the pure polymer, a T_g is not apparent for the KSD composition with the 4-98 grade. Also seen for each of the 4-38, 4-75 and 4-88 grades is an exothermic event indicative of ITZ crystallization with peak temperatures in the range of 117 – 127 °C. Interestingly, the magnitude of the exothermic event is inversely proportional to the degree of hydrolysis. This suggest that the physical stability of an ITZ amorphous dispersion in PVAL increases with increasing degree of hydrolysis. One possible explanation for this is that increasing the degree of hydrolysis increases the density of hydrogen bon donor sites on the polymer backbone that could interact with the hydrogen bond acceptor sites on ITZ to form a stable complex [86]. Another possible explanation is that the amphiphilic character of the polymer that stems from the ratio of hydrophilic PVAL-to-hydrophobic PVAC units approaches an optimum with regard to stabilizing interactions with ITZ as the percent hydrolysis is increased up to 88%.

When the degree of hydrolysis is low, as with the 4-38 grade, the dispersed ITZ phase would interact largely with the PVAC component which contains only hydrogen bond acceptor sites (assuming hydrogen bonding is forming the complex). Therefore, in this phase, the amorphous dispersion is stabilized by weaker intermolecular forces like Van der Waals forces. If the stable complex is formed by hydrophilic/hydrophobic microenvironments, then the fewer hydroxyl groups of the 4-38 grade would provide fewer areas for interaction. In either case, these weaker intermolecular forces are more easily disrupted by thermal perturbations; hence, post-T_g phase separation of amorphous ITZ and subsequent crystallization during the temperature ramp is observed to a greater extent with reduced degree of hydrolysis [135]. This is corroborated by the result for the fully hydrolyzed grade in which a crystallization exotherm was not detected.

Figure 2.6 also shows that for all KSD processed compositions, a minor ITZ endotherm was detected. For the KSD compositions with PVAL 4-38, 4-75 and 4-88, this endotherm is similar in magnitude to the crystallization exotherm, which suggest that the ITZ melting event is related entirely to ITZ that crystallized during the DSC scan. This result validates the findings of XRD in which no crystalline ITZ was detected. In the case of the 4-98 grade, where no crystallization exotherm was detected, the ITZ melting endotherm is likely due to residual crystalline ITZ remaining after processing. This could be due to incomplete dispersion of ITZ in the polymer on processing resulting from the highly crystalline nature and/or the high T_m of the PVAL 4-98 grade. It could also be the result of amorphous ITZ being forced out of its interaction with the polymer as the highly crystalline grade returned to its preferred crystalline orientation on quenching. This result appears to contradict the XRD analysis; however, considering its small magnitude, the melting endotherm represents a small fraction of the dispersed ITZ, the crystalline peaks of which could be easily masked by the high intensity peaks of PVAL 4-98.

Finally, it is interesting to note in Figure 2.6 the melting endotherms for the PVAL 4-75 and 4-88 are significantly reduced in comparison to the pure polymer; beyond what would be expected for a 20% dilution on the addition of ITZ. This suggests that the dispersed ITZ phase disrupts crystallization of PVAL upon cooling due to drug/polymer interactions. A similar melting endotherm, in terms of magnitude, between the pure polymer and the KSD composition for the 4-98 grade seems to suggest incomplete disruption of polymer crystallinity on processing and/or displacement of ITZ during the quenching process. Considering this, it seems that a sufficient fraction of PVAC on the polymer is required to disrupt PVAL crystallite structure to facilitate a molten transition by KSD processing and achieve a homogenous dispersion of the drug substance [136]. Additionally, PVAC units interspersed on the polymer backbone may act as defects within the PVAL crystallite structure that effectively make available sites for drug/polymer interactions [97]. However, one would expect to see a point of diminishing returns for increasing PVAC concentration as this would also lead to weaker drug/polymer interactions. From Figure 2.6, it would appear that this optimum PVAL:PVAC ratio for ITZ is near that of the 4-88 grade.

The reversing heat flow shown in Figure 2.7 shows similar trends to those of the nonreversing heat flow analysis, however with better resolution of the glass transition events. Specifically, the T_gs of the KSD compositions with the 4-88 and 4-98 grades are able to be resolved by reversing heat flow analysis and have respective midpoint values of 58.05 °C and 51.78 °C. Also provided in Figure 2.7 is a thermogram for pure amorphous ITZ which shows a T_g of 59 °C followed by two endothermic events at 74 °C and 90 °C that have been identified as mesophases of glassy itraconazole [137]. In comparing all of the KSD compositions in the figure, the 4-88 grade has the highest composite T_g. The T_g is more than 10 °C higher (roughly 20%) than KSD compositions with 4-38 and 4-75

grades as well as the pure 4-88 polymer and is close to the T_g of pure amorphous itraconazole. The anti-plasticizing effect of amorphous ITZ on the 4-88 grade indicates strong positive drug-polymer interactions [138]; most likely due to hydrogen bonding between the acceptor sites on ITZ and the donor sites on PVAL. The increased T_g relative to the other PVAL grades seems to also support the previously discussed hypothesis regarding an optimal ratio of PVAC to PVAL at which hydrogen bonding or hydrophilic/hydrophobic locations are maximized. From these results, it can be concluded that 4-88 is the best performer of the PVAL grades tested from a thermodynamic standpoint.

2.4.3 Non-sink, Gastric Transfer Dissolution Analysis

As discussed previously, PVAL is an interesting new carrier polymer in the area of supersaturating amorphous solid dispersions owing to its non-ionic nature and the high density of hydrogen bond donor sites on the polymer chain. These attributes make it a particularly attractive concentration enhancing carrier for weakly basic drugs which have been shown to interact strongly with anionic carrier polymers to yield substantial improvements in apparent solubility [40]. To investigate the concentration enhancing effects of PVAL on ITZ, the dissolution properties of the four KSD compositions were evaluated by a non-sink, gastric transfer dissolution method. The results of this analysis are presented in Figures 2.8 and 2.9.

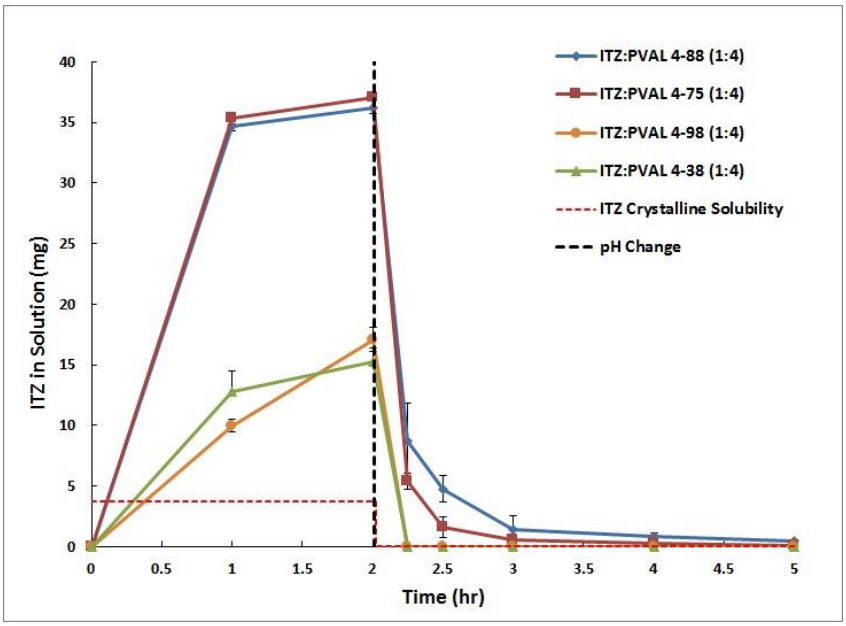

Figure 2.8: Dissolution Profiles for 4 mPa·s grades KSD compositions

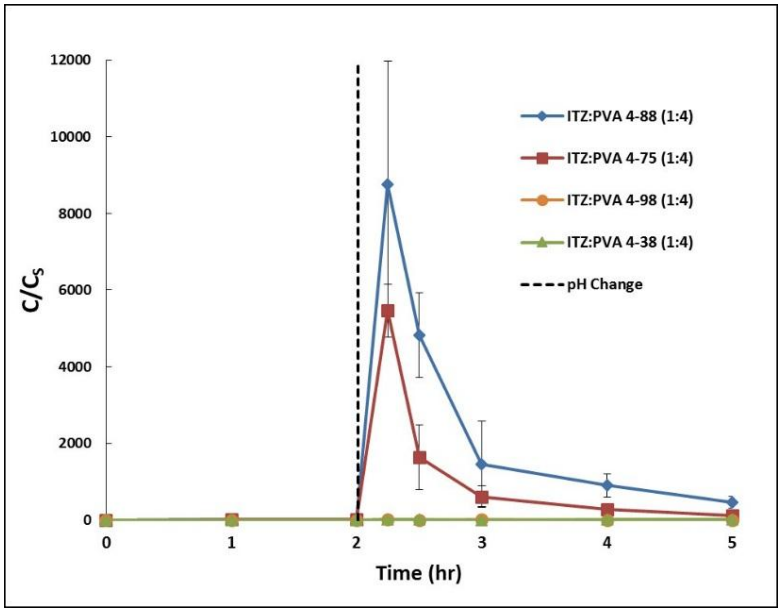

Figure 2.9: Dissolution Profiles for 4 mPa·s grades KSD compositions presented as concentration (C) relative to the saturation concentration (C_s) of ITZ at the respective pH.

Both the 4-75 and 4-88 compositions achieved complete drug dissolution before the pH change at 2 hours, while the 4-38 and 4-98 grades did not. Polyvinyl acetate is not

water soluble, which would explain why 4-38 did not go into solution like the higher hydrolyzed grades. Owing to its highly crystalline nature, the 4-98 grade dissolves at a very slow rate under the dissolution conditions of this study; hence, ITZ release from this composition is slow and incomplete. After the pH change, the 4-88 grade provided superior concentration enhancing effect presumably due to the greater PVAL content on the polymer and increased probability of ITZ interaction with the polymer in solution. The 4-38 and the 4-98 grades provided essentially no concentration enhancing effect due to the low concentration of dissolved polymer in the dissolution medium. Contrasting the dissolution AUCs after the pH change, gives a rank order of 4-88 > 4-75 > 4-98 > 4-38 with respective values of 640 ± 89, 442 ± 23, 130 ± 9 and 115 ± 8 mg·min. By way of comparison, DiNunzio *et al.* reported a post pH change dissolution AUC for Sporanox® capsules of 226 ± 23 mg·min [42]. In Figure 2.9, these dissolution results are presented in terms of concentration at each time point (C) relative to the saturation concentration (C_S) of ITZ at the respective pH. It should be noted that the C_S for ITZ decreases dramatically from 5 μg/ml to 1 ng/mL when the pH of the media is changed from 1.2 to 6.8 [5]. When plotted in this manner, the extent of supersaturation enabled by PVAL 4-88 at neutral pH becomes quite evident with solution concentrations nearly 9,000 times the saturation concentration of ITZ. These results therefore demonstrate that PVAL is an effective concentration enhancing polymer for ITZ and support the hypothesis that hydrogen bond donor sites are the key points of interaction with weakly basic compounds that provide stabilization/prolongation of aqueous supersaturation.

2.4.4 *In Vivo* Study

From solid state and dissolution evaluation of PVAL grades with varying degrees of hydrolysis, PVAL 4-88 emerged as the top performing polymer. In order to investigate

the effect of this polymer on the oral absorption of ITZ from an amorphous dispersion, the pharmacokinetics (PK) following oral administration to a rat model of this binary composition were comparatively evaluated against the commercially available ITZ product, Onmel™. The plasma concentration versus time profiles generated from this study are shown in Figure 2.10 while the key pharmacokinetic parameters as calculated by non-compartmental analysis are provided in Table 2.3 with the addition of previously obtained results for Sporanox®. Table 2.3 contains the plasma drug concentration $AUC_{(0\text{-last})}$, $AUC_{(0\text{-}\infty)}$, C_{max} and T_{max}.

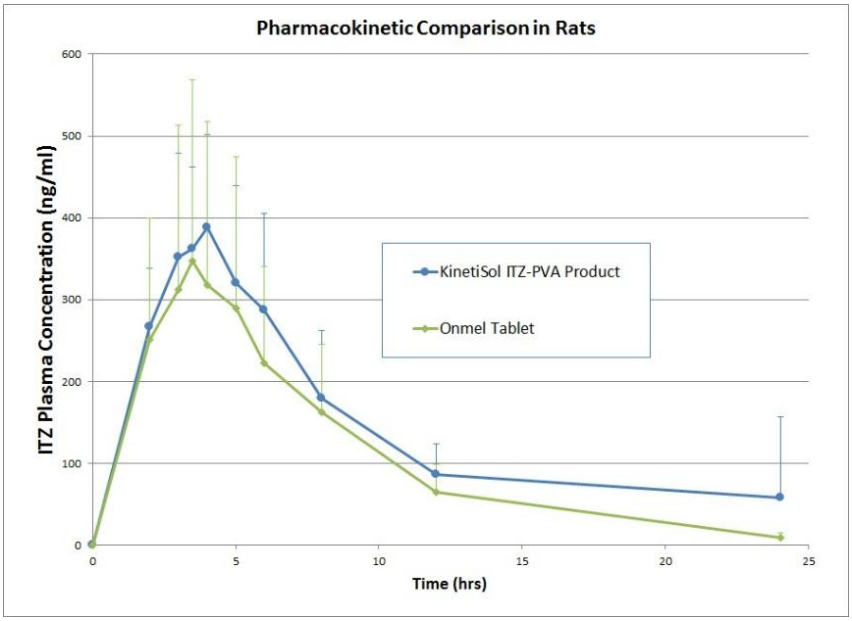

Figure 2.10: Rat PK of PVAL 4-88 compositions compared with Onmel™.

	$AUC_{(0\text{-}last)}$ (hr·ng/mL)	$AUC_{(0\text{-}\infty)}$ (hr·ng/mL)	C_{max} (ng/mL)	T_{max} (hr)
ITZ:PVAL 4-88 (1:4)	3,315 ± 1336	3,595 ± 1662	391 ± 111	3.88 ± 0.25
Onmel™	2,565 ± 1374	2,624 ± 1391	367 ± 202	3.50 ± 1.22
Sporanox® (From [42])	2,132 ± 1273		359 ± 261	5.5 ± 2.3

Table 2.3: Rat PK mean calculations

The mean AUC and C_{max} for the PVAL 4-88 composition was greater than that of Onmel™ and Sporanox®. However, it is noted that the drug loading of the ITZ:HPMC dispersion in the Onmel™ tablet is double that of the PVAL 4-88 composition. Similarly, the nonpareil beads in the Sporanox® composition are coated with a 40% w/w itraconazole and 60% w/w HPMC solid dispersion [139]. Therefore, the contrast with commercial products is not a true apple-to-apple comparison. Further studies will evaluate PVAL compositions at 40% w/w loading to have a more comparable result. Yet, considering the exploratory nature of this study, the analogous *in-vivo* performance of this first generation PVAL composition to commercial products is noteworthy.

2.5 CONCLUSION

This feasibility study has demonstrated that PVAL's pH independent solubility along with tunable density of functional groups allow it to function as a concentration enhancing polymer, effectively increasing the apparent solubility of poorly water soluble drug, itraconazole. The KinetiSol® technology enables the use of PVAL as the primary carrier for amorphous solid dispersion compositions. Solid-state and non-sink dissolution analysis revealed that the 88% hydrolyzed grade of PVAL was optimal for the ITZ compositions. Pharmacokinetic analysis in a rat model demonstrated that the ITZ/PVAL 4-88 composition yielded exposures that were possibly superior to Sporanox® and Onmel™.

Future research with ITZ will evaluate the effect of molecular weight in the range between the 4-88 and 26-88 PVAL grades tested in this study on dissolution performance. It will also explore increased drug loading levels, and evaluate storage stability. Additional separate studies are planned to determine the broad application of PVAL evaluating amorphous dispersions with neutral and weakly acidic drug substances. This supplementary information would offer a foundation for development scientists, who are looking for new options in formulating challenging drug substances, to have confidence in exploring polyvinyl alcohol.

Chapter 3

New Use of Polyvinyl Alcohol as a Solubility Enhancing Polymer for Poorly Water-soluble Drug Delivery (Part 2)

3.1 INTRODUCTION

One of the current challenges facing the pharmaceutical industry is addressing the increasing presence of poorly water soluble drugs in commercial products and development pipelines [2-4]. Using amorphous solid dispersions for oral delivery as a method to solve these challenges has increased in popularity in both commercial products and industry literature [1, 140-142]. For research purposes, itraconazole is often used as a model drug for concentration enhancement due to its aqueous solubility of approximately 1 ng/ml at neutral pH and approximately 4 μg/ml at 1.2 pH [41, 143, 144]. ITZ has been formulated in various polymeric carriers including hydroxypropylmethylcellulose (HPMC) [87, 89], copovidone (PVPVA) [94], polyethyleneglycols (PEG) [97], polymethacrylates [145], hypromellose acetate succinate (HPMCAS) [146], hypromellose phthalate (HPMCP) [41], Soluplus® [147], polyvinyl acetate phthalate (PVAP) and cellulose acetate phthalate (CAP) [42].

The KinetiSol® Dispersing (KSD) technology is a thermal process than can create solid amorphous systems from challenging drugs and very highly viscous polymers [71]. Utilizing this technology in our previous study, a broad range of molecular weights and degrees of hydrolysis of polyvinyl alcohol (PVAL) were investigated as a primary carrier in amorphous solid dispersion systems and for their solubility/bioavailability enhancing effect on itraconazole. EMD Millipore's PVAL was utilized in both studies and the nomenclature for describing different polymer grades is X-Y. X represents the viscosity (in mPa·s) of the 4% aqueous solution at 20 °C, which is a relative indication of the molar mass and Y is the degree of hydrolysis of the polyvinyl acetate. An examination of the

effects of molecular weight were conducted using PVAL 4-88, 26-88 and 40-88 with the 4-88 grade performing the best both from a KinetiSol® processing and dissolution enhancement point of view. Subsequently, 4-38, 4-75, 4-88 and 4-98 grades of PVAL were tested to ascertain the effect of the degree of hydrolysis for dissolution performance of ITZ. PVAL 4-38 did not fully release due to the fact that polyvinyl acetate, the predominant component of the grade, is less water soluble than PVAL. PVAL 4-98 also did not fully release due to the highly crystalline nature of the fully hydrolyzed grade which swelled in the aqueous environment, but did not completely dissolve. Both PVAL 4-75 and 4-88 released fully in the acidic portion of the dissolution test, but after the pH change to the neutral media the 4-88 grade provided best maintenance of supersaturated drug concentrations.

Research conducted on various molecular weights of HPMC on the dissolution performance of ITZ show that higher molecular weights are more efficient stabilizers of drug supersaturation after the pH change from the acidic gastric condition to the neutral intestinal environment [41, 132]. Similar to HPMC, PVAL has a wide spectrum of molecular mass from low to high viscosity ranges and it is anticipated that it will have an effect on the performance of the amorphous dispersion. Previous experimentation of PVAL 26-88 and 40-88 showed that these grades are excessively viscous as to pose processing challenges, which resulted in uneven drug distribution within the polymer. However, there are several grades between 4-88 and 26-88, namely 5-88, 8-88, 18-88 and 23-88, which could be investigated to determine if molecular weight effects post pH change dissolution performance. The current research comparatively evaluated the PVAL grades within a processable viscosity range (4-88 to 18-88) for their effect on the properties of amorphous dispersions of ITZ prepared by KSD.

Rendering a drug amorphous within a semi-crystalline polymeric carrier does raise concerns for the long term storage stability of the formulation [148-150]. Since the drug thermodynamically prefers the crystalline state, the polymeric carrier must prevent this occurrence through steric hindrance or molecular interaction. The concern of semi-crystalline polymers is that structured molecular geometry either allows for the formation of polymer rich and drug rich domains or that the crystalline geometry negatively influences the unstable amorphous drug. This is due to the stronger polymer-polymer interactions with semi-crystalline polymers (compared to amorphous ones) and hence the drug must compete with the polymer itself for binding sites on the formation and on the storage of the dispersion. PVAL does have at least one advantage over other semi-crystalline polymers like polyethylene glycol (PEG) in that it does have a higher T_g and T_m, which results in lower molecular mobility at temperature ranges associated with physical stability.

PVAL is known for providing solution stabilization as it is used in the pharmaceutical industry both as a stabilizing agent for emulsions [110] and as an emulsifier in creating PLGA nanoparticles [117, 118]. The previous research illustrated in both *in vivo* and *in vitro* studies PVAL's ability to increase free drug concentrations, and consequently oral absorption of the small molecule, itraconazole. Because of this performance, it is hypothesized that an in solution interaction exists between ITZ and PVAL and can be characterized. In an attempt to determine the mechanism of interaction that allows this apparent solubility increase, the current study employed the analytical tools of Fourier transform infrared spectroscopy (FTIR) and dissolution-ordered spectroscopy (DOSY).

3.2 MATERIALS

Itraconazole was purchased from Neuland Laboratories Limited (India). All grades of PVAL (EMD Millipore) were donated by Merck Millipore. All other chemicals used in this study were ACS grade

3.3 METHODS

3.3.1 KinetiSol® Dispersing (KSD)

Compositions for this study were produced by a lab scale, GMP pharmaceutical compounder designed and manufactured by DisperSol Technologies, L.L.C. (Georgetown, TX, USA). Prior to KSD processing, materials were weighed, dispensed into a polyethylene bag, manually shaken for approximately 1 minute, and charged into the compounder chamber. During processing, computer controls monitor processing parameters in real time and eject the material at a pre-set ejection temperature. Discharged material was immediately quenched in a cooling die under pressure in a pneumatic press. Cooled material was then cryomilled in a SPEX 6870 Freezer/Mill, with a 2 cycle run of 5 minutes each at 10 cycles per second after a 3 minute cool time and 2 minute timer between cycles. All further analyses was conducted on this powder.

3.3.2 Powder X-Ray Diffraction (XRD)

An Inel Equinox 100 X-ray diffractometer (INEL, Artenay, France) was used to detect the presence of ITZ crystallinity. Milled compositions, physical mixtures and unprocessed, pure ITZ were individually loaded on a rotating aluminum sample holder and placed in the radiation chamber. The Equinox 100 utilizes Cu K Alpha radiation (λ = 1.5418 Å) with a curved radius detector to simultaneously measure a 2θ range of 5 - 110°. Operating voltage and amperage were adjusted to 41 kV and 0.8 mA respectively and the scan time for each sample was 10 minutes.

3.3.3 Polarized Light Microscopy (PLM)

PLM analysis was conducted on a Meiji Techno MT 9300 polarizing light microscope with a first order red compensator. Pulverized samples were dusted on a glass slide and viewed under 400x magnification. The slide holder was rotated at least 90 degrees while being observed to detect any light refractions.

3.3.4 High Performance Liquid Chromatography (HPLC)

The ITZ content in processed samples and dissolution aliquots were analyzed with a Dionex Ultimate 3000 H/UPLC system equipped with diode array detector extracting at 263 nm. The system was operated under isocratic conditions with a 70:30:0.05 acetonitrile:water:diethanolamine mobile phase at a flow rate of 1.0 mL/min. The column used for analysis was a Phenomenex Luna 5 μm C18(2) 100 Å, 150 mm x 4.6 mm (Phenomenex, Torrance, CA, USA) HPLC column. Dionex Chromeleon 7.2 software was used to analyze all chromatography data.

3.3.5 Non-Sink Dissolution Analysis

Non-sink dissolution analysis was conducted with a VK 7000 dissolution tester (Varian, Inc., Palo Alto, CA, USA) configured as Apparatus 2. The test was performed similar to USP XXXVII (38) dissolution for delayed release dosage forms. Solid dispersions (n=3) were weighed to achieve a mass equivalent to 37.5 mg ITZ and dispensed in dissolution vessels on the surface of 750 ml of 0.1 N HCl (~10x ITZ equilibrium solubility in acid) equilibrated to a temperature of 37.0 ± 1 °C with a paddle rotation of 50 rpm. After 2 hours, a buffer medium of 250 mL of 0.2M Na_3PO_4, preheated to 37.0 ± 1 °C, was added to the dissolution vessels to adjust the pH to 6.80.

Drug content in solution was directly measured with a fiber optic Spectra™ instrument (Pion Inc., Billerica, MA, USA) fitted with 5 mm path length Pion Probes.

Readings were recorded every 5 minutes over the entire duration. Additionally, samples were taken at 2:00, 2:05, 2:10, 2:15, 2:30, 3:00, 3:30, 4:00 and 5:00 hours. Samples were immediately filtered using 0.2 μm PVDF with GMF membrane, 13 mm filters, diluted at a 1:1 ratio with mobile phase, mixed and then transferred into 1.5 mL vials for HPLC analysis. Pion data was correlated to match HPLC results by selecting appropriate 2nd derivative parameters.

3.3.6 Precipitation Inhibition Analysis

Solid dispersions (n=3) were weighed to achieve an equivalent of 37.5 mg ITZ and placed in suitable vessels containing 750 ml of 0.1 N HCl (to match concentrations in non-sink dissolution studies) that had been equilibrated to a temperature of 37.0 ± 1 °C. Containers were placed on stirring tables and agitated vigorously for several hours until solutions became clear. Media was then transferred to dissolution vessels within a VK 7000 dissolution tester (Varian, Inc., Palo Alto, CA, USA) configured as Apparatus 2 with a paddle rotation of 50 rpm. A buffer medium of 250 mL of 0.2M Na_3PO_4, preheated to 37.0 ± 1 °C, was added to the dissolution vessels to adjust the pH to 6.80. Samples were taken immediately before pH change, then after the pH change at 5, 10, 15, 30, 60, 90, 120, and 180 minutes. Samples were immediately filtered using 0.2 μm PVDF with GMF membrane, 13 mm filters, diluted to a 1:1 ratio with mobile phase, mixed and then transferred into 1.5 mL vials for HPLC analysis.

3.3.7 Fourier Transform Infrared Spectroscopy (FTIR)

Samples were tested in a Thermo Scientific Nicolet iS50 FT-IR Spectrometer (Thermo Electron Scientific Instruments LLC, Madison, WI, USA) with the Omni-Sampler module for attenuated total reflectance (ATR). The scan range was 2000 – 700

wavenumber (cm^{-1}) at a resolution of 4 cm^{-1} for 32 scans per sample. Data collection and analysis were performed with OMNIC™.

3.3.8 Diffusion-Ordered Spectroscopy (DOSY)

Amorphous dispersions and PVAL were dissolved in deuterated solutions of 0.1N DCl prepared by diluting concentrated DCL with D_2O. Samples were tested in a Varian VNMRS 600MHz nuclear magnetic resonance (NMR) spectrometer (Palo Alto, CA, USA) for solution with a *Doneshot* pulse sequence. The spectra was adjusted until water at 25 °C was 19.02 x 10^{-10} and all data generated is correlated to that reference. Figures were generated using Varian VNMRJ software.

3.4 Results and Discussion

3.4.1 Evaluation of PVAL Molecular Weight

To be consistent with our previous study, a drug loading of 20% ITZ was selected for the preparation of amorphous dispersions with PVAL grades of 4-88, 5-88, 8-88 and 18-88. All acceptable KSD compositions were verified to be amorphous by XRD and PLM, and HPLC analysis was conducted to establish dispersion potencies (data not shown). For dissolution testing, the samples were weight adjusted according to potency to achieve an equivalent amount of ITZ in each vessel. Figure 3.1 contains the dissolution curves of the listed PVAL grades for the 2 hour pH change dissolution method. Error bars are not shown due to data density making them indistinguishable.

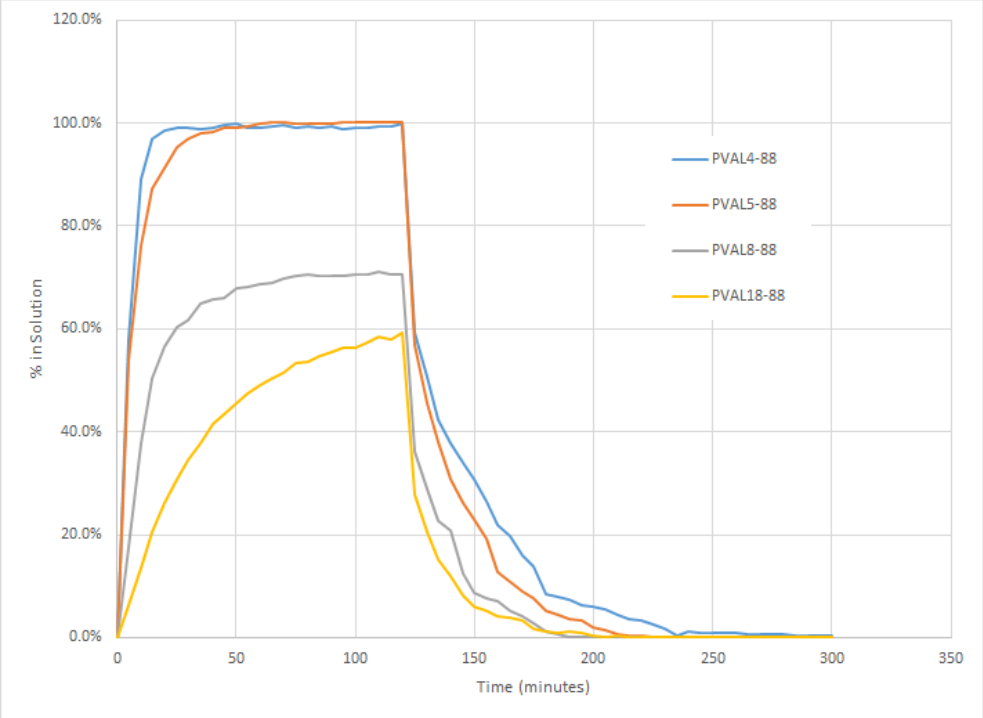

Figure 3.1: Dissolution profiles of 20% ITZ in PVAL 4-88, 5-88, 8-88 and 18-88.

Both PVAL 4-88 and 5-88 grades fully released ITZ at supersaturated levels with little variance between the two in the acid phase. PVAL 8-88 and 18-88 were not able to

achieve complete release, which was observed during the test with powder appearing at the bottom of the dissolution vessels after approximately an hour. After the pH change the precipitation inhibition performance followed the reverse order of molecular weights: 4-88 > 5-88 > 8-88 > 18-88.

Prior to the pH change, 8-88 had only reached 70% of drug in solution and 18-88 had only attained 60%. It was speculated that if these two grades could achieve 100% drug release the rank order of performance might change. An alternative dissolution study using the same amorphous dispersions, called precipitation inhibition analysis, was conducted which forced complete drug release from all polymer grades prior to the pH change with the results exhibited in Figure 3.2.

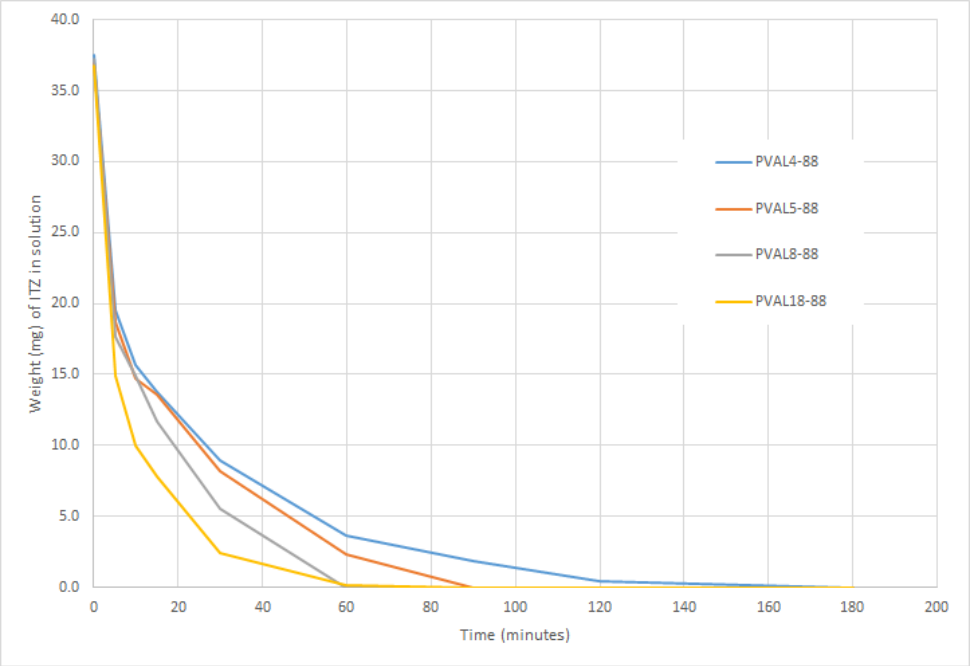

Figure 3.2: Precipitation inhibition curves of 20% ITZ in PVAL 4-88, 5-88, 8-88 and 18-88.

Even with the formulations at the same starting point, the lower molecular weights outperformed the larger ones in reducing the rate of drug precipitation. These results match

the previous study where PVAL 4-88 provided better performance than combinations containing the 26-88 and 40-88 grades. Thus, contrary to the trends observed with HPMC, for PVAL the lower molecular weights have superior dissolution performance over higher molecular weights.

This trend is confirmed by comparing the rates of dissolution for the polymers themselves in water. Product literature shows that lower molecular weights of the -88 grades have faster dissolution rates specifically in the temperature range between 20 and 40 °C [109]. Additionally, as shown in that same product literature, PVAL reduces interfacial tension, particularly the surface tension of water with respect to air, with differing effects according to molecular weight as seen in Figure 24. That figure specifically compares PVAL grades 40-88, 18-88, 8-88 and 4-88 for reduction in water surface tension. The rank order of greatest surface tension reduction to lowest is 4-88 > 8-88 > 18-88 > 40-88. Thus, the lower molecular weights have a greater reduction in surface tension of water.

Since amorphous dispersion powders were dispensed on the surface of the media in the vessels for the non-sink dissolution test, the lower surface tension and faster dissolution rate of the lower molecular weight grades would speak to the faster dissolution rate of ITZ. The effect on water surface tension indicates that lower molecular weight grades effectively function as a polymeric surfactant more than higher molecular weights. This would support the results for the precipitation inhibition analysis where the lower molecular weights were more effective in reducing the rate of drug precipitation.

3.4.2 Drug Loading Evaluation

All dissolution studies from the current and previous research have been conducted with 20% drug loading. It is noted that the drug loading of ITZ:HPMC in the commercial

product Onmel™ and the coating for the nonpareil beads in Sporanox® which is also ITZ in HPMC are both 40% [139]. Typically, the higher the drug load, the lower the dissolution performance because the ratio of drug to polymer decreases and solubility enhancement trends with increasing polymer concentration [151]. However, if higher drug loading can be achieved, the size of the dosage form can be reduced, typically improving patient convenience and compliance. Hence, optimal drug loading is a balance between performance and size of the final dosage form.

To investigate the effect of drug loading on dissolution performance, amorphous dispersions of ITZ in PVAL 4-88 were produced at 10, 20, 30, 40 and 50% drug loads. HPLC analysis measured actual potencies and samples were weight adjusted to ensure 37.5 mg of drug were contained in each dissolution vessel. The result from the non-sink dissolution test is found in Figure 3.3.

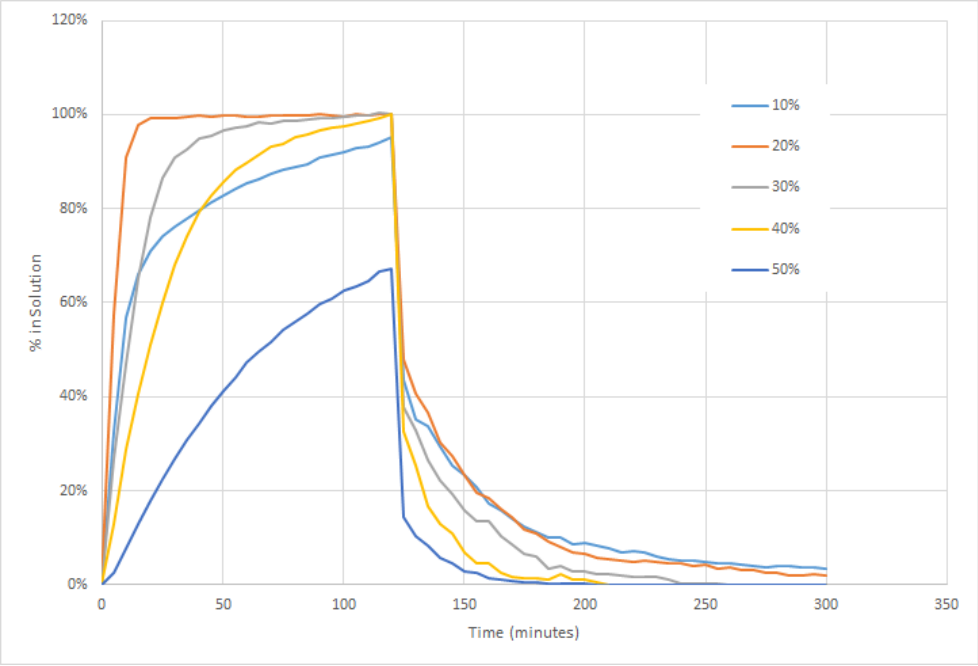

Figure 3.3: Dissolution comparison of different ITZ loadings in PVAL 4-88.

The rank order from highest dissolution performance in acid is as follows: 20% > 30% > 40% > 10% > 50%. Surprisingly, the 10% dispersion did not have the highest rate of dissolution. It exhibited a faster initial rate than 30% and 40%, but slowed after the initial 20 minutes to perform only better than the 50% loading. Only the 10% and 50% drug loading did not achieve 100% drug release within the two hour window of the acid portion of the experiment.

Toward the end of the 2 hour acid phase of the dissolution test, powder was visible at the bottom of the vessel of the 50% composition. All other vessels were clear at the bottom, however there was still powder floating at the top of the vessel of the 10% drug load sample. Keeping the relative amounts in perspective can provide probable explanations for this behavior. The 10% drug loading has a theoretical weight of 375 mg, the 20% drug loading has 187.5 mg weight on down to the 50% drug loading only having 75 mg of total amorphous intermediate powder. The 187.5 mg of 20% ITZ loaded powder floated on top (like all other samples) initially, then within a few minutes dispersed into the vessel and was dissolved within 20 minutes. Both the 30% and 40% loaded samples followed the same pattern, but with longer timeframes. In the case of the 10% ITZ dispersion, the time for the floating material to disperse within the aqueous environment and then dissolve was so prolonged that a very small amount of powder remained on the top surface at the end of the 2 hour acid phase. Visually, it was only a fraction of the initial 375 mg amount but it is unclear as to whether it could account for all of the undissolved amount of ITZ.

Results from the previous study and product literature show that increasing polymer crystallinity reduces polymer solubility and dissolution rate. The lowest drug loading at 10% would have the highest allowance for the formation, in some regions, for the preferred crystalline configuration which would slow dissolution and negatively affect solubility.

With the more crystalline configuration, ITZ could be entombed in highly crystalline regions which would account for the incomplete release and the more sustained drug solubility after the pH change due to higher polymer concentrations. Increasing drug load would decrease polymer crystallinity and allow for the faster dissolution for the 20% sample. However, increasing the drug loading also increases the hydrophobicity of the dispersion resulting in slower wetting and dissolution as seen with the 30% and 40%. The 50% dispersion would have the lowest polymer crystallization, but also the most reduced wetting and diminished release rate due to low polymer concentration.

After the pH change the rank order follows as was expected with 10% > 20% > 30% > 40% > 50%. 10% ITZ did start at a lower concentration than the 20%, but had higher actual amounts of drug in solution at 180 minutes which was an hour after the pH change. The 20% ITZ composition had the fastest dissolution rate and reduced the rate of precipitation at a similar level to the 10% composition. The 30% loading was a close second to 20% in the acid phase dissolution and exhibited a rate of precipitation only slightly lower than both the 10% and 20% compositions. Since, optimal drug loading is a balance between performance and size of the final dosage form, the 30% loading is probably closer to the optimal drug loading than all the other drug loadings tested.

3.4.3 Evaluation of the ITZ/PVAL Interaction

Because the ITZ is amorphous in the solid dispersion, it is not surprising to see apparent solubility levels much higher than the crystalline equilibrium solubility. However, without the aid of a solubility enhancing/stabilizing polymer, the thermodynamically unstable supersaturation would soon return to the crystalline equilibrium solubility. Especially, as the aqueous environment transitions from the acid gastric environment to the pH neutral environment of the intestinal tract, a weakly basic

drug like ITZ would return to solubility equilibrium quite rapidly [132]. Dissolution profiles contained in this and the previous study report concentration levels as high as 8,000 times the saturation concentration in neutral media and maintaining at least 4,000 times the saturation concentration for 30 minutes after the pH change. These results suggest an attractive interaction between the ITZ and PVAL.

FTIR-ATR has been reported as an analytical tool to investigate such possible interactions [53, 152, 153]. Peaks in the spectra can be associated with specific atomic bonding and shifting or changing shape can indicate molecular interactions. Figure 3.4 contains the FTIR spectra of amorphous itraconazole, preprocessed PVAL 4-88 and amorphous solid dispersions of 10% and 20% ITZ loading in PVAL 4-88.

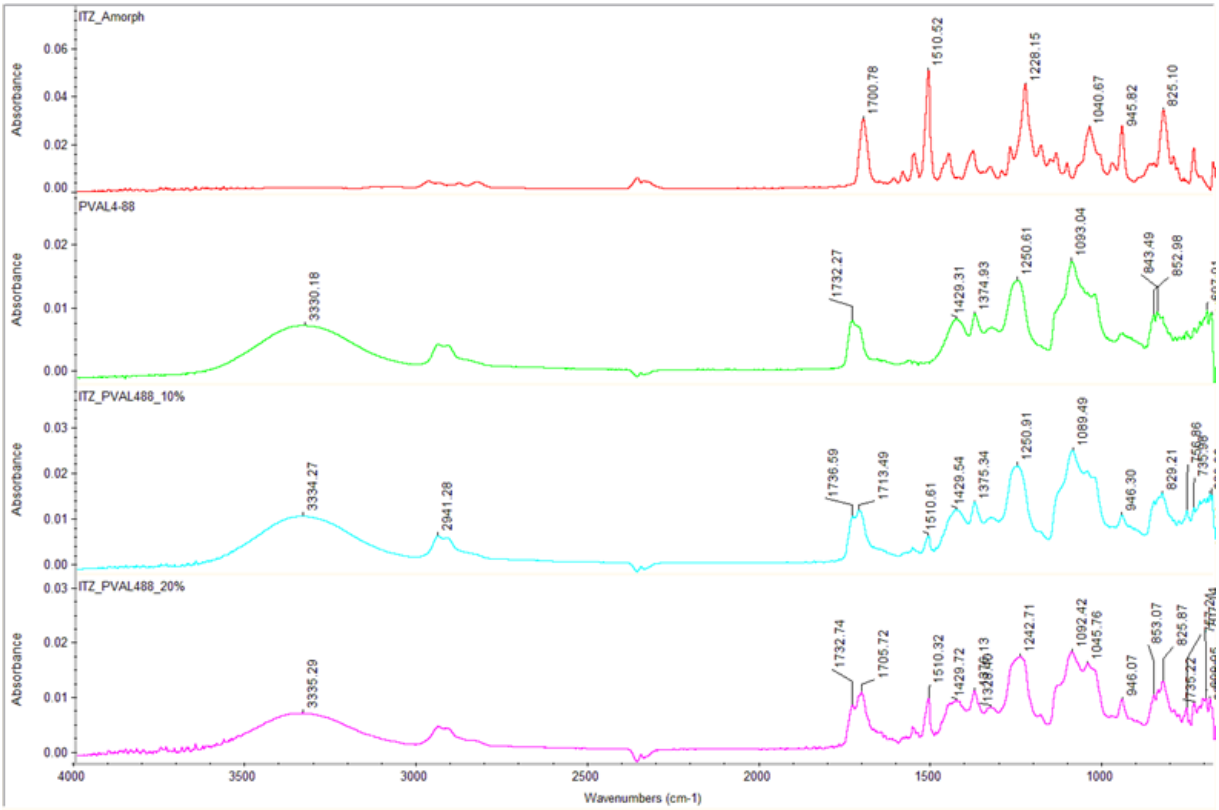

Figure 3.4: FTIR-ATR spectra of amorphous ITZ, PVAL 4-88, and amorphous dispersions.

The result for ITZ is similar to published literature [154, 155] and the PVAL result is consistent with product literature [109]. For PVAL, the broad peak at 3330 cm^{-1} is associated with O-H stretching, the small peak at 2941 cm^{-1} with C-H stretching, the 1732 cm^{-1} peak with C=O groups (from unhydrolyzed ester groups), the peak at 1429 cm^{-1} with CH_2 bending, the 1251 cm^{-1} peak with the C-O-C groups (also from unhydrolyzed ester groups) and, finally, the 1093 cm^{-1} peak is associated with C-O stretch and O-H bending. For ITZ, the first major peak at 1700 cm^{-1} is associated with C=O stretching, the 1511 cm^{-1} peak is related with $CO\text{-}NH_2$, and the 946 cm^{-1} linked with C-Cl. Most peaks do not show any difference between the individual components and the amorphous dispersions. Yet, the broad peak associated with O-H stretching on PVAL showed a shift from 3330 cm^{-1} to 3334 and 3335 cm^{-1} on the 10% and 20% ITZ loading in PVAL 4-88 respectively. The ITZ peak at 1700 cm^{-1} that correlates to C=O stretching, shows a change of 1713 and 1706 cm^{-1} for the same respective 10% and 20% ITZ loaded amorphous dispersions. As mentioned previously, the 10% amorphous dispersion will exhibit a higher degree of polymer crystal formation than the 20% load, which might explain the larger shift for the lower drug load. While it does appear that hydrogen bonding might be occurring, the magnitude of the shifts advocates that interactions, more than just hydrogen bonding alone, would account for the storage stability of the amorphous dispersion.

Diffusion-ordered spectroscopy (DOSY) or sometimes called diffusion-ordered NMR spectroscopy and diffusion-ordered correlation spectroscopy has been used to determine the drug complexation with cyclodextrins [156], drug release from a hydrogel matrix [157], identification of fake formulations of commercial products [158], and to see the interactions of polymers and drugs in solution [159]. DOSY is a measure of diffusion and can distinguish different components in a formulation by the rate of diffusion and location on the spectra. Small molecules have a faster diffusion rate than large polymers

and will have a different measurement of diffusion unless they are strongly bound by a covalent, ionic or hydrogen bond, which would give them the same measurement of diffusion as they act as single entity. Figure 3.5 has the DOSY map for PVAL 4-88 only and for the 20% drug loading in PVAL4-88.

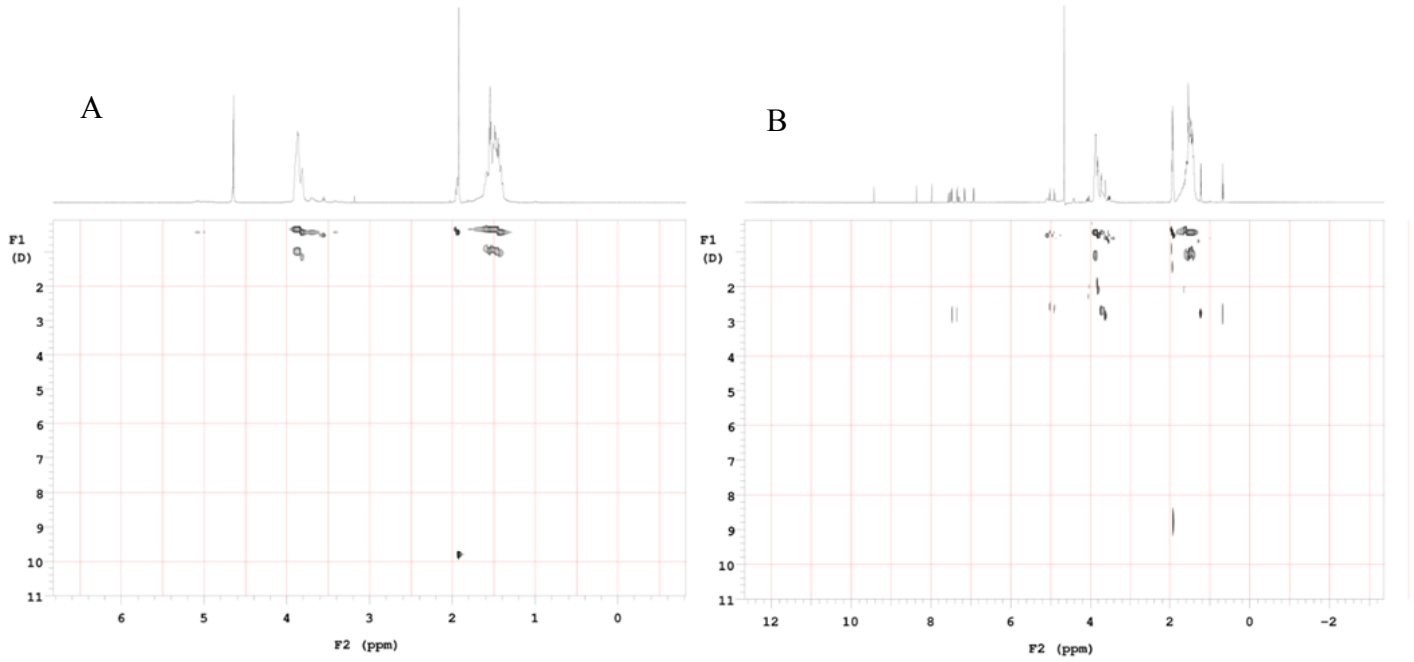

Figure 3.5: DOSY maps of (A) PVAL 4-88 and (B) 20% ITZ in PVAL 4-88 amorphous dispersion.

The Y or F1 axis is the measurement of diffusion or how well the molecules travel within the solution with lower numbers at the top representing slower diffusion and increasing with the numbers to reach the highest diffusion rates at the bottom. The X or F2 axis helps track any chemical shift from the top spectra. Figure 3.5A is a map of pure PVAL 4-88 that has not been processed. It is interesting to note that the polymer has two different diffusion coefficients, with the first band around 0.4 and the second one around

1.0 on the F1 axis. Product literature speaks specifically about PVAL's propensity toward complex formation in the presence of certain acids or salts [109]. Since the solution is 0.1N DCl, it is possible to have PVAL form a bimolecular complex. Additionally, in the discussion regarding PVAL reduction of water surface tension, it was mentioned that PVAL 4-88's greater effect on surface tension would allow it to function with surfactant-like properties, which would allow for molecules to self-associate in solution. Thus, it appears that the two different diffusion coefficients is formed by some molecules going into solution in groups and other by themselves. Whatever the actual cause is for the grouping phenomena, it appears that acetate groups on the PVAL molecular chain play a part because the spectra associated with acetate (around 2 on the F2 axis) is only observed in the slower diffusion group. Also on Figure 3.5A is an area that is around 10 on the F1 axis and around 2 on the F2 axis; this charts the residual acetyl groups within the bulk polymer.

Figure 3.5B is a map of the amorphous dispersion containing 20% ITZ in PVAL4-88. At the top, again, is the two different diffusion coefficients of the PVAL 4-88. Around 3 on the F1 axis is the spectra of itraconazole, which illustrates a different measurement of diffusion for the drug than the polymer. This illustrates clearly that the drug is not tightly bound to the polymer by strong intermolecular interactions. If there is any hydrogen bonding, the drug/polymer association would have to be flexible enough to allow ITZ movement along PVAL to account for the different rates of diffusion. Ideally, a third DOSY map of only ITZ in solution would be very useful to see if the interaction of the polymer changes the diffusion for the drug to illustrate a practical interaction between the two, but, unfortunately, the concentration of ITZ in solution was below the limit of detection for this analytical test. There is an area around 2 on the F1 axis that lies between the diffusion of PVAL 4-88 and ITZ that could possibly be a slower measured diffusion

for ITZ that would indicate an interaction. However, it could also be a software interpretation error due to peaks of both PVAL 4-88 and ITZ both occurring in that area. Thus, the key conclusion that can be drawn from these results is that the concentration enhancing effect of PVAL on ITZ is likely the result of weak intermolecular interactions, such as van der Waals forces/hydrophobic interactions, as it appears that strong intermolecular interactions between ITZ and PVAL do not occur in solution. This conclusion is supported by other research efforts that have looked at amorphous dispersions of ITZ with various polymeric carriers and concluded that hydrogen bonding was not the mechanism of action in solution between the drug and polymer [42, 132].

3.4.4 Evaluation of Stability

One of the main concerns to be addressed when creating amorphous dispersions is the stability of the matrix to prevent the drug from returning to its crystalline state within the delivery form before dosage [54, 57, 160]. Physical stability of the drug substance can be achieved through kinetic stabilization or freezing the amorphous drug within the polymeric carrier. This can be achieved by having a T_g of the composite matrix 50 °C above ambient storage conditions [52]. It can also be achieved by thermodynamic stability which is attained by molecular interactions that provide stability [56]. Many amorphous dispersions are formulated in a metastable region where the mode of stabilization is a combination of both kinetic and thermodynamic mechanisms [57]. Drug loading also influences stability because as loading is increased, at some point miscibility is exceeded and then drug molecule proximity within the polymer matrix becomes critical. Stability tends to decrease because recrystallization becomes more probable as drug molecules are increasingly found in close proximately to other drug molecules.

The drug loading portion of the current study concluded that 30% ITZ in PVAL 4-88 is probably closer to the optimal drug loading than all the other drug loadings tested. A container (without desiccant) containing milled amorphous intermediate powder of 30% ITZ was stored at ambient conditions for 30 months. A new sample that was identical in

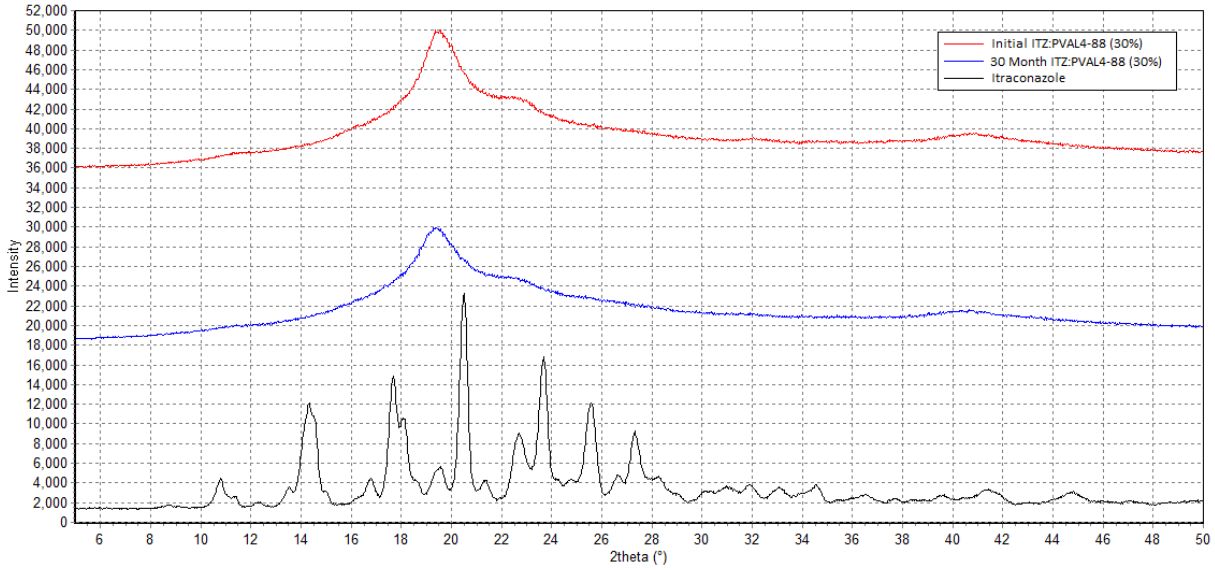

Figure 3.6: XRD profiles of ITZ, initial and 30 month old amorphous dispersions.

Both the initial and 30 month XRD profiles contain no peaks that correspond with ITZ indicating that both are substantially amorphous. The major broad peak in the amorphous dispersions at approximately 19 2-theta and minor peaks at approximately 23 and 41 2-theta are related to the crystallinity of the PVAL 4-88. No visual crystal structures were observed in either samples by PLM. Since it is possible to have crystals below the limit of detection of XRD and PLM, a dissolution study was conducted to confirm the dissolution performance of the amorphous compositions. These results are presented in Figure 3.7. As stated in the methods section, the first 120 minutes of the dissolution was

performed in 0.1 N HCL after which a buffer is added to change to a neutral pH. Thus, in the acidic environment full release of ITZ is realized after which the pH change resulted in precipitation of ITZ. Since only two dissolution profiles are compared in this figure, error bars were included to show the significance of any variation.

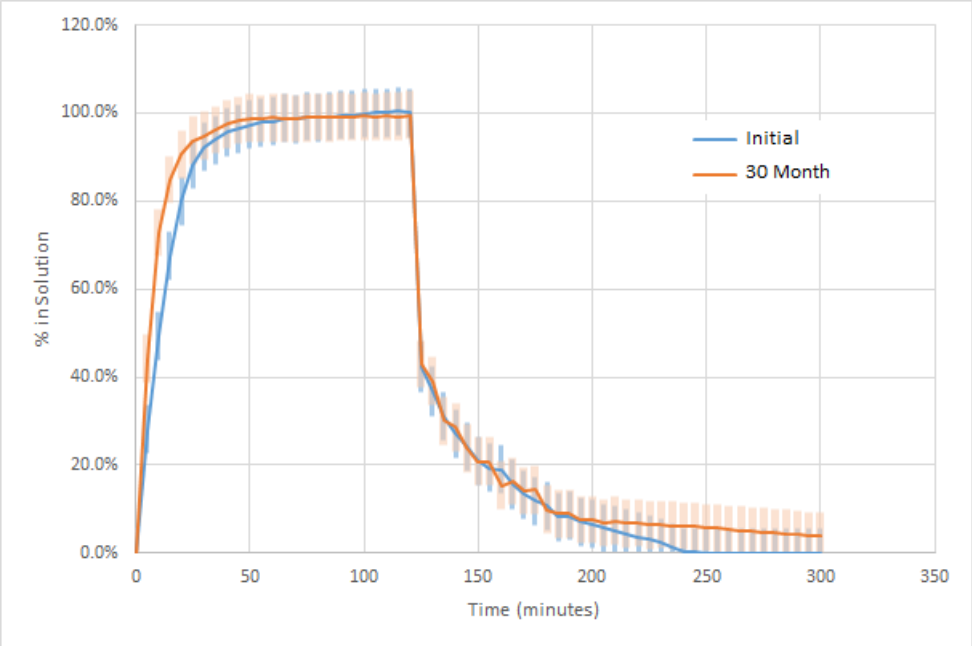

Figure 3.7: pH change dissolution comparing initial and 30 month ambient storage amorphous dispersions of ITZ:PVAL 4-88 (30% drug loading).

The dissolution performance in 0.1 N HCl of the two compositions are comparable with the 30 month old composition performing slightly better. Two different lots of PVAL 4-88 were used to make these compositions, which could explain the slight variance. Another possibility is that the stored material had some water absorption that would allow for better wetting and faster release. Since the purpose of the test was to determine crystal growth during storage, the reason for this variance was not investigated. After the pH change, the two compositions performed similarly with the two curves staying within the error bars. Because the dissolution performance is similar, it can be concluded that the

solid-state properties of ITZ in the PVAL matrix did not change during storage. Therefore, dissolution performance and XRD results demonstrate acceptable real-time ambient stability for the lead ITZ:PVAL 4-88 composition.

3.5 CONCLUSION

PVAL has been further investigated as a solubility enhancing polymer in amorphous solid dispersions as enabled by KinetiSol® Dispersing. PVAL 4-88 was confirmed to provide the best solubility enhancement and in solution stability as compared with 5-88, 8-88 and 18-88 presenting a trend that lower molecular weights function better than higher molecular weight polyvinyl alcohols. In a drug loading study, 20, 30 and 40% ITZ drug loads achieve full drug release in 0.1 N HCl in 2 hours, and were able to retard the return to the crystalline equilibrium solubility after the pH change in the expected rank order of 10%>20%>30%>40%>50% with the 30% loading selected as optimal. DOSY and FTIR were used confirm that weak molecular interactions are the likely cause of solid state and solution stability of amorphous ITZ. A 30 month stability study showed the optimal ITZ:PVAL 4-88 amorphous dispersion remained entirely amorphous as determined by XRD and PLM and the dissolution performance was unchanged.

Chapter 4

Novel formulation approach for multiparticulate abuse deterrent development

4.1 INTRODUCTION

The misuse and abuse of prescription drugs poses a serious public threat in the United States today. The Centers for Disease Control and Prevention (CDC) have declared that the United States is in the midst of an epidemic of prescription drug overdose deaths [161]. The CDC reported that drug overdose deaths were second only to motor vehicle crash deaths among the leading causes of unintentional injury death in 2007 [162]. That same report issued statistics that the number of deaths involving opioid analgesics was 1.93 times the number involving cocaine and 5.38 times the number involving heroin. A 2010 Substance Abuse and Mental Health Services Administration survey found that 16 million Americans age 12 years and older had taken a prescription pain reliever, tranquilizer, stimulant, or sedative for nonmedical purposes at least once in the previous year; 7 million had used psychotherapeutic drugs nonmedically within the past month. Of these drug abusers, 55% said they obtained the drug they most recently used from a friend or relative for free [163]. These statistics express the rising need for drug formulators and regulators to create barriers to prescription drug abuse.

To combat this growing epidemic, the U.S. Food and Drug Administration has released a guidance document for drug formulation companies to follow for formulating prescription drugs prone to abuse [164]. That guidance document offers several suggested approaches that are summarized in Table 4.1.

Approach	Brief Description
Physical/chemical barriers	Physical barriers can prevent chewing, crushing, cutting, grating or grinding of the dosage form. Chemical barriers can resist extraction of the drug using common solvents like water or organic solvents.
Agonist/antagonist combinations	A drug antagonist can be added to interfere with, reduce or defeat the euphoria associated with abuse.
Aversion	Substances can be added to the product to produce an unpleasant effect if the dosage form is manipulated or is used at a higher dose than directed.
Delivery system	Certain drug release designs or method of delivery can offer resistance to abuse like a sustained-release subcutaneous implant.
New molecular entities and Prodrugs	The properties of a NME or prodrug could include the need for enzymatic activation, different receptor binding profiles, slower central nervous system penetration or other effects.
Combination	Two or more of the above methods could be combined to deter abuse.
Novel approaches	This category encompasses novel approaches that are not captured in the previous categories.

Table 4.1: Categories for abuse deterrence as defined by the U.S. FDA.

The first category, physical and chemical barriers, represent the most prevalent approach in currently available commercial products. The most financially successful commercial abuse deterrent formulation has been Purdue Pharma's OxyContin®, which

was reformulated in a polyethylene oxide matrix as a physical barrier and approved by the FDA in April 2010 [165, 166]. The original product label did not contain any information on abuse deterrence despite having *in vitro* evidence to support such a claim. After product launch several studies investigated the public health impact of the OxyContin® reformulation to support the relabeling of the product with abuse deterrent information. One study looked at patients entering treatment programs with opioid dependency [167]. The selection of OxyContin® as a primary drug of abuse decreased from 35.6% of respondents before the release of the abuse-deterrent formulation to just 12.8% 21 months later. Those same respondents reported that of all opioids used to 'get high in the past 30 days' OxyContin® fell about 40% while the use of heroin nearly doubled over the same time period. Another study reported that abuse of the reformulated OxyContin® was 41% lower than historic abuse of the original formulation [168]. 'Real world' *in vitro* testing demonstrated the relative difficulty of manipulation of the reformulation [169] along with human *in vivo* testing [170] assessed the actual abuse deterrent properties of the reformulation. While not completely tamper proof, the reformation of OxyContin® did prove to be a deterrent in all evaluations.

The use of a polyethylene oxide (PEO) matrix has been utilized in Opana® (an oxymorphone reformulation by Endo Pharmaceuticals) and in Nucynta® (a tapentadol reformulation by Ortho-McNiell-Janssen Pharmaceuticals) but neither have been allowed to state abuse deterrence on product labels by the FDA even with some post-marketing studies [166]. Remoxy® (Pain Therapeutics, Inc.) is an oxycodone extended release product that does not use PEO to provide a physical barrier but rather a formulation containing sucrose acetate isobutyrate in a gelatin capsule [171]. The formulation creates a viscous mass that resists size reduction even when frozen and only releases a fraction of the oxycodone when submerged in high-proof alcohol for hours. Clinical trials showed

significant pain reduction and survey data from drug counselors demonstrated that it was less preferred for abuse as compared to the original ER oxycodone formulation [172, 173]. However, the FDA issued a complete response letter in June, 2011, indicating additional studies were required before approval would be granted. Since sucrose acetate isobutyrate is not considered GRAS by the FDA, there appears to be an opportunity for creating a solid matrix product out of GRAS excipients that does not contain PEO as a barrier approach in abuse deterrent formulation.

There are commercial products that belong to other abuse deterrent categories. Suboxone® is categorized as an agonist/antagonist combination of buprenorphine and naloxone, where the buprenorphine acts as a partial opioid agonist combined with the opioid agonist naloxone. It was approved in 2003 by the FDA for the treatment of opioid dependence but is commonly used off-label as a pain therapeutic [174]. Embeda® is also an agonist/antagonist combination of morphine and naltrexone. When taken orally as intended, the naltrexone is not released. But, if the tablet is chewed or crushed prior to taken orally, the naltrexone is released with the morphine and the agonist activity is limited [175]. This complex formulation encountered manufacturing issues and was recalled in March, 2011. Oxecta® is an immediate release formulation of oxycodone that contains aversive ingredients. Since the active ingredient is readily available via the oral route, the aversion abuse deterrent approach is to reduce non-oral abuse. The formulation contains sodium lauryl sulfate which irritates the nasal cavity to deter insufflation and it also contains excipients that form a gel when exposed to water to deter intravenous use [176].

Dysphagia, or difficulty in swallowing tablets, greatly influences patient compliance. A study has shown that up to ¼ of the general population may have problem swallowing, with the very young having the most difficulty followed by elderly patients [177]. Unfortunately, these age groups are commonly issued prescriptions for drugs that

are likely to be abused. For example, in 2007, 3.1 million youths aged 12 to 17 received treatment or counseling for problems with behavior or emotions with a significant percentage receiving psychotherapeutic drugs [178]. On the other hand, different studies have shown that the age group most likely to suffer from chronic pain is age 50 to 64 [179, 180]. It would be highly beneficial to have a delivery form that could simultaneously provide ease of dosing for patent compliance while at the same time delivering abuse deterrence.

One such approach would be to have a physical barrier formulation in a multiparticulate delivery form rather than a single, larger abuse deterrent tablet. The smaller particles would allow for oral delivery by sprinkling onto soft food for consumption to help with patient who suffer with dysphagia. In addition to ease of dosing, there are other biopharmaceutical advantages with having a multiparticulate delivery form. Gastrointestinal tract (GIT) transit time for small particles would not depend upon gastric emptying, which would result in a more uniform distribution in the GIT and less variable pharmacokinetic profiles among patients. However, the challenge with a multiparticulate approach is that the smaller particle size has higher susceptibility to certain mechanical abuse techniques such as size reduction by a coffee grinder or mortar and pestle. The high surface area also lends faster drug release when submerged in ethanol, which is also a common abuse technique. So, while the theory of a multiparticulate delivery is appealing, the technical details to the approach are challenging.

Currently, the most published multiparticulate approach is a platform technology called DETERx (Collegium Pharmaceuticals, Inc.) that creates a complex of drug with fatty acid and then places it with a hydrophobic waxy matrix in submillimeter, spherical particles for extended release [181-183]. The spherical particles are prepared using a standard spray congealing process and are specifically designed to retain the time-release

mechanism following common methods of tampering (e.g. crushing, chewing, heating for IV injection, etc.). The release profile can be adjusted by excipient ratios and particle size. Not much information is available on the challenge of creating the drug/fatty acid ionic complex, but a simple drug-in-a-matrix approach would be less complex and would possibly allow for a broader range of drugs to be incorporated in the platform.

The KinetiSol® Dispersing (KSD) technology is a thermal process than can create solid amorphous systems from challenging drugs and very highly viscous polymers [71]. While most publications on this technology deal with amorphous systems, the process can produce dispersions of crystalline drug just as straightforward as amorphous ones. Polymers with viscosity too large for process via extrusion have been successfully processed with KSD with the resulting solid systems being very difficult to mill once cooled [132]. While there is more to abuse deterrent systems than being difficult to mill, the viscous polymers do inherently provide resistance to crushing and powder formation. Additionally, the flexibility of KSD for polymer selection will allow for formulating with polymers that have inherent ethanol resistance like using polyvinyl alcohol (PVAL). It is hypothesized that through KSD, very viscous polymers like high molecular weight hydroxypropylmethylcellulose (HPMC) can be combined with other excipients to create abuse deterrent formulations. Furthermore, if combined with excipients that retard drug release, very viscous polymers can be formed into a multiparticulate extended release delivery form, providing dosing benefit to patients with dysphagia while not needing the complex processing of DETERx.

4.2 MATERIALS

Theophylline (THEO) was purchased from Acros Organics (Thermo Fisher Scientific). HPMC grades were received from Dow Chemical Company or purchased from Ashland Chemical Company. Ethocel (EC) grades were also sourced from Dow Chemical Company. TEC and DBS was purchased from Vertellus. EVAC and PVAL grades were purchased from Sigma-Aldrich.

4.3 METHODS

4.3.1 KinetiSol® Dispersing (KSD)

Compositions for this study were produced by a lab scale, GMP pharmaceutical compounder designed and manufactured by DisperSol Technologies, L.L.C. (Georgetown, TX, USA). Prior to KSD processing, materials were weighed, dispensed into a polyethylene bag, manually blended for approximately 1 minute, and charged into the compounder chamber. For compositions with liquid components, the non-liquid components were weighed and placed into a food processor. The liquid components were then weighed out in syringes that had been tared after being flushed with the liquid component (to compensate for the weight of residual liquid in the syringe after injection). The liquid was slowly added to the non-liquid components and then mixed on low setting for 2 minutes. During processing in the compounder, computer controls monitor processing parameters in real time and eject the material at a pre-set ejection temperature. Discharged material was immediately quenched in a cooling die under pressure in a pneumatic press. Cooled material was then milled in a FitzMill L1A with a 0.156 inch (approximately 5 mesh) screen after which particles smaller than a 12 mesh screen size were removed from the resulting material. Formulations with high impact resistance required cooling with liquid nitrogen prior to milling.

4.3.2 Non-Sink Dissolution Analysis

Non-sink dissolution analysis was conducted with a VK 7000 dissolution tester (Varian, Inc., Palo Alto, CA, USA) configured as Apparatus 2. Samples equivalent to 37.5 mg THEO were weighed and added to the surface dissolution vessels filled with 750 ml of 0.1 N HCl equilibrated to a temperature of 37.0 ± 1 °C with a paddle rotation of 50 rpm. Drug content in solution was directly measured at 270 nm with a fiber optic Spectra™ instrument (Pion Inc., Billerica, MA, USA) fitted with 5 mm path length Pion Probes. Readings were recorded every 10 minutes for 24 hours. For dissolution containing ethanol, 300 ml of ethanol was added to 450 ml of 0.1 N HCl and equilibrated to a temperature of 37.0 ± 1 °C prior to adding samples.

4.3.3 Dart Impact Test

Dart impact tests were conducted on a custom made testing device. Essentially, a dart (solid steel cylinder) weighing 1.198 kg is placed with in PVC tube that is mounted vertically. A string and pulley system allows the dart to be raised to a specific height and then released. At the base of the PVC tube is a flat steel plate where a tablet is placed to be hit by the falling dart. The dart is raised to 213 cm in height so that the tablet is hit with 25 J of energy. A tablet passed the test if it remained intact in one piece without visual cracks.

4.3.4 Coffee Grinder Size Reduction Test

Approximately one gram of the multiparticulates is weighed out and placed in a KitchenAid coffee grinder. The coffee grinder is turned on for 15 seconds followed by a 15 second pause. This is repeated for a total time of 5 minutes. The ground material is then placed on top of a screen stack containing 20, 40, 60, and 200 mesh with a pan at the bottom to collect all fines that would pass through the 200 mesh. The screen stack was

mechanically shaken for two minutes. Each screen was weighted prior to sieving and then weighted afterward to determine the total weight of material in each size range.

4.3.5 Syringeability Test

Approximately 500 mg of the multiparticulates were placed on a metal pan and held over a propane torch set on the lowest setting. The height from the pan to the flame was slowly reduced until the heat was sufficient to start melting the particle surfaces. Once molten, the pan could be tipped so the melted material could pool on the lip of the pan and be drawn up by a 20 gauge needle. The needle and syringe were pre-weighed so that any material drawn up by the needled could be quantified by weighing the needle, syringe and drawn material.

4.3.6 Water Extraction Test

Three 150 ml beakers were filled with 100 ml of distilled water and placed in three different conditions. The first beaker was left at room temperature, the second one was placed on a hot plate and brought to a mild boil, and the last one was placed in an ice water bath to reach approximately 3 °C. Once the three beakers achieved the desired conditions, 25 mg of multiparticulate were placed in the water. Drug content in solution was directly measured at 270 nm with a fiber optic Spectra™ instrument (Pion Inc., Billerica, MA, USA) fitted with 5 mm path length Pion Probes. Readings were recorded every 2 minutes for 3 hours. Test was concluded as soon as the water in the heated beaker reached a level that would not allow for complete submersion of the fiber optic tip. The final volume was measured and concentrations were calculated on the average of the beginning and final volumes.

4.4 Results and Discussion

4.4.1 Formulation Development

In the previous chapters and in other research [132] where amorphous solid dispersions were created using high molecular weight polymers, it was discovered that milling the KSD discharged material was a challenge. It was also discovered if the drug was not rendered amorphous, then the discharged material was significantly easier to mill. In general, it is known that drugs can function as plasticizers once they are rendered amorphous or molten and it has been found that ITZ works well as a plasticizer in cellulosic polymers [184]. Since drugs that are abused typically do not need bioavailability enhancement, it would be preferred to make solid dispersion with drugs in their unaltered or crystalline state. However, not only would the composition not gain the benefit of the drug acting like a plasticizer, but the small, crystalline molecules would also have a negative impact on mechanical properties of the polymer.

To compensate for this, a small component of the formulation must have some plasticizing effect to retain impact properties sufficient to resist crushing or milling. A screening study was conducted with 15 different excipients with HPMC E50 and 20% THEO by processing the compositions by KSD and then directly forming a tablet for dart impact testing. For confidentiality reasons, the 15 excipients will not be listed in this chapter. Six of the formulations successfully passed the impact test; two of them were selected to move forward with formulation development: triethyl citrate (TEC) and dibutyl sebacate (DBS). TEC was selected because of the elastomeric properties that it imparted on HPMC, which makes it particularly impact resistant. DBS was selected because it is less water soluble than TEC and might provide a slower release in dissolution testing.

The desired release rate from an extended release delivery form is drug and therapy dependent. In this study, THEO is being used as a surrogate for an opioid like oxycodone

because of its high melting point and water/alcohol solubility. For pain therapy, opioids have been tested for in 4-6 hour and 12 hour release [185]. For a starting point, the authors thought that a release profile around 6 hours could be representative of a target product profile and was selected as the development goal. Several formulations were made from the selected group of materials, HPMC, EC, PVAL, EVAC, TEC and DBS, and tested in dissolution. Formulations that required at least 3 hours to achieve full drug in solution are listed in Table 4.2. Along with the time to achieve full release, the table also contains an impact rating, which was a subjective categorization after manually bending the discharged after cooling in the compression mold. A rating of 1 was very easy to break, a rating of 2 required some effort to break, and a rating of 3 was very difficult or impossible to break.

Formulation	Time to full release	Impact rating
62% HPMC E50 / 10% HPMC K100M / 8% TEC	3:00	3
44% PVAL 4-38 / 36% K100M	3:10	2
40% PVAL 4-88 / 40% PVAL 4-98	3:20	1
40% EVAC 12 / 30% HPMC K100M / 10% EC 10	4:00	1
40% EVAC 12 / 40% HPMC K100M	4:10	2
52% HPMC E50 / 10% EC 10 / 10% HPMC K100M / 8% TEC	4:10	2
42% HPMC E50 / 20% EC 10 / 10% HPMC K100M / 8% TEC	4:30	1
30% HPMC E15 / 30% HPMC K100M / 20% DBS	5:40	3
35% HPMC E15 / 35% HPMC K100M / 10% DBS	6:40	3
55% EC 10 / 25% DBS	35% in 24:00	1
80% EVAC 12	20% in 24:00	3

Table 4.2: Formulations tested to determine excipient trends (n=1).

Many of the formulations initially tested attained full release in around 2 hours, so the formulation focus turned to determining combinations that released THEO very slowly. EVAC is used for extended release transdermal drug delivery [186] and is used in the plastic industry as an impact modifier [187]; consequently, it was not surprising that it

required more than 24 hours to release and received an impact rating of 3. EVAC was introduced into formulations containing HPMC E50 and it did slow the release. But, the time to full release was still faster than three hours and the impact rating of the compositions were 2 or less. When combined with HPMC K100M, a release time of 4 hours was achieved but again the impact rating was 2 or less. Ethyl Cellulose is used in formulations for extended release and lends itself well to thermal processing [188]. Mixed with a high percentage of DBS yielded a composition that required more than 24 hours to release. However, EC is brittle and very easy to grind or mill. It was added at 10 and 20% in several formulations and generally aided in slow down release. Unfortunately, the negative impact on the mechanical properties even at 10% was sufficient to make all formulations a rating of 2 or less even with the impact augmenting effects of TEC.

HPMC K100M in combination with both plasticizers proved to be the best mechanical property enhancing approach in formulation development, but most of the release times were between 3 and 4 hours. Other HPMC grades were added to the formulations both to make the composition easier to process and to alter the release profile. Eventually, a combination of E15, K100M and DBS generated a release profile around 6 hours and earned an impact rating of 3.

As mentioned in the introduction section, one of the common methods for abuse is to consume alcohol simultaneously with the dosage form to defeat the extended release feature and attain dose dumping. Thus, the last step of the formulation process was to see the release profile in 40% ethanol compared with the release in 0.1 N HCl to determine if further formulation adjustments were needed. Figure 4.1 contains the dissolution profiles of the two conditions for the lead formulation of 20% THEO / 35% HPMC E15 / 35% HPMC K100M / 10% DBS.

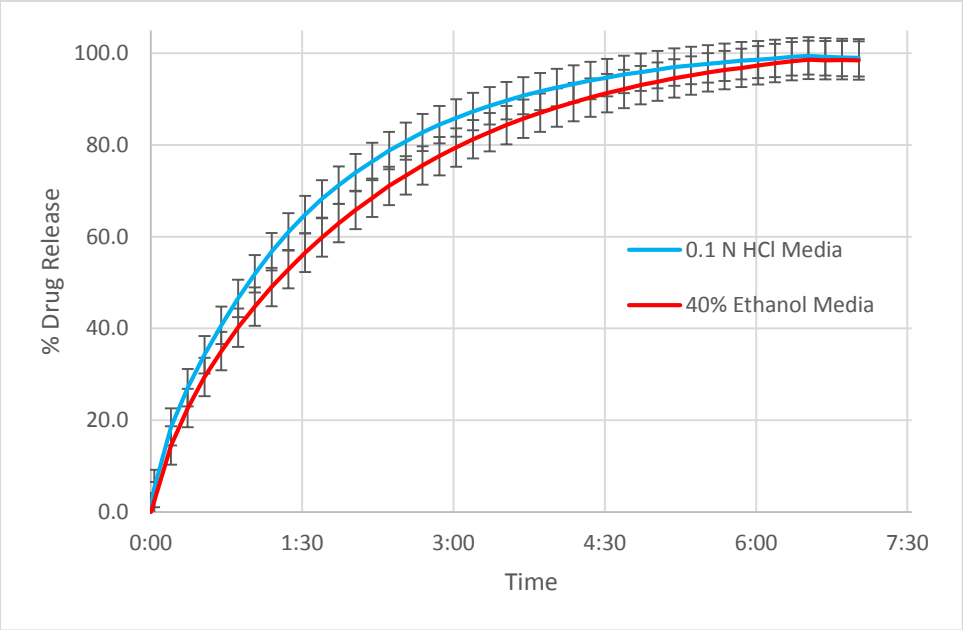

Figure 4.1: Dissolution profiles of lead formulation in 0.1 N HCl and 40% Ethanol (n=3).

The lead formulation actually had a slightly slower dissolution rate in the media containing 40% ethanol than it did the standard media. An F2 similarity factor was calculated to compare the two dissolution profiles and a value of 90 was obtained [189]. This indicated that there is less than 2% variance between the two profiles. Thus, the lead formulation meets to the main performance criteria of releasing the drug over 6 hours, having good mechanical properties for impact resistance, and having a release profile that is not significantly altered by ethanol.

4.4.2 Abuse Testing

A reduction in particle size will cause an increase in the dissolution rate. Thus, one of the abuse methods is to reduce the delivery form to a fine powder to have an immediate

release rate. The multiparticulates produced in this study are in the size range of 1.7 to 4 mm. All the particles that were smaller than a 12 mesh screen were removed from the multiparticulates, so the smallest size corresponds with the 12 mesh screen which is 1.7 mm. The 4 mm size on the large end of the spectrum corresponds with the milling screen size. The coffee grinder size reduction test was conducted on the lead formulation with the results of the mass fraction analysis shown in Figure 4.2.

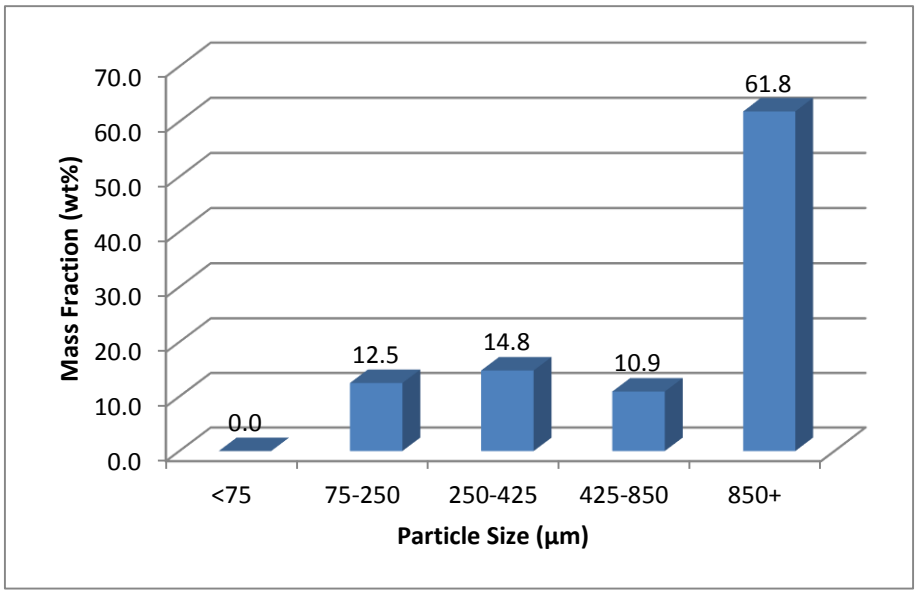

Figure 4.2: Post Coffee Grinder Test Particle Size distribution.

The small sieve stack was limited in sizes, so the percentage of particles larger than 12 mesh could not be measured. However, almost 62% of the multiparticulates were over the 20 mesh size which shows that very little size reduction did occur on the majority of the particles. None of the particles were reduced in size to a fine powder (less than 75 microns) which is a positive result to keep the delivery form from being rendered an immediate release. The remaining particles were scattered in sizes ranging from 75 to 850

microns. The real indication of the effect of the coffee grinder size reduction test is to perform a dissolution comparison which is illustrated in Figure 4.3.

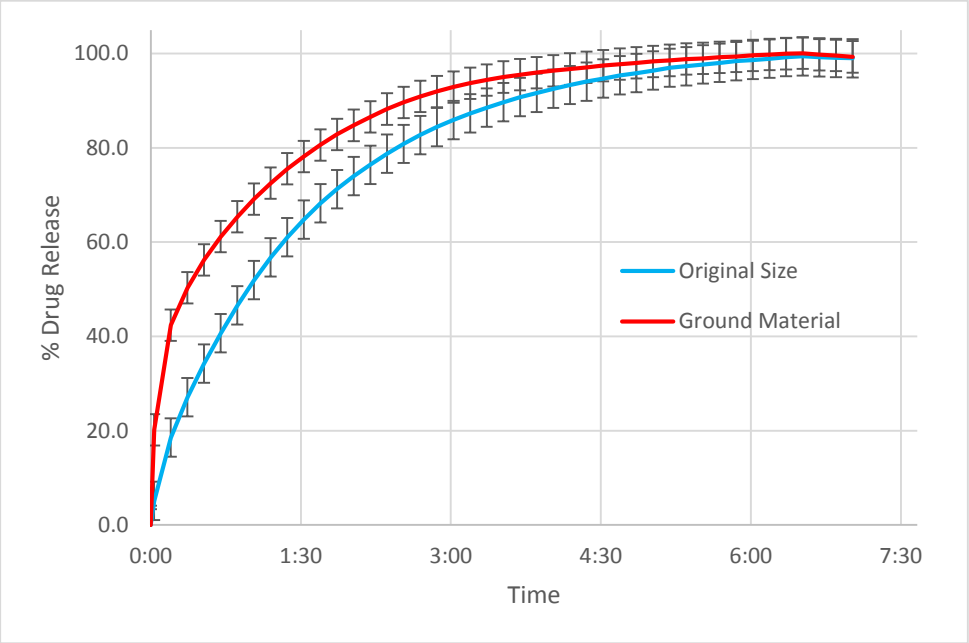

Figure 4.3: Dissolution Profile of Original Size and Coffee Ground Material (n=3).

As expected, the ground material had a faster dissolution rate than the original size material, but it was not an immediate release profile. The T95 (time where 95% of the drug has been released) and T80 (time for 80%) was 4:42 and 2:32 for the original size and 3:32 and 1:42 for the coffee ground material, which is approximately a time reduction of 30%. An F2 similarity factor was calculated for the entire profile and for the first three hours with values of 84 and 67 respectively, which is a difference of roughly 5%. While it is a change in the dissolution performance, the ground material still retained an extended release profile to serve as an abuse deterrent.

Skeptics of this test might argue that the coffee grinder was only run intermittently for 5 minutes and if it were processed consistently for a longer duration of time that the particle size reduction would allow for immediate release. Prior to having access to a Fitzmill in early KSD research studies, coffee grinders were used for size reduction of the discharge of amorphous dispersions. Several coffee grinders were broken until a method was discovered to grind high molecular weight polymers without causing damage to the grinder. If the coffee grinders were run continuously, the surfaces of the particles are heated up by the friction occurring in the grinder. As the surface temperatures of the particles rises, they become soft and tacky. The tacky surfaces create a much higher resistance to rotation, which will result in breaking the drive shaft or burning out the electric motor. It is likely that an individual attempting to abuse the delivery form for the first time would not take such precautions and cause damage to the coffee grinder, which would probably motivate the person to change to a different method of tampering.

A mortar and pestle was employed to see if size reduction could be achieved. Figure 4.4 is a picture of the material after test to show that no particle size reduction or powder was formed.

Figure 4.4: Mortar and Pestle approach for size reduction of multiparticulates.

After 5 minutes of vigorously attempting size reduction in the mortar and pestle, no size reduction was observed. A hammer test was briefly attempted, where the multiparticulates were placed in a polyethylene bag and hit with a hammer. The first impact did substantial damage to the plastic bag and the second impact caused some multiparticulates to fly across the room. No size reduction was observed and the test was ceased for safety reasons. With the results from the coffee grinder, mortar and pestle, and hammer testing, it was concluded that the lead formulation did provide good resistance to size reduction.

The syringeability test was then conducted on the lead formulation as illustrated in Figure 4.5.

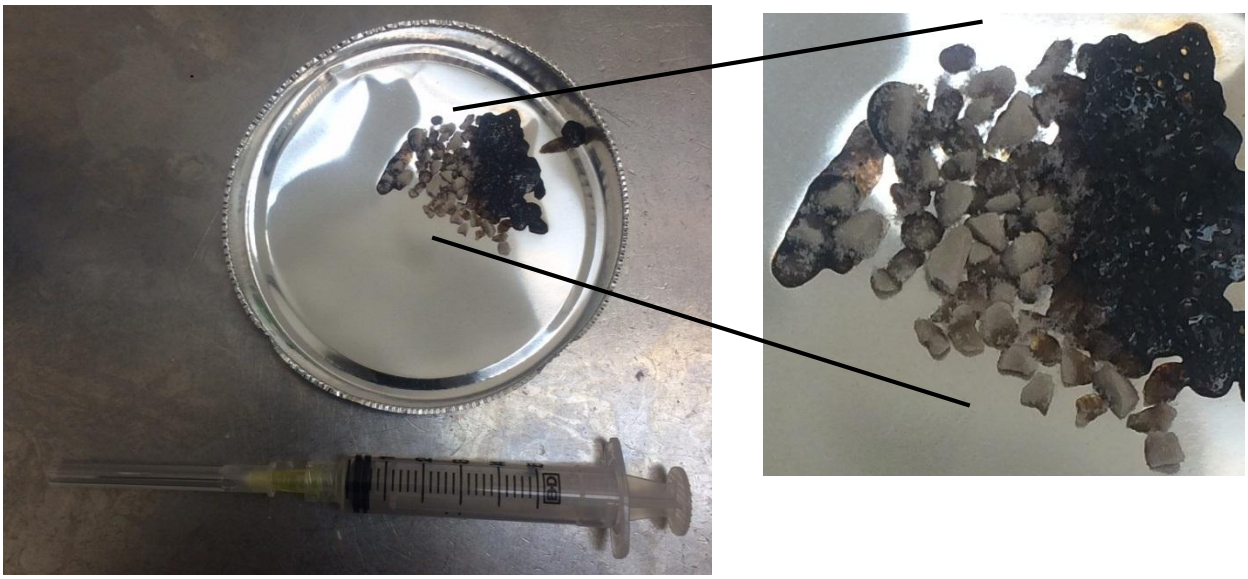

Figure 4.5: Result of Syringeability test of lead formulation.

As the particles were heated up, the surfaces in contact with the pan would melt and then instantly char. Some of the particles in the figure demonstrate this as the bottom is black while the top is still unmelted. It is possible that the heat transfer rate is too high from the propane torch and causing the surface to burn before the top portion of the particle

received enough heat to melt. Consequently, the test was conducted on a hot plate where the temperature was slowly raised over approximately 15 minutes to allow time for sufficient heat transfer. Even with the slower heat transfer rate, the particles burned on the bottom and remained solid on the top (picture not shown). Thus, this action was not a result of the method of heating, but rather the performance of the formulation.

As the bottom of the particles started to melt/char, the pan was tilted to get the material to flow the lip of the pan for possible collection in the needle. Interestingly, the particles would move, but the portion that melted on the bottom would not flow. The particle would slowly disintegrate as it slid along the pan, which would leave a trail, but would stop moving once the particle completely melted. A trail can be seen in the picture on the left hand side. The right hand side of the picture shows the portion of particles completely melted together. After the particles on the right were melted, the pan was slopped so that the material would flow to the right; however, the material would not pour. As the pan was removed from the heat source, the liquefied portions became hard within a few seconds. Because of the behavior of the material, none of it was able to be drawn through the needle into the syringe. It was concluded that abuse by this method is not practical.

The final step for testing abuse deterrence in this study was the water extraction test. The results are shown in Figure 4.6.

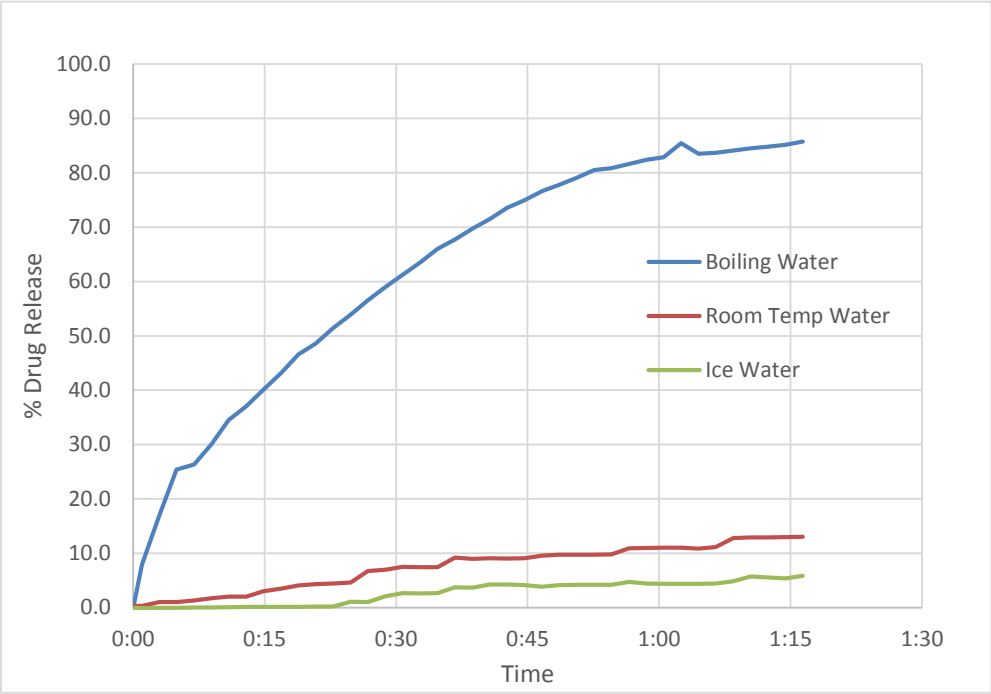

Figure 4.6: Dissolution Profiles from the Water Extraction Test.

The delivery form did release slowly in ice water and room temperature water; at the 1:15 time point there was 5% and 13% released respectively. However, the boiling water allowed for around 40% of the drug to be released in the first 15 minutes. Intriguingly, the multiparticulates in the boiling water appeared to have little or no physical change as they were similar in hardness and color at the end of the test. The multiparticulates placed in the room temperature and ice water baths had increased in size due to water absorption, turned white in color and had taken a gelatin consistency. It seems hydration of the formulation is key in retarding drug release and that hot water prevents water absorption. This finding is consistent with product literature on HPMC [190, 191].

It is beyond the scope of this study to reformulate in an attempt to address the hot water release issue. Possibly, using a lower grade of HPMC, like E3, along with a different plasticizer or combination of plasticizers would allow for the composition to hydrate in

boiling water while retaining the mechanical properties of the lead formulation. Effort on achieving a more narrow range of particle sizes would provide a more uniform release rate and varying the average particle size could modify the time to full drug release. Many aspects could be investigated and optimized to improve this basic concept. However, the study has shown that high molecular weight polymers, especially HPMC, can be formulated for mechanical resistance to abuse methods and provide extended drug release.

4.5 CONCLUSION

Abuse of prescription medication is a large social challenge facing the United States today. Abuse deterrent formulations have been introduced into the market and have shown to discourage abusers from using those medicaments nonmedically. Some patient populations struggle with swallowing those formulations and would benefit from a multiparticulate abuse delivery form. This study has shown that high molecular weight polymers, primarily HPMC, can be combined with plasticizers to create a delivery form that is resistant to size reduction by coffee grinder, mortar and pestle and hammering. The same formulation shows ethanol will not cause dose dumping and also resistance to syringeability. While good water extraction resistance was established, it could be improved upon to resist extraction in hot water. Further research could allow this concept to be developed commercially and aid in the fight against the epidemic of prescription drug overdose deaths.

Bibliography

1. Brough, C. and R.O. Williams Iii, *Amorphous solid dispersions and nano-crystal technologies for poorly water-soluble drug delivery.* International Journal of Pharmaceutics, 2013. **453**(1): p. 157-166.
2. Ku, M.S. and W. Dulin, *A biopharmaceutical classification-based Right-First-Time formulation approach to reduce human pharmacokinetic variability and project cycle time from First-In-Human to clinical Proof-Of-Concept.* Pharmaceutical Development and Technology, 2012. **17**(3): p. 285-302.
3. Takagi, T., et al., *A provisional biopharmaceutical classification of the top 200 oral drug products in the United States, Great Britain, Spain, and Japan.* Molecular pharmaceutics, 2006. **3**(6): p. 631-643.
4. Dahan, A., J.M. Miller, and G.L. Amidon, *Prediction of solubility and permeability class membership: provisional BCS classification of the world's top oral drugs.* The AAPS journal, 2009. **11**(4): p. 740-746.
5. Kipp, J.E., *The role of solid nanoparticle technology in the parenteral delivery of poorly water-soluble drugs.* International Journal of Pharmaceutics, 2004. **284**(1–2): p. 109-122.
6. Singh, A., Z.A. Worku, and G. Van den Mooter, *Oral formulation strategies to improve solubility of poorly water-soluble drugs.* Expert Opinion on Drug Delivery, 2011. **8**(10): p. 1361-1378.
7. Keserü, G.M. and G.M. Makara, *The influence of lead discovery strategies on the properties of drug candidates.* Nature Reviews Drug Discovery, 2009. **8**(3): p. 203-212.
8. Lipinski, C.A., et al., *Experimental and computational approaches to estimate solubility and permeability in drug discovery and development settings.* Advanced Drug Delivery Reviews, 2012. **64, Supplement**(0): p. 4-17.
9. Lipinski, C.A., *Drug-like properties and the causes of poor solubility and poor permeability.* Journal of Pharmacological and Toxicological Methods, 2000. **44**(1): p. 235-249.

10. Serajuddin, A.T.M., *Salt formation to improve drug solubility.* Advanced Drug Delivery Reviews, 2007. **59**(7): p. 603-616.
11. Serajuddin, A.T.M. and M. Pudipeddi, *Salt-selection strategies.* Handbook of pharmaceutical salts: properties, selection, and use. Weinheim: Wiley-VCH, 2008: p. 135-160.
12. Stella, V.J. and Q. He, *Cyclodextrins.* Toxicologic Pathology, 2008. **36**(1): p. 30-42.
13. Neslihan Gursoy, R. and S. Benita, *Self-emulsifying drug delivery systems (SEDDS) for improved oral delivery of lipophilic drugs.* Biomedicine & Pharmacotherapy, 2004. **58**(3): p. 173-182.
14. Muchow, M., P. Maincent, and R.H. Müller, *Lipid nanoparticles with a solid matrix (SLN®, NLC®, LDC®) for oral drug delivery.* Drug development and industrial pharmacy, 2008. **34**(12): p. 1394-1405.
15. Fenske, D.B., A. Chonn, and P.R. Cullis, *Liposomal Nanomedicines: An Emerging Field.* Toxicologic Pathology, 2008. **36**(1): p. 21-29.
16. Letchford, K. and H. Burt, *A review of the formation and classification of amphiphilic block copolymer nanoparticulate structures: micelles, nanospheres, nanocapsules and polymersomes.* European Journal of Pharmaceutics and Biopharmaceutics, 2007. **65**(3): p. 259-269.
17. Gullapalli, R.P., *Soft gelatin capsules (softgels).* Journal of Pharmaceutical Sciences, 2010. **99**(10): p. 4107-4148.
18. Schultheiss, N. and A. Newman, *Pharmaceutical cocrystals and their physicochemical properties.* Crystal Growth and Design, 2009. **9**(6): p. 2950-2967.
19. Stephenson, G.A., A. Aburub, and T.A. Woods, *Physical stability of salts of weak bases in the solid-state.* Journal of Pharmaceutical Sciences, 2011. **100**(5): p. 1607-1617.
20. Singhal, D. and W. Curatolo, *Drug polymorphism and dosage form design: a practical perspective.* Advanced Drug Delivery Reviews, 2004. **56**(3): p. 335-347.

21. Yu, L.X., et al., *Biopharmaceutics classification system: the scientific basis for biowaiver extensions.* Pharmaceutical Research, 2002. **19**(7): p. 921-925.
22. Wu, C.-Y. and L.Z. Benet, *Predicting drug disposition via application of BCS: transport/absorption/elimination interplay and development of a biopharmaceutics drug disposition classification system.* Pharmaceutical Research, 2005. **22**(1): p. 11-23.
23. Curatolo, W., J.A. Nightingale, and S.M. Herbig, *Utility of hydroxypropylmethylcellulose acetate succinate (HPMCAS) for initiation and maintenance of drug supersaturation in the GI milieu.* Pharmaceutical Research, 2009. **26**(6): p. 1419-1431.
24. Huang, L.-F. and W.-Q. Tong, *Impact of solid state properties on developability assessment of drug candidates.* Advanced Drug Delivery Reviews, 2004. **56**(3): p. 321-334.
25. Dressman, J.B., et al., *Estimating drug solubility in the gastrointestinal tract.* Advanced Drug Delivery Reviews, 2007. **59**(7): p. 591-602.
26. Zhao, Y.H., et al., *Rate-limited steps of human oral absorption and QSAR studies.* Pharmaceutical Research, 2002. **19**(10): p. 1446-1457.
27. Möschwitzer, J., et al., *Nanocrystal formulations for improved delivery of poorly soluble drugs.* Nanomedicine in Health and Disease, 2011: p. 79.
28. Dokoumetzidis, A. and P. Macheras, *A century of dissolution research: from Noyes and Whitney to the biopharmaceutics classification system.* International Journal of Pharmaceutics, 2006. **321**(1): p. 1-11.
29. Galli, C., *Experimental determination of the diffusion boundary layer width of micron and submicron particles.* International Journal of Pharmaceutics, 2006. **313**(1): p. 114-122.
30. Shchekin, A. and A. Rusanov, *Generalization of the Gibbs–Kelvin–Köhler and Ostwald–Freundlich equations for a liquid film on a soluble nanoparticle.* The Journal of chemical physics, 2008. **129**: p. 154116.

31. Kesisoglou, F., S. Panmai, and Y. Wu, *Nanosizing — Oral formulation development and biopharmaceutical evaluation.* Advanced Drug Delivery Reviews, 2007. **59**(7): p. 631-644.
32. Shegokar, R. and R.H. Müller, *Nanocrystals: Industrially feasible multifunctional formulation technology for poorly soluble actives.* International Journal of Pharmaceutics, 2010. **399**(1–2): p. 129-139.
33. Junghanns, J.U.A.H. and R.H. Müller, *Nanocrystal technology, drug delivery and clinical applications.* International journal of nanomedicine, 2008. **3**(3): p. 295.
34. Choi, J.-Y., et al., *Role of polymeric stabilizers for drug nanocrystal dispersions.* Current Applied Physics, 2005. **5**(5): p. 472-474.
35. Van Eerdenbrugh, B., G. Van den Mooter, and P. Augustijns, *Top-down production of drug nanocrystals: Nanosuspension stabilization, miniaturization and transformation into solid products.* International Journal of Pharmaceutics, 2008. **364**(1): p. 64-75.
36. Lee, J., J.Y. Choi, and C.H. Park, *Characteristics of polymers enabling nano-comminution of water-insoluble drugs.* International Journal of Pharmaceutics, 2008. **355**(1–2): p. 328-336.
37. Voorhees, P.W., *The theory of Ostwald ripening.* Journal of Statistical Physics, 1985. **38**(1-2): p. 231-252.
38. Merisko-Liversidge, E., G.G. Liversidge, and E.R. Cooper, *Nanosizing: a formulation approach for poorly-water-soluble compounds.* European Journal of Pharmaceutical Sciences, 2003. **18**(2): p. 113-120.
39. Hancock, B.C. and M. Parks, *What is the true solubility advantage for amorphous pharmaceuticals?* Pharmaceutical Research, 2000. **17**(4): p. 397-404.
40. Miller, D.A., et al., *Targeted intestinal delivery of supersaturated itraconazole for improved oral absorption.* Pharmaceutical Research, 2008. **25**(6): p. 1450-1459.
41. Miller, D.A., et al., *Enhanced in vivo absorption of itraconazole via stabilization of supersaturation following acidic-to-neutral pH transition.* Drug development and industrial pharmacy, 2008. **34**(8): p. 890-902.

42. DiNunzio, J.C., et al., *Amorphous compositions using concentration enhancing polymers for improved bioavailability of itraconazole.* Molecular pharmaceutics, 2008. **5**(6): p. 968-980.
43. Guzmán, H.R., et al., *Combined use of crystalline salt forms and precipitation inhibitors to improve oral absorption of celecoxib from solid oral formulations.* Journal of Pharmaceutical Sciences, 2007. **96**(10): p. 2686-2702.
44. Brouwers, J., M.E. Brewster, and P. Augustijns, *Supersaturating drug delivery systems: The answer to solubility-limited oral bioavailability?* Journal of Pharmaceutical Sciences, 2009. **98**(8): p. 2549-2572.
45. Janssens, S. and G. Van den Mooter, *Review: physical chemistry of solid dispersions.* Journal of Pharmacy and Pharmacology, 2010. **61**(12): p. 1571-1586.
46. Lindfors, L., et al., *Nucleation and crystal growth in supersaturated solutions of a model drug.* Journal of colloid and interface science, 2008. **325**(2): p. 404-413.
47. Janssens, S., et al., *Formulation and characterization of ternary solid dispersions made up of Itraconazole and two excipients, TPGS 1000 and PVPVA 64, that were selected based on a supersaturation screening study.* European Journal of Pharmaceutics and Biopharmaceutics, 2008. **69**(1): p. 158-166.
48. Raghavan, S.L., et al., *Crystallization of hydrocortisone acetate: influence of polymers.* International Journal of Pharmaceutics, 2001. **212**(2): p. 213-221.
49. Raghavan, S.L., et al., *Formation and stabilisation of triclosan colloidal suspensions using supersaturated systems.* International Journal of Pharmaceutics, 2003. **261**(1–2): p. 153-158.
50. Vasanthavada, M., et al., *Phase behavior of amorphous molecular dispersions I: Determination of the degree and mechanism of solid solubility.* Pharmaceutical Research, 2004. **21**(9): p. 1598-1606.
51. Wang, X., A. Michoel, and G. Van den Mooter, *Solid state characteristics of ternary solid dispersions composed of PVP VA64, Myrj 52 and itraconazole.* International Journal of Pharmaceutics, 2005. **303**(1–2): p. 54-61.

52. Hancock, B.C., S.L. Shamblin, and G. Zografi, *Molecular mobility of amorphous pharmaceutical solids below their glass transition temperatures.* Pharmaceutical Research, 1995. **12**(6): p. 799-806.
53. Konno, H. and L.S. Taylor, *Influence of different polymers on the crystallization tendency of molecularly dispersed amorphous felodipine.* Journal of Pharmaceutical Sciences, 2006. **95**(12): p. 2692-2705.
54. Huang, J., R.J. Wigent, and J.B. Schwartz, *Drug–polymer interaction and its significance on the physical stability of nifedipine amorphous dispersion in microparticles of an ammonio methacrylate copolymer and ethylcellulose binary blend.* Journal of Pharmaceutical Sciences, 2008. **97**(1): p. 251-262.
55. Karavas, E., et al., *Investigation of the release mechanism of a sparingly water-soluble drug from solid dispersions in hydrophilic carriers based on physical state of drug, particle size distribution and drug–polymer interactions.* European Journal of Pharmaceutics and Biopharmaceutics, 2007. **66**(3): p. 334-347.
56. Chokshi, R.J., et al., *Stabilization of low glass transition temperature indomethacin formulations: Impact of polymer-type and its concentration.* Journal of Pharmaceutical Sciences, 2008. **97**(6): p. 2286-2298.
57. Qian, F., J. Huang, and M.A. Hussain, *Drug–polymer solubility and miscibility: Stability consideration and practical challenges in amorphous solid dispersion development.* Journal of Pharmaceutical Sciences, 2010. **99**(7): p. 2941-2947.
58. Waterman, K.C. and B.C. MacDonald, *Package selection for moisture protection for solid, oral drug products.* Journal of Pharmaceutical Sciences, 2010. **99**(11): p. 4437-4452.
59. Möschwitzer, J.P., *Drug nanocrystals in the commercial pharmaceutical development process.* International Journal of Pharmaceutics, 2012.
60. Möschwitzer, J., *Particle Size Reduction Technologies in the Pharmaceutical Development Process.* American Pharmaceutical Review, 2010 (April), 2010: p. 54-59.

61. Merisko-Liversidge, E.M. and G.G. Liversidge, *Drug Nanoparticles: Formulating Poorly Water-Soluble Compounds.* Toxicologic Pathology, 2008. **36**(1): p. 43-48.
62. Merisko-Liversidge, E. and G.G. Liversidge, *Nanosizing for oral and parenteral drug delivery: A perspective on formulating poorly-water soluble compounds using wet media milling technology.* Advanced Drug Delivery Reviews, 2011. **63**(6): p. 427-440.
63. Cooper, E.R., *Nanoparticles: A personal experience for formulating poorly water soluble drugs.* Journal of Controlled Release, 2010. **141**(3): p. 300-302.
64. Arunkumar, N., M. Deecaraman, and C. Rani, *Nanosuspension technology and its applications in drug delivery.* Asian journal of pharmaceutics, 2009. **3**(3): p. 168.
65. Texter, J., *Precipitation and condensation of organic particles.* Journal of dispersion science and technology, 2001. **22**(6): p. 499-527.
66. de Waard, H., W.L.J. Hinrichs, and H.W. Frijlink, *A novel bottom–up process to produce drug nanocrystals: Controlled crystallization during freeze-drying.* Journal of Controlled Release, 2008. **128**(2): p. 179-183.
67. Vehring, R., *Pharmaceutical particle engineering via spray drying.* Pharmaceutical Research, 2008. **25**(5): p. 999-1022.
68. Wu, C. and J.W. McGinity, *Influence of ibuprofen as a solid-state plasticizer in Eudragit® RS 30 D on the physicochemical properties of coated beads.* AAPS PharmSciTech, 2001. **2**(4): p. 35-43.
69. Crowley, M.M., et al., *Pharmaceutical applications of hot-melt extrusion: part I.* Drug development and industrial pharmacy, 2007. **33**(9): p. 909-926.
70. Fini, A., et al., *Ultrasound-compacted and spray-congealed indomethacin/polyethyleneglycol systems.* International Journal of Pharmaceutics, 2002. **247**(1–2): p. 11-22.
71. Miller, D.A., et al., *KinetiSol: A New Processing Paradigm for Amorphous Solid Dispersion Systems.* Drug Development and Delivery, 2012. **12**(9).

72. Fakes, M.G., et al., *Enhancement of oral bioavailability of an HIV-attachment inhibitor by nanosizing and amorphous formulation approaches.* International Journal of Pharmaceutics, 2009. **370**(1–2): p. 167-174.

73. Zheng, W., et al., *Selection of oral bioavailability enhancing formulations during drug discovery.* Drug development and industrial pharmacy, 2012. **38**(2): p. 235-247.

74. Vogt, M., K. Kunath, and J.B. Dressman, *Dissolution enhancement of fenofibrate by micronization, cogrinding and spray-drying: Comparison with commercial preparations.* European Journal of Pharmaceutics and Biopharmaceutics, 2008. **68**(2): p. 283-288.

75. Kwong, E., J. Higgins, and A.C. Templeton, *Strategies for bringing drug delivery tools into discovery.* International Journal of Pharmaceutics, 2011. **412**(1): p. 1-7.

76. Thombre, A.G., et al., *In vitro and in vivo characterization of amorphous, nanocrystalline, and crystalline ziprasidone formulations.* International Journal of Pharmaceutics, 2012. **428**(1–2): p. 8-17.

77. Thombre, A.G., S.M. Herbig, and J.A. Alderman, *Improved Ziprasidone Formulations with Enhanced Bioavailability in the Fasted State and a Reduced Food Effect.* Pharmaceutical Research, 2011. **28**(12): p. 3159-3170.

78. Sigfridsson, K., et al., *A formulation comparison, using a solution and different nanosuspensions of a poorly soluble compound.* European Journal of Pharmaceutics and Biopharmaceutics, 2007. **67**(2): p. 540-547.

79. Shen, L.J., *Nanomedicines in renal transplant rejection–focus on sirolimus.* International journal of nanomedicine, 2007. **2**(1): p. 25-32.

80. Wu, Y., et al., *The role of biopharmaceutics in the development of a clinical nanoparticle formulation of MK-0869: a Beagle dog model predicts improved bioavailability and diminished food effect on absorption in human.* International Journal of Pharmaceutics, 2004. **285**(1–2): p. 135-146.

81. Hoy, S.M., L.J. Scott, and G.M. Keating, *Intramuscular paliperidone palmitate.* CNS drugs, 2010. **24**(3): p. 227-244.

82. Kawabata, Y., et al., *Formulation design for poorly water-soluble drugs based on biopharmaceutics classification system: Basic approaches and practical applications.* International Journal of Pharmaceutics, 2011. **420**(1): p. 1-10.

83. Klein, C.E., et al., *The tablet formulation of lopinavir/ritonavir provides similar bioavailability to the soft-gelatin capsule formulation with less pharmacokinetic variability and diminished food effect.* JAIDS Journal of Acquired Immune Deficiency Syndromes, 2007. **44**(4): p. 401-410.

84. Sherman, E.M. and J.G. Steinberg, *Heat-stable ritonavir tablets: a new formulation of a pharmacokinetic enhancer for HIV.* Expert Opinion on Pharmacotherapy, 2011. **12**(1): p. 141-148.

85. Bauer, J., et al., *Ritonavir: An Extraordinary Example of Conformational Polymorphism.* Pharmaceutical Research, 2001. **18**(6): p. 859-866.

86. Chemburkar, S.R., et al., *Dealing with the Impact of Ritonavir Polymorphs on the Late Stages of Bulk Drug Process Development.* Organic Process Research & Development, 2000. **4**(5): p. 413-417.

87. Verreck, G., et al., *Characterization of solid dispersions of itraconazole and hydroxypropylmethylcellulose prepared by melt extrusion—part I.* International Journal of Pharmaceutics, 2003. **251**(1–2): p. 165-174.

88. Lee, S., et al., *Preparation and characterization of solid dispersions of itraconazole by using aerosol solvent extraction system for improvement in drug solubility and bioavailability.* Archives of Pharmacal Research, 2005. **28**(7): p. 866-874.

89. Six, K., et al., *Characterization of solid dispersions of itraconazole and hydroxypropylmethylcellulose prepared by melt extrusion, part II.* Pharmaceutical Research, 2003. **20**(7): p. 1047-1054.

90. Shah, N., et al., *Development of Novel Microprecipitated Bulk Powder (MBP) Technology for Manufacturing Stable Amorphous Formulations of Poorly Soluble Drugs.* International Journal of Pharmaceutics, 2012.

91. Harmon, A., *A Roller Coaster Chase for a Cure*, in *The New York Times*2010.

92. Harmon, A., *After Long Fight, Drug Gives Sudden Reprieve*, in *The New York Times*2010.
93. Van Drooge, D., et al., *Characterization of the molecular distribution of drugs in glassy solid dispersions at the nano-meter scale, using differential scanning calorimetry and gravimetric water vapour sorption techniques.* International Journal of Pharmaceutics, 2006. **310**(1): p. 220-229.
94. Verreck, G., et al., *The effect of pressurized carbon dioxide as a temporary plasticizer and foaming agent on the hot stage extrusion process and extrudate properties of solid dispersions of itraconazole with PVP-VA 64.* European Journal of Pharmaceutical Sciences, 2005. **26**(3): p. 349-358.
95. Shibata, Y., et al., *Effect of characteristics of compounds on maintenance of an amorphous state in solid dispersion with crospovidone.* Journal of Pharmaceutical Sciences, 2007. **96**(6): p. 1537-1547.
96. Urbanetz, N.A., *Stabilization of solid dispersions of nimodipine and polyethylene glycol 2000.* European Journal of Pharmaceutical Sciences, 2006. **28**(1): p. 67-76.
97. Janssens, S., et al., *The use of a new hydrophilic polymer, Kollicoat IR< sup>®</sup>, in the formulation of solid dispersions of Itraconazole.* European Journal of Pharmaceutical Sciences, 2007. **30**(3): p. 288-294.
98. Albers, J., et al., *Mechanism of drug release from polymethacrylate-based extrudates and milled strands prepared by hot-melt extrusion.* European Journal of Pharmaceutics and Biopharmaceutics, 2009. **71**(2): p. 387-394.
99. Chokshi, R.J., et al., *Characterization of physico-mechanical properties of indomethacin and polymers to assess their suitability for hot-melt extrusion processs as a means to manufacture solid dispersion/solution.* Journal of Pharmaceutical Sciences, 2005. **94**(11): p. 2463-2474.
100. Tanno, F., et al., *Evaluation of hypromellose acetate succinate (HPMCAS) as a carrier in solid dispersions.* Drug development and industrial pharmacy, 2004. **30**(1): p. 9-17.

101. Friesen, D.T., et al., *Hydroxypropyl methylcellulose acetate succinate-based spray-dried dispersions: an overview.* Molecular pharmaceutics, 2008. **5**(6): p. 1003-1019.
102. Ghosh, I., et al., *Comparison of HPMC based polymers performance as carriers for manufacture of solid dispersions using the melt extruder.* International Journal of Pharmaceutics, 2011. **419**(1): p. 12-19.
103. Chowdary, K. and K. Suresh Babu, *Dissolution, bioavailability and ulcerogenic studies on solid dispersions of indomethacin in water soluble cellulose polymers.* Drug development and industrial pharmacy, 1994. **20**(5): p. 799-813.
104. Onoue, S., et al., *Improved dissolution and pharmacokinetic behavior of cyclosporine A using high-energy amorphous solid dispersion approach.* International Journal of Pharmaceutics, 2010. **399**(1): p. 94-101.
105. Newa, M., et al., *Preparation, characterization and in vivo evaluation of ibuprofen binary solid dispersions with poloxamer 188.* International Journal of Pharmaceutics, 2007. **343**(1): p. 228-237.
106. DiNunzio, J.C., et al., *Applications of KinetiSol< sup>®</sup> Dispersing for the production of plasticizer free amorphous solid dispersions.* European Journal of Pharmaceutical Sciences, 2010. **40**(3): p. 179-187.
107. Djuris, J., et al., *Preparation of carbamazepine–Soluplus® solid dispersions by hot-melt extrusion, and prediction of drug–polymer miscibility by thermodynamic model fitting.* European Journal of Pharmaceutics and Biopharmaceutics, 2013. **84**(1): p. 228-237.
108. Rowe, R.C., et al., *Handbook of pharmaceutical excipients*. Vol. 6. 2006: Pharmaceutical press London.
109. Alcohol, M.-P., *Technical Brochure*, 1999, Clariant GmgH: Sulzbach, Germany.
110. Galindo-Rodriguez, S., et al., *Physicochemical parameters associated with nanoparticle formation in the salting-out, emulsification-diffusion, and nanoprecipitation methods.* Pharmaceutical Research, 2004. **21**(8): p. 1428-1439.

111. Abdel-Mottaleb, M.M., et al., *Physically cross-linked polyvinyl alcohol for the topical delivery of fluconazole.* Drug development and industrial pharmacy, 2009. **35**(3): p. 311-320.

112. Bourges, J.L., et al., *Intraocular implants for extended drug delivery: Therapeutic applications.* Advanced Drug Delivery Reviews, 2006. **58**(11): p. 1182-1202.

113. Davies, N.M., et al., *Evaluation of mucoadhesive polymers in ocular drug delivery. I. Viscous solutions.* Pharmaceutical Research, 1991. **8**(8): p. 1039-1043.

114. McDonald, C., et al., *A randomised, crossover, multicentre study to compare the performance of 0.1%(w/v) sodium hyaluronate with 1.4%(w/v) polyvinyl alcohol in the alleviation of symptoms associated with dry eye syndrome.* Eye, 2002. **16**(5): p. 601-607.

115. Winterton, L.C., et al., *The elution of poly (vinyl alcohol) from a contact lens: The realization of a time release moisturizing agent/artificial tear.* Journal of Biomedical Materials Research Part B: Applied Biomaterials, 2007. **80B**(2): p. 424-432.

116. Thanoo, B., M. Sunny, and A. Jayakrishnan, *Controlled Release of Oral Drugs from Cross-linked Polyvinyl Alcohol Microspheres.* Journal of Pharmacy and Pharmacology, 1993. **45**(1): p. 16-20.

117. Sahoo, S.K., et al., *Residual polyvinyl alcohol associated with poly (D, L-lactide-co-glycolide) nanoparticles affects their physical properties and cellular uptake.* Journal of Controlled Release, 2002. **82**(1): p. 105-114.

118. Mu, L. and S. Feng, *A novel controlled release formulation for the anticancer drug paclitaxel (Taxol< sup>®</sup>): PLGA nanoparticles containing vitamin E TPGS.* Journal of Controlled Release, 2003. **86**(1): p. 33-48.

119. Riis, T., et al., *pH-independent drug release of an extremely poorly soluble weakly acidic drug from multiparticulate extended release formulations.* European Journal of Pharmaceutics and Biopharmaceutics, 2007. **65**(1): p. 78-84.

120. Davaran, S., et al., *Development of a novel prolonged-release nicotine transdermal patch.* Pharmacological research, 2005. **51**(3): p. 233-237.

121. DeMerlis, C. and D. Schoneker, *Review of the oral toxicity of polyvinyl alcohol (PVA).* Food and Chemical Toxicology, 2003. **41**(3): p. 319-326.
122. De Jaeghere, W., et al., *HOT-MELT EXTRUSION OF POLYVINYL ALCOHOL FOR ORAL IMMEDIATE RELEASE APPLICATIONS.* International Journal of Pharmaceutics, 2015.
123. Keen, J.M., J.W. McGinity, and R.O. Williams III, *Enhancing bioavailability through thermal processing.* International Journal of Pharmaceutics, 2013. **450**(1): p. 185-196.
124. Gray, V., et al., *The science of USP 1 and 2 dissolution: present challenges and future relevance.* Pharmaceutical Research, 2009. **26**(6): p. 1289-1302.
125. Azarmi, S., W. Roa, and R. Löbenberg, *Current perspectives in dissolution testing of conventional and novel dosage forms.* International Journal of Pharmaceutics, 2007. **328**(1): p. 12-21.
126. Galia, E., et al., *Evaluation of various dissolution media for predicting in vivo performance of class I and II drugs.* Pharmaceutical Research, 1998. **15**(5): p. 698-705.
127. Hughey, J.R., et al., *Dissolution enhancement of a drug exhibiting thermal and acidic decomposition characteristics by fusion processing: a comparative study of hot melt extrusion and kinetisol® dispersing.* AAPS PharmSciTech, 2010. **11**(2): p. 760-774.
128. Sarode, A.L., et al., *Hot melt extrusion (HME) for amorphous solid dispersions: predictive tools for processing and impact of drug–polymer interactions on supersaturation.* European Journal of Pharmaceutical Sciences, 2013. **48**(3): p. 371-384.
129. Trey, S.M., et al., *Delivery of itraconazole from extruded HPC films.* Drug development and industrial pharmacy, 2007. **33**(7): p. 727-735.
130. Nunes, C., A. Mahendrasingam, and R. Suryanarayanan, *Quantification of crystallinity in substantially amorphous materials by synchrotron X-ray powder diffractometry.* Pharmaceutical Research, 2005. **22**(11): p. 1942-1953.

131. Wang, B., et al., *Viscometric, light scattering, and size-exclusion chromatography studies on the structural changes of aqueous poly(vinyl alcohol) induced by γ-ray irradiation.* Journal of Polymer Science Part B: Polymer Physics, 2000. **38**(1): p. 214-221.

132. Hughey, J.R., et al., *Preparation and characterization of fusion processed solid dispersions containing a viscous thermally labile polymeric carrier.* International Journal of Pharmaceutics, 2012. **438**(1): p. 11-19.

133. Hutchinson, J.M. and P. Kumar, *Enthalpy relaxation in polyvinyl acetate.* Thermochimica acta, 2002. **391**(1): p. 197-217.

134. Lu, J., T. Wang, and L.T. Drzal, *Preparation and properties of microfibrillated cellulose polyvinyl alcohol composite materials.* Composites Part A: Applied Science and Manufacturing, 2008. **39**(5): p. 738-746.

135. Stoclet, G., R. Seguela, and J.-M. Lefebvre, *Morphology, thermal behavior and mechanical properties of binary blends of compatible biosourced polymers: Polylactide/polyamide11.* Polymer, 2011. **52**(6): p. 1417-1425.

136. Richardson, M., P. Flory, and J. Jackson, *Crystallization and melting of copolymers of polymethylene.* Polymer, 1963. **4**: p. 221-236.

137. Six, K., et al., *Investigation of thermal properties of glassy itraconazole: identification of a monotropic mesophase.* Thermochimica acta, 2001. **376**(2): p. 175-181.

138. Chokshi, R.J., et al., *Characterization of physico-mechanical properties of indomethacin and polymers to assess their suitability for hot-melt extrusion processs as a means to manufacture solid dispersion/solution.* Journal of Pharmaceutical Sciences, 2005. **94**(11): p. 2463-2474.

139. Rambali, B., et al., *Itraconazole formulation studies of the melt-extrusion process with mixture design.* Drug development and industrial pharmacy, 2003. **29**(6): p. 641-652.

140. Vasconcelos, T., B. Sarmento, and P. Costa, *Solid dispersions as strategy to improve oral bioavailability of poor water soluble drugs.* Drug Discovery Today, 2007. **12**(23–24): p. 1068-1075.

141. Vo, C.L.-N., C. Park, and B.-J. Lee, *Current trends and future perspectives of solid dispersions containing poorly water-soluble drugs.* European Journal of Pharmaceutics and Biopharmaceutics, 2013. **85**(3): p. 799-813.

142. Van den Mooter, G., *The use of amorphous solid dispersions: A formulation strategy to overcome poor solubility and dissolution rate.* Drug Discovery Today: Technologies, 2012. **9**(2): p. e79-e85.

143. Six, K., et al., *Clinical study of solid dispersions of itraconazole prepared by hot-stage extrusion.* European Journal of Pharmaceutical Sciences, 2005. **24**(2): p. 179-186.

144. Mellaerts, R., et al., *Increasing the oral bioavailability of the poorly water soluble drug itraconazole with ordered mesoporous silica.* European Journal of Pharmaceutics and Biopharmaceutics, 2008. **69**(1): p. 223-230.

145. Miller, D.A., et al., *Targeted intestinal delivery of supersaturated itraconazole for improved oral absorption.* Pharmaceutical Research, 2008. **25**(6): p. 1450-1459.

146. DiNunzio, J.C., et al., *Production of advanced solid dispersions for enhanced bioavailability of itraconazole using KinetiSol® Dispersing.* Drug development and industrial pharmacy, 2010. **36**(9): p. 1064-1078.

147. Zhang, K., et al., *Increased dissolution and oral absorption of itraconazole/Soluplus extrudate compared with itraconazole nanosuspension.* European Journal of Pharmaceutics and Biopharmaceutics, 2013. **85**(3): p. 1285-1292.

148. Law, D., et al., *Physicochemical considerations in the preparation of amorphous ritonavir–poly(ethylene glycol) 8000 solid dispersions.* Journal of Pharmaceutical Sciences, 2001. **90**(8): p. 1015-1025.

149. Bley, H., B. Fussnegger, and R. Bodmeier, *Characterization and stability of solid dispersions based on PEG/polymer blends.* International Journal of Pharmaceutics, 2010. **390**(2): p. 165-173.

150. Newa, M., et al., *Preparation, characterization and in vivo evaluation of ibuprofen binary solid dispersions with poloxamer 188.* International Journal of Pharmaceutics, 2007. **343**(1): p. 228-237.

151. Craig, D.Q., *The mechanisms of drug release from solid dispersions in water-soluble polymers.* International Journal of Pharmaceutics, 2002. **231**(2): p. 131-144.

152. Kazarian, S. and G. Martirosyan, *Spectroscopy of polymer/drug formulations processed with supercritical fluids: in situ ATR–IR and Raman study of impregnation of ibuprofen into PVP.* International Journal of Pharmaceutics, 2002. **232**(1): p. 81-90.

153. van der Weerd, J. and S.G. Kazarian, *Combined approach of FTIR imaging and conventional dissolution tests applied to drug release.* Journal of Controlled Release, 2004. **98**(2): p. 295-305.

154. Nesseem, D.I., *Formulation and evaluation of itraconazole via liquid crystal for topical delivery system.* Journal of pharmaceutical and biomedical analysis, 2001. **26**(3): p. 387-399.

155. Garg, A., R. Sachdeva, and G. Kapoor, *Comparison of crystalline and amorphous carriers to improve the dissolution profile of water insoluble drug itraconazole.* Int. J. Pharm. Bio. Sci. 2013; 4 (1): 934, 2013. **948**.

156. Calderini, A. and F. Pessine, *Synthesis and characterization of inclusion complex of the vasodilator drug minoxidil with β-cyclodextrin.* Journal of Inclusion Phenomena and Macrocyclic Chemistry, 2008. **60**(3-4): p. 369-377.

157. Crescenzi, V., et al., *Synthesis and partial characterization of hydrogels obtained via glutaraldehyde crosslinking of acetylated chitosan and of hyaluronan derivatives.* Biomacromolecules, 2003. **4**(4): p. 1045-1054.

158. Trefi, S., et al., *The usefulness of 2D DOSY and 3D DOSY-COSY 1H NMR for mixture analysis: application to genuine and fake formulations of sildenafil (Viagra).* Magnetic Resonance in Chemistry, 2009. **47**(S1): p. S163-S173.

159. Laurienzo, P., et al., *Novel alginate–acrylic polymers as a platform for drug delivery.* Journal of Biomedical Materials Research Part A, 2006. **78**(3): p. 523-531.

160. Ambike, A.A., K. Mahadik, and A. Paradkar, *Stability study of amorphous valdecoxib.* International Journal of Pharmaceutics, 2004. **282**(1): p. 151-162.

161. Office, U.S.G.A., *Prescription Pain Reliever Abuse.* Report to Congressional Requesters, 2011.

162. Prevention, C.f.D.C.a., *Unintentional Drug Poisoning in the United States.* CDC Brief, 2010.

163. Abuse, S. and M. Administration, *Results from the 2010 national survey on drug use and health: Summary of national findings, NSDUH Series H-41, HHS Publication No.(SMA) 11-4658*, in *Substance Abuse and Mental Health Services Administration*2011, Rockville, MD.

164. Food, U. and D. Administration, *Guidance for industry abuse-deterrent opioids-evaluation and labeling.* Center for Drug Evaluation and Research, 2013.

165. Ma, L., L. Deng, and J. Chen, *Applications of poly (ethylene oxide) in controlled release tablet systems: a review.* Drug development and industrial pharmacy, 2014. **40**(7): p. 845-851.

166. Alexander, L., et al., *Development and impact of prescription opioid abuse deterrent formulation technologies.* Drug and alcohol dependence, 2014. **138**: p. 1-6.

167. Cicero, T.J., M.S. Ellis, and H.L. Surratt, *Effect of abuse-deterrent formulation of OxyContin.* New England Journal of Medicine, 2012. **367**(2): p. 187-189.

168. Butler, S.F., et al., *Abuse rates and routes of administration of reformulated extended-release oxycodone: initial findings from a sentinel surveillance sample of*

individuals assessed for substance abuse treatment. The Journal of Pain, 2013. **14**(4): p. 351-358.

169. Cone, E.J., J. Giordano, and B. Weingarten, *An iterative model for in vitro laboratory assessment of tamper deterrent formulations.* Drug and alcohol dependence, 2013. **131**(1): p. 100-105.
170. Harris, S.C., et al., *Abuse potential, pharmacokinetics, pharmacodynamics, and safety of intranasally administered crushed oxycodone HCl abuse-deterrent controlled-release tablets in recreational opioid users.* The Journal of Clinical Pharmacology, 2014. **54**(4): p. 468-477.
171. Raffa, R.B. and J.V. Pergolizzi Jr, *Opioid formulations designed to resist/deter abuse.* Drugs, 2010. **70**(13): p. 1657-1675.
172. Butler, S.F., et al., *Estimating Attractiveness for Abuse of a Not-Yet-Marketed "Abuse-Deterrent" Prescription Opioid Formulation.* Pain Medicine, 2010. **11**(1): p. 81-91.
173. Merrigan, T., et al. *Abuse-resistant, controlled-release oxycodone treats chronic pain*. in *American Academy of Pain Medicine 24th Annual Meeting*. 2008.
174. Barry, D.T., et al., *Pain and associated substance use among opioid dependent individuals seeking office-based treatment with buprenorphine–naloxone: A needs assessment study.* The American Journal on Addictions, 2013. **22**(3): p. 212-217.
175. Duggan, S.T. and L.J. Scott, *Morphine/naltrexone.* CNS drugs, 2010. **24**(6): p. 527-538.
176. Engel, K., et al., *Anti-inflammatory effect of pimecrolimus in the sodium lauryl sulphate test.* Journal of the European Academy of Dermatology and Venereology, 2008. **22**(4): p. 447-450.
177. Andersen, O., et al., *[Problems when swallowing tablets. A questionnaire study from general practice].* Tidsskrift for den Norske laegeforening: tidsskrift for praktisk medicin, ny raekke, 1995. **115**(8): p. 947-949.
178. Aldworth, J., *Results from the 2007 national survey on drug use and health: National findings*2009: DIANE Publishing.

179. Von Korff, M., et al., *An epidemiologic comparison of pain complaints.* Pain, 1988. **32**(2): p. 173-183.
180. Bouhassira, D., et al., *Prevalence of chronic pain with neuropathic characteristics in the general population.* Pain, 2008. **136**(3): p. 380-387.
181. Kopecky, A., A.B. Fleming, and P.K. Noonan, *Safety and pharmacokinetics of oxycodone DETERx administered intranasally in recreational opioid users.* Drug & Alcohol Dependence, 2015. **146**: p. e163.
182. Gudin, J., et al., *Comparing the Effect of Tampering on the Oral Pharmacokinetic Profiles of Two Extended-Release Oxycodone Formulations with Abuse-Deterrent Properties.* Pain Medicine, 2015.
183. Fleming, A.B., et al., *Evaluation of an Extended-Release, Abuse-Deterrent, Microsphere-in-Capsule Analgesic for the Management of Patients with Chronic Pain With Dysphagia (CPD).* Pain Practice, 2015.
184. Coppens, K.A., et al., *Hypromellose, ethylcellulose, and polyethylene oxide use in hot melt extrusion.* 2006.
185. Hale, M.E., et al., *Efficacy and safety of controlled-release versus immediate-release oxycodone: randomized, double-blind evaluation in patients with chronic back pain.* The Clinical Journal of Pain, 1999. **15**(3): p. 179-183.
186. Saltzman, W.M. and W.L. Olbricht, *Building drug delivery into tissue engineering design.* Nature Reviews Drug Discovery, 2002. **1**(3): p. 177-186.
187. Utracki, L.A., *Compatibilization of polymer blends.* 2002.
188. Crowley, M.M., et al., *Physicochemical properties and mechanism of drug release from ethyl cellulose matrix tablets prepared by direct compression and hot-melt extrusion.* International Journal of Pharmaceutics, 2004. **269**(2): p. 509-522.
189. Shah, V.P., et al., *In vitro dissolution profile comparison—statistics and analysis of the similarity factor, f2.* Pharmaceutical Research, 1998. **15**(6): p. 889-896.
190. Rajabi-Siahboomi, A., et al., *Structure and behaviour in hydrophilic matrix sustained release dosage forms: 2. NMR-imaging studies of dimensional changes*

in the gel layer and core of HPMC tablets undergoing hydration. Journal of Controlled Release, 1994. **31**(2): p. 121-128.

191. Sarkar, N., *Kinetics of thermal gelation of methylcellulose and hydroxypropylmethylcellulose in aqueous solutions.* Carbohydrate Polymers, 1995. **26**(3): p. 195-203.

Vita

Chris Eugene Brough graduated from high school at Hong Kong International School in 1991. After which he attended Brigham Young University in Provo, Utah. He received B.S. and M.S. degrees in mechanical engineering and also completed a Master's degree in Business Administration from the Marriott School of Management. Upon completing his education, he formed a company called ReSyk to exploit the technology he developed in his master's thesis.

ReSyk sold machines, called compounders, to companies that were looking to recycle plastic directly into commodity products. ReSyk had 7 licensees of the technology within the United States and Mexico when it sold to IntegriCo Composites in 2005. IntegriCo moved to Temple, Texas, in 2006 to set up a large manufacturing facility to produce plastic railroad ties from recycled post-industrial and post-consumer plastic. At this time, Chris came into contact with Dave Miller, who was a Ph.D. student at the University of Texas. Dave was trying to produce viscous, pharmaceutical amorphous dispersions via hot melt extrusion with limited success. Chris and Dave tested a few of these compositions in the large industrial compounders and had immediate success.

With this result, IntegriCo decided to form a spin-off company, called DisperSol Technologies, to develop the technology for the pharmaceutical fields. Chris built a small, lab scale compounder and placed it at the University in 2008 and worked with Ph.D. candidates on the technology. At DisperSol's persistent request, Chris became a student in 2011 to explore new areas with the technology.

Email address: chris.brough@dispersoltech.com

This dissertation was typed by the author.